Cognitive-Empowered Femtocells: An Intelligent Paradigm for a Robust and Efficient Media Access

by

Xiao Yu Wang

A thesis
presented to the University of Waterloo
in fulfillment of the
thesis requirement for the degree of
Doctor of Philosophy
in
Electrical and Computer Engineering

Waterloo, Ontario, Canada, 2010

I hereby declare that I am the sole author of this thesis. This is a true copy of the thesis, including any required final revisions, as accepted by my examiners.

I understand that my thesis may be made electronically available to the public.

Abstract

Driven by both the need for ubiquitous wireless services and the stringent strain on radio spectrum faced in today's wireless communications, cognitive radio (CR) have been investigated as a promising solution to deploy Wireless Regional Area Networks (WRANs) for an efficient spectrum utilization. Communication devices with CR capabilities are able to access spectrum bands licensed for other wireless services in an opportunistic and secondary fashion, while preventing harmful interference to incumbent licensed services. However, a lesson learned from early experiences in developing such macro-cellular networks is that it becomes increasingly less economically viable to develop CR macrocellular infrastructures for increasing data rates in both line-of-sight as well as non-line-of-sight situation of WRAN, and the corresponding quality of service (QoS) in macrocellular networks is also noticeably degraded due to path loss, shadowing, and multipath fading due to wall penetration.

Moreover, there are several challenges to make the real-world CR enabling dynamic spectrum access a difficult problem to implement without harmful interference. First, the hardware design of cognitive radio on the physical layer involves the tuning over a broad range of spectrum to detect a weak signal in a dynamic environment of fading channels, which in turn makes identification of the spectrum opportunities hard to achieve in an efficient and accurate manner. Second, opportunistic media access based on imperfect spectrum usage information obtain from physical layer brings up undesirable interference issue, as well as reliability issues introduced by mutual interference. Third, the curial issue is to determine which channels to use for data transmissions in presence of the dynamic and opportunistic nature of wireless environments, in the case where pre-defined dedicated control channel is not available in the complex and heterogenous networks.

In this dissertation, a novel framework called Cognitive-Empowered Femtocell (CEF), which combines CR techniques with femtocell networking, is introduced to tackle these challenges and achieve better spectrum reuse, lower interference, easy integration, wider network coverage, as well as fast and cost effective early stage WRAN. In this framework, a sensing coordination scheme is proposed to gracefully unshackles the master/slave relationship between central controllers and end users, while maintaining order and coordination such that better sensing precision and efficiency can be achieved. As such, the network intelligence can be expanded from controlling the intelligence paradigm to better understand the satisfy wireless user needs. We also discuss design and deployment aspects such as sensing with reasoning approach, gossip-enabled stochastic media access without a dedicated control channel, all of which are important to the success of the CEF framework.

We illustrate that such a framework allows wireless users to intelligently capture spectrum opportunities while mitigating interference to other users, as well as improving the network capacity. Performance analysis and simulations were conducted based on these techniques to provide insight on the future direction of interference suppression for dynamic spectrum access.

Acknowledgements

I would like to express my deepest gratitude to my thesis supervisor, Dr. Pin-Han Ho, for immensely helpful comments and suggestion. His guidance, background knowledge, patience and editing skills contributed enormously to the completion of this thesis. He has contributed tremendously to my growth as a dedicated researcher.

I would like to thank my parents Wenyi Zhang and Linquan Wang for giving me the encouragement and strength I needed to complete my goals. I wish to thank my family members for their support and generosity.

I would like to thank all of the funding agencies and corporations that supported my research through financial support. I would like to thank the Natural Sciences and Engineering Research Council (NSERC) of Canada, MITACS.

Special recognition goes out to my friend Alexander Wong for insightful discussions and unconditional support.

Finally, I would like to acknowledge my lovely cat Xiaohua, who spent a lot of time ignoring my research efforts from the beginning to the end, and my cutest cat Cici, who spent a lot of time distracting me from my research at the end.

Contents

List of Tables

List of Figures

List of Acronyms

3GPP	3G Partnership Project
ACK	acknowledge
A/D	Analog-to-Digital
AP	Access Point
ATSC	Advanced Television System Committee
ATV	Analog Television
AWGN	Additive White Gaussian Noise
BPSK	Binary Phase Shift Keying
BS	Base Station
CAAC	Channel-Aware Access Control
CDT	Channel Detection Time
CDF	Cumulative Distribution Function (CDF)
CDMA	Code-Division Multiple-Access
CEF	Cognitive-Empowered Femtocell
CMT	channel move time
CR	Cognitive Radio
CSMA/CA	Carrier Sense Multiple Access With Collision Avoidance
DCF	Distributed Coordination Function
DF	Data Fragment
DOSP	Dynamically Optimization Spatiotemporal Prioritization
DSL	Digital Subscriber Line
DTV	Digital Television
EIRP	Effective Isotropic Radiate Power
EKBR	Extended Knowledge-Based Reasoning
FCC	Federal Communication Commission
FCFS	First-Come First-Serve
GCL	Gossip confidence level

GESMA	Gossip-Enabled Stochastic Media Access
i.i.d	identical and independent distributed
JTRS	Joint Tactical Radio System
LOS	Line-of-Sight
LTE	Long Term Evolution
MAC	Media Access Control
MCMC	Markov-Chain Monte-Carlo
MHz/GHz	Multi/Giga Hertz
NTSC	National Television System Committee
OFDMA	Orthogonal Frequency-Division Multiple Access
P2P	peer-to-peer
PDF	Probability Density Function
PHY	Physical Layer
PSD	Power Spectral Density
QoS	Quality of Service
RIP	Received Interference Power
RF	Radio Frequency
RSS	Received Signal Strength
RTS/CTS	Request-to-Send / Clear-to-Send
std	standard deviation
SCA	Software Communications Architecture
SCF	Spectrum Correlation Function
SDR	Software Defined Radio
SDCI	Software Defined and Cognitive Interfaces
SINR	Signal to Interference plus Noise Ratio
SIR	Signal to Interference Ratio
SMA	Stochastic Medium Access
SNR	Signal-to-Noise Ratio
TH-CDMA	time hopped CDMA
TV	television
UMTS	Universal Mobile Telecommunications System
VHF/UHF	Very / Ultra High Frequency
WiFi	Wireless Fidelity
WiMAX	Worldwide Interoperability for Microwave Access
WLAN	Wireless Local Area Network
WRAN	Wireless Regional Area Network
WSS	Wide-Sense Stationary

List of Symbols

b_m	time bin
B_*	signal bandwidth of different signals as $* = p$: DTV signals, v: ATV signals, m: wireless microphone signals, and (2):secondary user signals
$\bar{B}_i$	expectation of busy period
c_i	the cutoff point of Butterworth function
C	cost associated with each fine sensing
C_0	coordination channel
C_i	channel indexed with i
$\mathbf{C}$,$\mathbf{C}^*$	sequence, instructed channel sequence
d, d_{min}	distance, minimum distance
E_i, E_i'	edges representing recorded possible data transmission on channel i between two vertices and empty entries, respectively
f_c^i	center frequency of channel C_i
f_*^i	feature carrier frequency
f_v^i	video carrier of ATV
$f_{\tilde{t}_b}(t)$	probability density function of backoff time of secondary users
$f_{T_i^{(1)}}(t)$	two-stage hyper exponential distribution of primary user behavior on channel i with mean $1/\lambda_i^{(1)}$, and α variability
$f(U_i, t)$	estimated channel preference ratio
$f_X(x)$	distribution of request class X
$f_X(\bar{N}^X, \sigma^X)$	rule of sub-band allocation with mean $\bar{N}_X$, and standard deviation σ_X
$F(t, \mu^j)$	probability distribution of the j^{th} femto traffic arrival with aggregate arrival rate μ^j
$g_i(t)$	impulse response of channel i for interfering signals
$g_{\aleph_k}$	decay rate of the reliability of other femto user $\aleph_k$
$G = (V, E_i)$	graphical model with a set of vertices
$G'(\cdot)$,$G''(\cdot)$	confidence-weighted graphical model, full graphical model

G_t, G_r	transmitter, receiver antenna gain
h_c	channel impulse response
J, $J_0(\cdot)$	modified Bessel function, first order Bessel function
I_F	interference within a femtocell
I_{FF}	interference from neighboring femtocells
I_{FM}, I_{FM}	femtocell interference to/from a macrocell
$I(i)$	indication function
$I_i(x_o)$,$\bar{I}_i(x_o)$	total interference power received at the victim receiver x_o on channel i, average value
$I(\lambda_i^{(1)})$	average probability of interference to the primary user
$\bar{I}_i$	expectation of idle period
$I(t)$	aggregate interfering signal
$\mathbb{I}_i^{(1)}$	average idle period in the primary network
k	number of obtained available channels
k_Γ	degree of freedom of Gamma distribution
k^x	positive parameter of Pareto index of request class X
K	number of channels
K_I	finite number of interference
K_{FF}, K_F, K_{MF}	number of interference I_{FF}, I_F, I_{MF}
L	system loss factor
L_{fr}	maximum length on data fragment
L_p	length of the data packet (frame)
M	number of samples
m_i	fading severity of channel i
n	number of floors in the path
n^*	optimal number of channels to be finely sensed
n_{ava}	number of successfully identified channels
n_{com}	number of available common channels with other competing femto users
n_{max}	limited number of channel negotiation attempts
n_{req}	requested number of mutually available channels
$N_{(2)}$	number of femto users
N_{CDT}, $\bar{N}_{CDT}$	number of available channels with CDT-fresh sensing results, and mean value

N_s	number of actual sensed channels
N^X,$\bar{N}^X$	maximum number of instructed channels, mean value
N_j^X	number of instructed channels for femto users $\aleph_j$
N_ξ, N_1, $N_\xi^{(i)}$	information rate of modulation symbols of OFDM, that of BPSK, i^{th} N_ξ
$o, \bar{o}^\star$	sensing overhead, its upper bound
$\hat{p}$	interference probability from secondary transmission
p_{cn}	probability of a successful channel negotiation
p_d^*	probability of detection of signal type $*$
p_f^*	probability of false alarm of signal type $*$
$p_i^{(1)}(t)$	probability of no arrival of primary user signal within time period t
$p(i)$	probability of residing on channel i
$p(S)$	target distribution of MCMC approach
$p_i(t)$	likely hood of channel availability of channel i at PHY
$p_{i,re}$	probability that there is no primary user returning to the channel i
$p_{rts,i}$	probability of a successful transmission of RTS message
p_s, $\bar{p}_s$	success rate of spectrum sensing, its mean value
$p_{tx,i}$	probability of successful data transmission on channel i
p_X	probability of the request class X
$p^X(N_{CDT} = n)$	probability of obtaining number of N_{CDT} channels
P_i^o	outage probability on channel i
$P_{i,F}$	probability of interference on channel i within a femtocell
$P_{i,FF}$	probability of interference from neighboring femtocell on channel i
$P_{i,FM}$,$P_{i,MF}$	probability of interference of femtocell to/from the macrocell
$P_{i,(2)}^{\max}$	maximum allowable transmission power of a femto transmitter
$P_{i,(2)}$	average transmitting power of femto user
$P_{i,(1)}^I$,$P_{i,(1)}^{I,max}$	existing interference power at a primary receiver, maximum value
$P_r(d)$	received power at distance d
$P_s(C_i)$,$\hat{P}_s(C_i)$,$\bar{P}_s(C_i)$	short-term statistics on channel i, estimated value, normalized value
$\bar{P}_s'$	normalized aggregate probability of unavailable channel
P_t	transmitted power
P_ξ,$P_{-\xi}$	probability of getting channels of class ξ,probability of the noise that is not in any range of class ξ

q_i^0, q_i^j	probability of channel i are selected by the reference CEF BS and j^{th} neighboring CEF BS
$Q(\cdot)$	proposed probability distribution in MCMC
$r_i(t)$	received waveform on channel i
$\bar{R}$,$\bar{R}^*$	expected basic data transmission rate obtained in n^* iterations fine sensing, that of reasoning approach
$R_{(i)}$	aggregate data transmission rate after i^{th} fine sensing
R_j	aggregate data transmission rate when fine sensing process terminated at j^{th} iteration
$Re\{\cdot\}$	real part of a complex value
R_k	data transmission rate of OFDMA of k channels with BPSK modulation
R_u	temporal usage rate
$R_x(\cdot)$	autocorrelation
$\hat{s}_1, \hat{s}_2, ..., \hat{s}_j$	optimal sequence of channels for negotiation
S, s	random variable taking on a channel, its realization
S_k	equivalent low-pass representation of received k^{th} interfering signal
$S_{LP}(t)$	equivalent low-pass representation of DTV/ATV signal
$S_x(f)$	spectrum correlation function
Δt	processing time of the proposed EKBR scheme and other consumed system time
δt	time difference between current time instance and time stamp assoicated with edge E_i
t_i, $\bar{t}_i$	femto user transmission time, average value
t_s	sample time of OFDM system
T	observation time of signal $x_i(t)$
T_0	period of wide-sense cyclostationary signal
T_b, $\tilde{T}_b$,$T_{b,max}$	the back-off time determined by back-off mechanism during channel access, radome variable, maximum value
$T_{f,i}^{rts}$	failed busy period on non-residing channel
$T_{f,i}^{c}$	failed busy period due to collision
$\bar{T}_{f,i}$	average failed busy period
$T_i^{(1)}$	inter-arrival time of primary users
T_i,T_i^{ava}	time used on available channel i by femto users, available time on channel i
T_k	arrival time of k^{th} interfering signal

T_s^{bas}	average duration of a successful transmission on other commonly available channel
T_s^{rts}	average duration of a successful transmission on the residing channel
$\bar{T}_s$	average time consumed on sensing process
$\bar{T}_{s,i}$	average successful busy period on channel i
T_X	inter-arrival time of the request class X from femto users
$\bar{T}_s^X$	upper bound on the average time consumed on sensing for request class X
T_Σ	overall data transmission processing time
u_i	test statistics of signal on channel i
$u_m(t)$	number of usage out of the overall observation in time bin b_m
$\bar{u}$	factor of line of sight signal
$\bar{U}_i$	average utilization time for successful data transmission
$U_i(t)$	total volume of usage on channel i
V	represents the number of femto users and the set of edges
w_i	weights of channel selection of sensing coordination
$w_{LP}(t)$	equivalent low-pass representation of an AWGN
$W(\forall E_i, t)$	gossip confidence level
x_o	victim receiver
$x(t)$, $x_i(t)$	wide-sense cyclostationary signal, and that on channel i
X	requested number of channels
X_i	spectrum offer at the i^{th} fine sensing
y_k	k^{th} interfering transmitter
$Y_{(i)}$	net spectrum offer return at the i^{th} fine sensing step
Y_s	binary indicator on the results of channel negotiation on s
z_k	distance between the victim receiver x_o and k^{th} interfering transmitter y_k
$\underline{a}$	vector of path loss factor
α_i	probability of primary user transmission
β_i	Nakagami-m fading factor
γ	category of modulation schemes
γ^*,γ^o	SIR, threshold
γ_*	detection threshold of signal type $*$
Γ	Gamma function
Γ_i,$\mathbf{\Gamma}$	probability of selecting channel i, sequence
δ	transmission time of control message

$\delta(\cdot)$	Dirac delta function
ϵ	penetration loss
ε_i	distance factor of interference power from the femto user
η	number of channel with reliable sensing results
η_i	average number of primary users per unit area
η_ξ	number of available channels of class ξ
θ_m	percentage of missed spectrum opportunities
θ_j^X	the probability of a number of N_j^X instructed channels
Θ,Θ'	a set of selected channel for channel negotiation, feasible set of common available channels for data transmission
λ	interference intensity
$\lambda_i^{(1)}$, $\hat{\lambda}_i^{(1)}$	mean arrival rate of primary users, estimated value
$\lambda_i^{(2)}$, $\lambda^{(2)}$	secondary arrival rate on channel i, aggregate value over channels
$\lambda_X^{(2)}$	mean arrival rate of class X in secondary user network
λ_w	wavelength
$\lambda(\Omega(x_o))$	aggregated interference intensity
$\lambda_{FF}(), \lambda_F(), \lambda_{MF}()$	aggregated intensity of I_{FF}, I_F, I_{MF}
Λ	aggregate primary traffic volume
μ^j	aggregate arrival rate of j^{th} femto traffic
ν_i	probability of instructing channel i to more than two femto users in the vulnerable time
ξ	channel class
$\varpi(\bullet)$	absorbing state
ρ, ρ_i	throughput, channel utilization on channel i
ϱ	number of classes of request
σ^X	standard deviation of distribution $f_X(\bar{N}^X, \sigma^X)$
Σ_s	total number of different channels sensed by the same set of femto users
$\bar{\Sigma}_d$, $\bar{\Sigma}_f$	total time consumed on energy detection and fine sensing at femto users
τ	radio propagation delay
τ_d,τ_f	time consumed for each energy detection, each fine sensing
τ_s	short-term statistics observation time window
Υ	probability of sensing conflict

Φ	number of mutually exclusive states
χ^2	chi-square distribution
χ^x	positive minimum possible value of request class X
ψ_{η_ξ}	probability that the femto user decides to continue the fine sensing process based on the proposed reasoning approach
ω, $\bar{\omega}_*$	instantaneous SNR, average SNR of different signals
$\Omega_i^{\tau_s} = \{\omega_i(\tau_1), ..., \omega_i(\tau_n)\}$	observation for channel i for spectrum sensing
$\Omega_k^i = \{\omega_k^i(t_1), \omega_k^i(t_2), ..., \omega_k^i(t_n)\}$	observation of other femto user $\aleph_k$ on channel i for media access
$\Omega(x_o)$	radio range of the victim receiver x_o
$\aleph_c$	femto BS
$\aleph_j$,$\aleph_k$	femto user j, other femto user k
$\ell(d)$	path loss
$\Re$	absorbing states
$\mathcal{P}_k$	transmission power of k^{th} interfering transmitter y_k

Chapter 1

Introduction

In recent years, a dramatic increase in demand for ubiquitous wireless services has been straining the already limited and scarce radio spectrum, especially on those standardized for legacy voice and data transmission. This leads to awkward situations where outgoing calls fail despite having full signal power in the handset, as well as the inability to access Wireless Local Area Network (WLAN) services despite sufficiently strong wireless connections. The main reason for these situations lies in the shortage of spectrum resources associated with the corresponding devices. On the other hand, a large portion of licensed spectrum has not been explored and utilized, which causes a significant number of spectrum holes [1]. According to statistics provided by the Federal Communications Commission (FCC), up to 85% of the licensed spectrum is not used in certain geographical areas, such as rural areas and thinly populated areas. Even in the areas with high population densities, there is still 15% of the licensed spectrum being underutilized. Therefore, the FCC decided to deregulate the spectrum for increasing broadband usage rates. This deregulation opens a door for the unlicensed use of licensed spectrum and consequently opens the door for research in the area. As such, it has attracted extensive attention from both industry and academia on how to utilize the temporarily released spectrum in an efficient and opportunistic manner.

1.1 What is Cognitive-Empowered Femtocell

To fully understand and appreciate the concept of Cognitive-Empowered Femtocell, it is important to discuss the fundamental concept behind cognitive radio and femtocell networking.

1.1.1 Cognitive Radio

Cognitive radio (CR) [1, 2] has been consequently proposed to solve the inefficiency in spectrum assignments of legacy static radio. Various definitions for CR have appeared in different circumstances. According to [3], cognitive radio is an intelligent radio with the capability of accessing radio spectrum resources by exploiting the radio environment for user centric communication. Therefore, in a radio communication system, nodes equipped with CRs can opportunistically gain access to an already-licensed spectrum band, such as television (TV) bands within the 30MHz-3GHz range, to fill in the spectrum holes. In this sense, these nodes act as "secondary" users relative to the licensed (or "primary") users. Since CRs can efficiently increase the utilization of spectrum as well as the capacity of a network, it has attracted a lot of attention and has become a promising solution to the spectrum shortage problem.

Cognitive radio is an extension of software defined radio (SDR). A SDR is a radio communication system equipped with programmable hardware that can tune to any frequency band and receive any modulation across a large frequency spectrum. The concept of the SDR can be traced back to 1992, where the SpeakEasy project was launched for military purposes. The objective of the project was to produce a radio which can operate with existing different military radios. Furthermore, the radio was designed to incorporate diverse coding and modulation standards. In 1997, the Joint Tactical Radio System (JTRS) project was launched for the purpose of unifying different radio communication systems used by the U.S. military in field operations. The essence of the project is to build an open architecture framework which defines the software structures of a SDR. This framework, known as Software Communications Architecture (SCA), enables interpretability among many existing military and civilian radios. The idea of Cognitive radio was first presented by Joseph Mitola III and Gerald Q. Maguire, Jr. [2] in 1999, who extended upon the basic concepts of the SDR by integrating automated reasoning such that radios are capable of adapting system parameters based on its environment. Cognitive radios are also able to conduct collaborations among peers for the use of radio spectrum.

Cognitive Radio (CR) vs. Software Defined Radio (SDR) Since cognitive radio extends upon the basic concepts of SDRs, it is important to describe the characteristics that differentiate CRs from SDRs. Software Defined Radio (SDR), also known as reconfigurable radio, is a radio communication system that relies on embedded software to transform the waveform properties (e.g., modulation, coding, access, and duplex modes, and protocol structure of transmission method [4]) such that it can be interpreted by another type of radio without hardware changes. The term *reconfigurability* refers to the radio's ability to

dynamically support multiple variable systems, protocols and interfaces.

Cognitive Radio (CR), as its name implies, carries a level of awareness of the environment, such as spectrum availability, network status, available resources, and user behavior. Furthermore, it also carries a level of cognition or intelligence that permits decision-making. In wireless communications, the cognition or intelligence can be interpreted as the ability of a transmitter or receiver to detect whether a particular segment of the radio spectrum is currently in use and jump into the temporarily unused spectrum very rapidly without interfering with others' ongoing transmissions.

It can be seen by the descriptions of SDR and CR that the CR is the next logical evolution of SDR. SDRs change transmission mode parameters in a passive way to support diverse system interfaces, while CRs actively sense the environment, track changes, and create new waveforms on their own to opportunistically access free spectrum.

1.1.2 IEEE 802.22 Wireless Regional Area Networks

The charter of IEEE 802.22 [5], the working group on Wireless Regional Area Networks (WRANs), is to develop a standard for a cognitive radio-based physical (PHY) and media access control (MAC) layers for license-exempt ("secondary") users operating in the TV broadcast bands between 54 MHz and 863 MHz covering a typical range of 33 km, and up to 100 km. A centralized approach for the detection of spectrum holes is being pursued by the working group together with the FCC. Two different types of sensing, i.e., fast sensing and fine sensing, are proposed for incumbent sensing. The fast sensing stage is a speedy sensing stage which simply uses energy detection to detect channel availability. Based on the results of fast sensing, more detailed sensing is performed during the fine sensing process on the target channels. Orthogonal Frequency-Division Multiple Access (OFDMA) is proposed as the modulation scheme for transmission in up- and down-links. While the technical requirements of WRAN were finalized in 2007 [6], many pending items are listed in their first draft and only limited details has been defined. For example, the particular functionalities of the PHY/MAC layers has not been specified.

1.1.3 Femtocell Networking

A lesson learned from early experiences in developing such macrocellular networks is that it is expensive to develop infrastructure for radio communications in the typical range of 33 km [6] in both line-of-sight (LOS) as well as non-line-of-sight situations, and it

becomes increasingly less economically viable for increasing data rates. Besides expenditure concerns, quality of service (QoS) in macrocellular networks is also noticeably degraded due to path loss, shadowing, and multipath fading. For example, in a macrocellular network, the significant signal loss at the high frequency bands from wall penetration results in low data rates and poor voice quality inside buildings [7].

A femtocell is a small cellular area covering homes or offices, while femtocell devices are simple, low cost miniature base stations designed for alleviating indoor wireless coverage issues associated with macrocellular networks. The investigation into femtocell devices is driven commercially by existing cellular network providers, who are seeking new sources of revenue from voice and data services while reducing operating costs and capital expenditure [8]. As such, in terms of network structure, femtocell networks are end-user deployed hotspots that underlay the planned macrocellular networks of mobile operators. One of the highlighted key technical challenges associated with such a two-tier cellular network is dealing with cross-tier and inner-tier interference, i.e., interference to/from the macrocell and other femtocells. In the limited literature available, most proposed resource management approaches require modifications on existing macrocell BS. However, due to the design requirement for simplicity with minimum modifications on the macrocell protocols running at the BS, these interference management approaches may not be efficient and scalable. Note that the coverage of a macrocell could be over thousands of femtocells. Therefore, it is not a scalable solution to jointly consider those femtocell users in the design of macrocell resource allocation and scheduling schemes.

1.1.4 Cognitive-Empowered Femtocell

Motivated by the principles and challenges of femtocell networks, a new idea began to emerge: what if we apply CR techniques in femtocell networks? Combining CR techniques with femtocell networking technology, which has never been developed before, can have a significant impact on ubiquitous broadband communications. The proposed Cognitive-Empowered Femtocells (CEFs) [9] underlaying macrocell networks form a two-tier macrocell-femtocell/primary-secondary network.

The underlying goal of CEF technology is to improve the utilization of spectrum resources and in turn solve the issue of spectrum resource starvation for ubiquitous wireless services. The enabling feature of CEF networking solutions is coordinated spectrum management, which provides the capability for opportunistic access of radio spectrum resources by exploiting the radio environment for user-centric communications. Moreover, CEF networking solutions use a small cellular area to cover offices, homes, and public areas where

the demand of spectrum resources of high-speed wireless broadband services is stringent, as well as where the mobile wireless communications suffer from indoor communication barriers associated with macrocellular networks. Therefore, the CEF users can opportunistically gain access to an already-licensed spectrum band, such as any television (TV) bands within 400-800MHz Ultra High Frequency (UHF) TV bands, to fill in the "white space" spectrum. The design principle is to develop simple, low cost, plug-and-play, user-installed, self-configuring CEF BSs that can be made available at prices comparable to WiFi access point (AP), while providing indoor coverage for mobile users by the mobile operators.

In a nutshell, CEF can provide significant benefits when compared to existing wireless services:

- **Better spectrum reuse.** CEF techniques make the reuse of spectrum possible for femtocells to be not only limited in mobile bands allocated to macrocellular techniques, such as Worldwide Interoperability for Microwave Access (WiMAX), Universal Mobile Telecommunications System (UMTS), Long Term Evolution (LTE), etc., but also extended into the spectrum allocated to UHF/VHF TV broadcast services. As such, it can better solve the spectrum resource starvation problem in those regions.

- **Lower interference.** CEF techniques continually monitor the spectrum to avoid possible interference with the license users. Therefore, CEF techniques can be used to protect femtocell users from interference with macrocell users and neighboring femtocell users, allowing for more reliable, high data rate transmissions while improving coverage.

- **Easy integration.** CEF devices are simple, low cost, and can be widely deployed for improved coverage, making them an ideal practical application platform for using CR techniques. Since CR techniques are integrated into the femtocell underlayer, no modifications on the macrocell devices are required.

- **Fast and cost effective deployment.** Rather than developing macrocellular infrastructures to promote spectrum reuse in certain regions, which can be time consuming and costly, CEFs allow for fast and cost effective early stage WRAN deployment for spectrum reuse in those regions.

1.2 Challenges of CEF

Given the benefits of combining CR technology and femtocell networking, let us explore the challenges for CR techniques in the context of femtocell integration for developing CEFs on spectrum sensing, media access and interference avoidance.

1.2.1 Challenges of Spectrum Sensing

To identify the spectrum availability for femtocell users, spectrum sensing is a key process which involves the identification of available spectrum and the boundaries of sub-bands that are currently unused by licensed macrocell users, as well as avoidance of harmful interference. There are many challenges associated with the design of CR due to the wide range of available licensed spectrum. Many previous studies [10–12] assumed the existence of an ideal physical layer (PHY), which is capable of perfect detection and utilization of free spectrum. However, such an assumption is seldom true due to several important issues associated with designing an efficient and accurate spectrum sensing techniques following PHY constraints.

First of all, research on CR faces challenges caused by the broad range of available spectrum. Radio frequency (RF) hardware for CR should be capable of tuning to any part of a multi-gigahertz-wide bandwidth from 20MHz to 3GHz. Therefore, such hardware devices require an extremely high-speed analog-to-digital (A/D) converter to detect a weak signal, which might be infeasible. The major PHY design issues related to this have been addressed by Cabric et al. [13].

Second, reliable detection on the presence of macrocell and/or other incumbent users is also a crucial problem in a fading environment, where figuring out whether a channel is free or in deep fading is hard [14]. A commonly-used energy detection method can be adopted to detect the presence of an unknown signal in noise. The widely adopted propagation model [15] can be defined as follows:

$$P_r(d) = \frac{P_t G_t G_r \lambda_w^2}{(4\pi)^2 d^2 L} \tag{1.1}$$

where P_t is the transmitted power, $P_r(d)$ is the received power, G_t is the transmitter antenna gain, G_r is the receiver antenna gain, d is the distance between transmission pair, L is the system loss factor, and λ_w is the wavelength. This propagation model is designed for predicting received signal strength (RSS) in free space, where there is a clear

and line-of-sight (LOS) path between a transmitter and a receiver. However, in real life, reflection, diffraction, scattering, multi-path fading and indoor penetration loss can not be ignored, especially when signals are traveling long distances in large-scale networks. It is often not sufficient for determining whether the macrocell and/or other incumbent user is indeed present. Moreover, due to the susceptibility to unknown noise, setting a threshold for detection on the presence of macrocell and/or other incumbent users is hard for every license class [13]. Another disadvantage of energy detection is that it can not differentiate between signal types even though it detects the presence of macrocell and/or other incumbent users. Therefore, a number of feature detection techniques have been proposed to differentiate the noise energy from the modulated signal energy.

Cyclostationary feature detection has drawn much attention in the area of digital signal processing. *Cyclostationary* processes are signals characterized by cyclical time-varying statistics. Modulated signals exhibit built-in cyclostationarity, which facilitates receivers in the detection of a random signal with a particular modulation type from noise or other modulated signals [13]. In the general case, modulated signals are treated as wide-sense stationary (WSS) processes with time invariant autocorrelation function defined as follows:

$$R_x(t,\tau) = E\left\{x\left(t\right)x\left(t-\tau\right)^*\right\} \tag{1.2}$$

where signal $x(t)$ is a wide-sense cyclostationary signal with period T_0 and must satisfy the following:

$$R_x(t,\tau) = R_x(t+T_0,\tau) \quad \forall t,\tau \tag{1.3}$$

The spectrum correlation function (SCF) is given by transforming Eq. (1.2) into the frequency domain:

$$S_x(f) = F\{R_x(\tau)\} = \int_{-\infty}^{\infty} R_x(\tau)e^{-j2\pi f\tau}d\tau \tag{1.4}$$

$S_x(f)$ contains the frequency information related to timing parameters in modulated signals [16]. The main disadvantage of feature detection methods is that they require a much longer observation time than that taken by the energy detection method, as well as being computationally complex in comparison [17]. The technique of feature detection is beyond of the scope of this work, but an overview of feature detection can be found in [16].

Finally, an important characteristic of CRs is that they are highly flexible. Since the CRs are given lower priority than the macrocell and/or other incumbent users, a fundamental requirement is that CRs' transmission should not affect macrocell and/or other incumbent users' channel initiations and transmissions. Through observing certain

signal patterns, the CRs must determine whether the macrocell and/or other incumbent users have the intention of using their assigned channels. If it is determined that the macrocell and/or other incumbent users have the intention of using the channels, the CRs must immediately clear the channels for the macrocell and/or other incumbent users and prevent interference within an acceptable range. At the same time, the CRs must switch to other free channels to maintain their ongoing transmission for real-time traffic. Therefore, continuous spectrum sensing is required. For non-real-time traffic, the CRs terminate the ongoing transmission and resume them whenever they detect available channels. This also requires frequent spectrum sensing to lower the latency and packet discard rate of the system. Therefore, a problem unique to the CRs is to find available radio channels without interfering with macrocell and/or other incumbent users.

1.2.2 Challenges of Wireless Medium Access

Since the major research problems on PHY layer dealing with how to correctly and quickly detect the existence of macrocell and/or other incumbent users' signal and spectrum opportunities have not been solved, the Medium Access Control (MAC) layer protocols can not be properly designed based on the assumption of an ideal PHY layer. People start to solve the problem from a MAC design point of view while taking the aforementioned PHY layer issues as design constraints. The challenge of MAC design is to further improve the sensing reliability, sensitivity and flexibility under non-ideal situations where there is no perfect knowledge of the PHY layer. Even in an ideal situation where all PHY layer problems can be solved, the MAC designs still correspond to many CEF coordination functions, such as those associated with detection timing, access efficiency and sharing of medium resources. The issues related to a CEF MAC design are enumerated as follows:

1. **Timing**: Opportunities for spectrum access are all over the spectral band and fluctuate from time to time. A tradeoff exists between the time consumed in terms of how quickly available channels are accessed and the time consumed in waiting for good quality channels.

2. **Efficiency**: A CEF MAC has to determine how many channels to go through in each sensing and spectrum access. Since each channel across the whole spectrum may or may not be accessible at a moment, the more channels sensed, the better chance the CEF user can obtain spectrum access with the desired quality. Conversely, given the size of data to be sent as well as a given bound on the latency of both sensing and

transmission, a lengthy sensing process reduces the time left for transmission, which subsequently reduces the chance of successfully delivering the data. Furthermore, a lengthy sensing process will certainly consume more energy at the node. Therefore, a harmonic design on the length of a sensing process in presence of the time and/or energy constraint is highly desired for an efficient CEF MAC.

3. **Channel selection**: The CEF MAC must also choose between a single channel or multiple channels. If a single channel is chosen for a transmission request, the problem falls in the category of the **Timing** issue mentioned above, which is to statistically compromise between timely access and better-quality access. If multiple channels are chosen, the issue of interest becomes determining how many channels (or how much bandwidth in total) should be enough to achieve a certain level of quality for data transmission. This falls in the category of the **Efficiency** issue mentioned above.

4. **Hidden and exposed terminal problem**: These are classical problems in distributed wireless networks. Within CEF, hidden and exposed terminals can be femto users within the same or different femtocell, as well as macrocell and/or other incumbent users, which cause interferences and in turn degrade the network throughput.

5. **Protocols**: For peer-to-peer communications within CEF, radio links are established using precisely defined handshake communication protocols. The handshake communication protocols specify how CEF users communicate over radio frequencies and also defines the control signaling methods. The protocols must provide a great amount of details regarding channel reliability to ensure that data is properly sent and received between a communication pair.

6. **Saturation and jam on common control channel**: In cognitive MAC design, the use of a common control channel is heavily debated. If a common control channel is used for exchanging control or management signals, the common control will soon be saturated and jammed. In the case where there is no common control channel available, the problem revolves around how to communicate spectrum resource allocation information between source and destination nodes. For example, the source node and the destination may have allocated different freely available channels. However, since there is no common control channel, the information regarding available channels that each individual node has cannot be communicated between the two nodes. Therefore, they are unable to determine a common available channel for establishing communication link.

1.2.3 Challenges of Interference Avoidance

While the design of spectrum sensing and MAC protocols should take interference into consideration, it is important to deal with interference avoidance as a whole as a separate entity. This is due to the fact that a different mentality must be applied to the design of interference avoidance, where it is more effective to study it from an interference point-of-view. Once an effective design of interference avoidance has been established in this separate study, it can be integrated back into the overall design of spectrum sensing and MAC protocols. Therefore, in this section, we address several interference issues associated with the two-tier macrocell-femtocell/primary-secondary network:

1. **Femtocell interference to/from macrocells**: also known as cross-tier interference. Within the two-tier network, the possible causes of this interference include: 1) the indoor femtocell users are not able to identify severely faded outdoor macrocell users' signals, and thus leading to unwanted accesses to unavailable channels that are being used by macrocell users, and 2) macrocell users returning to previously identified available channels that have been used by femtocell users. The challenge associated with the first cause of interference falls into the category of the **challenges of spectrum sensing** mentioned in Section 1.2.1.

   The challenge associated with the second cause of interference is due to the nature of that femtocell user that occupy channels purely on a secondary basis. As long as macrocell and/or other incumbent users intend to allocate channels, the CEF users are forced to imperceptibly move to other segments of spectrum to continue transmissions. To the femtocell users, there are two factors that need to be considered: transparency of temporarily occupied spectrum, and seamlessness of moving from channels to channels. The issue of transparency can be interpreted as having the femtocell users access the channel without affecting the performance of macrocell and/or incumbent services.

2. **Interference from neighboring femtocells**: also known as inner-tier interference, where victim receivers are the femtocell users that are most likely on the edge of femtocell or in the intersections of neighboring femtocells. The cause of this form of interference is that the same channels are accessed by neighboring femtocell users. Since the spectrum are shared within several equal-tier and independent femtocell systems, interference mitigation must be achieved through a certain level of coordination amongst neighboring femtocells.

3. **Interference within a femtocell**: Within a femtocell, interference is mainly caused by contention on the same channels; therefore, the spectrum sensing serves this purpose by gaining channel status before accessing the channel, and reliable MAC protocols are required to efficient share the spectrum. Since reliable spectrum detection is still an open issue in the PHY layer design, MAC layer spectrum sensing and control signaling is expected to take an important role in interference avoidance by considering imperfect information obtained from PHY layer.

1.3 Methodology

This dissertation defines, designs, develops, and analyzes the CEF concept. Stochastic approaches are promoted for CEF users to achieve timely, efficient, accurate and practical media access and spectrum sharing in the context of complex, dynamic networks with limited interference.

In particular, this work defines the framework of CEF, differentiating it from other cross-layer paradigms and technologies in wireless communications. The concept of combining CR techniques with femtocell technology is highly novel and has never been thoroughly investigated before, with the potential of significantly improving the capacity for ubiquitous broadband communication services while lowering the burden of mobile operators. This framework is inclusive enough to incorporate different objectives, network architectures, protocol stacks, and cognitive processes. Several cognitive elements that use direct and indirect network observations as inputs to the decision making process are designed and developed.

A novel spectrum sensing coordination framework for CEF networks is introduced, which aims to take the best of the cooperative and stand-alone spectrum sensing strategies while avoiding the respective disadvantages. By loosening the ties upon the master/slave relationship between central controllers and femtocell users, both order and coordination are maintained among the femtocell users.

The decision making process utilizes a reasoning approach at the femtocell users to determine a set of action choices, implementable in the network parameters. Since efficiency is a major objective of the CEF system, the tradeoff between performance and complexity is gracefully balanced using efficient optimization algorithms, such as stochastic expectation maximization and Markov-chain Monte-Carlo algorithms.

To give insight into the applicability and limitation of the developed CEF system,

rigorous mathematical analysis is conducted using probability theory, multi-dimensional absorbing Markov chains, renewal theory, and shot noise processes.

1.4 Thesis Statement

The work in this dissertation represents the first investigation of CEF. In Chapter 3, the first definition, framework, development for CEF is presented. Rather than having a complete control on spectrum sensing and access, the CEF BS are designed to assist and coordinate the CEF users for better capturing spectrum opportunities while mitigating the cross-tier and inner-tier interference. With a novel information-adaptive spectrum management coordination framework, the network intelligence can be expanded from controlling the resources through an egocentric paradigm to an individualized intelligence paradigm to better understand and satisfy user needs.

In Chapter 4, as an important realization of the spectrum management of CEF framework, a sensing coordination scheme is introduced. The proposed sensing coordination scheme intends to initiate a graceful compromise between stand-alone and cooperative sensing by taking the best of the two while mitigating their respective disadvantages. With a sensing coordination module equipped on the femto BS, the fine sensing activities of all the surrounding femto users are coordinated and scheduled such that better sensing precision and efficiency can be achieved.

In Chapter 5, a novel scheme for spectrum sensing at individual CEF users in Medium Access Control (MAC) layer, called Extended Knowledge-Based Reasoning (EKBR) [18], is proposed. The target of EKBR is to improve the fine sensing efficiency by jointly considering a number of network states and environmental statistics, including coordination instructions, short-term statistical information, channel quality, data transmission rate, and channel contention characteristics. This is for a better estimation on the optimal range of spectrum for fine sensing so as to adaptively reduce the overall channel sensing time. As such, better performance can be achieved than that by the state-of-the-art techniques while yielding less computation complexity and sensing overhead.

In Chapter 6, a novel Gossip-Enabled Stochastic Medium Access (GESMA) scheme that takes interference constraints into account to improve spectrum sharing efficiency is proposed. Specifically, the proposed GESMA scheme is developed to maximize the probability of successful channel access, serving in an ad hoc manner where CEF users from the same and/or different femtocells try to communicate with each other without

available common control channels. The formulated optimization problem is then solved by using a dynamic Markov-Chain Monte-Carlo scheme with obtained gossip knowledge. Moreover, the thesis introduces a suite of mechanisms for implementation of the proposed scheme, including segmentation of long packets and contention resolution, which is working on top of power controlled Request-to-Send (RTS) and Clear-to-Send (CTS) exchanges in a multichannel environment. The proposed GESMA scheme is expected to serve as a value-added complement to the state-of-the-art multi-channel MAC protocols with pre-defined dedicated control channels in distributed and highly dynamic CR networks.

In Chapter 7, the overall mathematic model of the interference associated with the proposed CEF framework is thoroughly studied through a *shot noise* process.

In Chapter 8, results are summarized and conclusions are drawn. Based on the interference analysis of the CEF framework, future work yet to be done for mitigating the interference is presented.

Chapter 2

Related Work

CEF encompass many areas of research, such as accurate spectrum sensing, and efficient media access with limited interference, which are associated with the time line of setting up a communication link, as well as conducting interference management. This chapter describes related work which both inspires and guides this research.

2.1 Spectrum Sensing

A spectrum sensing scheme concerns how the employed spectrum sensing technique is deployed in a communication system (which most likely distributed and autonomous in nature). *Cooperative sensing* and *stand-alone sensing* are the two most popular dynamic spectrum sensing schemes.

2.1.1 Cooperative Sensing

Given the increasing importance of CR, which is expected to effectively solve the bandwidth issues in future heterogeneous wireless networks, cooperative sensing has been proposed for achieving an efficient exploration of spectrum resource for secondary users, and is currently subject to extensive research efforts from both industry and academia. With cooperative spectrum sensing, individual secondary users perform local spectrum sensing and share their sensing information with one another to collectively determine the likelihood of channel availability.

Cooperative spectrum sensing algorithms can be categorized into three classes in terms of the mechanisms of sharing the sensing results. The first class of cooperative spectrum sensing algorithms are those that exchange a set of informative sensing results among secondary users to facilitate overall decision making [19–21]. The study in [19] proposed a spectrum sensing architecture which consists of Software Defined and Cognitive Interfaces (SDCI) along with a cognitive engine. The purpose of SDCI is to observe the system internal status as well as the external environment. The raw data containing structured information are processed by the cognitive engine, which is composed of an analysis module and a decision module. This class of approaches can share the sensing information among peers at the expense of taking extra communication overhead due to the required information exchange.

To reduce communication overhead, the second class of approaches have each secondary user send the local decision with respect to the presence of primary users to a decision node instead of the whole sensing results. The decision node makes a final decision by manipulating the local decision received from the other secondary users [22–30]. Generally, the data fusion is performed using a series of "AND" or/and "OR" operations. Since each local decision may not be correct, an improper global decision may be made, resulting in missed spectrum opportunities or interference with the primary users in the network. In [26, 27], a cooperative sensing scheme was developed such that only the secondary users who are confident in their spectrum sensing results will exchange information with other secondary users. However, it is still subject to problems associated with determining the confidence of each secondary users on their local decisions. As an extension of [26], the study in [28] has the secondary users grouped based on their multiple access methods to cooperatively detect the presence of primary users. Each group is assigned a different sensing task, where the final decision on the presence of primary users is made after information exchange within the group, in order to improve sensing accuracy and decrease delay between sensing and decision. In [29], a relay-based sensing scheme is proposed to gain spatial diversity in centralized secondary networks. Cognitive relay nodes help to sense the presence of primary users and relay their decision to the cognitive based station through a predefined control channel.

Intuitively, the second class of approaches are subject to lower communication overhead. However, the resulting voting-based cooperative spectrum sensing mechanism requires the secondary users to cast their decision at the same time in each round, thereby introducing additional delay on the decision making process. Thus, the common problem for the second class of approaches is that the final decision at the decision node may be based on stale network states due to time sensitivity of spectrum usage information. Furthermore, the

sensing accuracy of both classes of approaches are highly dependent on the density of secondary user nodes, where the situation of low secondary user densities could lead to inaccurate decisions [31]. Finally, the previous studies on the two classes of approach did not consider to take advantage of prior knowledge about user behaviour to help improve sensing accuracy.

The third class of approaches proposed in [32, 33] improves the spectrum sensing accuracy by sharing long-term statistical channel availability information with other cooperative secondary users to improve the accuracy of the spectrum sensing process. Such a way allows the knowledge gained by other cooperative secondary users to be retained in the secondary user network even when any of the cooperative secondary users leaves the network or become inactive. As such, this class of approaches is robust to the density of secondary user nodes by fully taking advantage of user behaviour history in the network environment to improve overall sensing accuracy. However, the approach in [32] may subject to a big challenge in determining the importance of the individual statistical characteristics and selecting a proper weight on each of them during the statistical fusion process. The proposed dynamically optimization spatiotemporal prioritization (DOSP) [33] spectrum sensing algorithm extends the study in [32] by intelligently selecting the weighting on the long-term, short-term, and instantaneous statistical information through sequential quadratic programming [34] in determining the likelihood of channel availability. Through statistical learning and dynamic optimization, the proposed algorithm can achieve improved channel prioritization by minimizing the sensing error rate.

2.1.2 Stand-alone Sensing

An alternative approach to cooperative sensing is stand-alone spectrum sensing, where each secondary user has a complete control over when to sense and which channels to sense. To improve sensing efficiency, a stand-alone sensing method usually provides an estimation on the duration of the sensing activity by considering the overhead of sensing [35, 36], as well as the tradeoff between the quality and quantity of spectrum opportunities [37, 38, 36, 39, 40].

Kim et al. [41] proposed the use of two modes of MAC-layer spectrum sensing, reactive and proactive, as well as the associated tradeoff between the two modes. They also introduced an energy-efficient approach for determining the appropriate mode of sensing, as well as a sensing-period adaptation technique for finding the optimal sensing period. More recently, they proposed a spectrum sensing algorithm in [36] that attempts to determine a sensing sequence that minimizes the average delay of discovering idle channels based

on channel capacity and probability of channel availability. Datla et al. [38] took a more heuristic approach to the problem of spectrum sensing, where a linear backoff scheme is employed to reduce the preference of sensing a channel whenever the channel is identified as being occupied. Jia et al. [39] introduced a spectrum sensing algorithm that takes some constraints on sensing and transmission into account. By considering the limitations associated with bandwidth and fragmentation (transmission constraints) and the limitations with sensing capacity (sensing constraints), Jia et al. formulates the tradeoff between spectrum opportunities and sensing overhead as a stopping problem to determine whether the sensing process should proceed. More recently, Huang et al. [40] formulated the spectrum sensing and transmission problems together as an optimal stopping algorithm that aims to maximize the average reward per unit time, where an award is received by a secondary user for each successful transmission. Chang et al. [42] also employed a joint channel sensing and transmission strategy that aims to maximize reward using a threshold-based structure.

2.1.3 Comparison of Spectrum Sensing strategies

The advantages and disadvantages associated with both strategies are provided in Table. 2.1.

Table 2.1: Comparison between Cooperative and Stand-Alone Sensing

	Cooperative Sensing	**Stand-alone Sensing**
Density	Highly dependent on the density of sensing nodes. Highly dependent on observation independency.	N/A
Heterogeneity Signals	May result in the situation where secondary users submit different sensing results and conclusions due to different perceptions of heterogeneity signals.	N/A
Communication Overhead	Heavier communication overhead.	N/A
Time Sensitivity	Introduce additional delay from collecting sensing results from sensing nodes to making the decision, resulting staled sensing results.	Able to promptly use available sub-bands once availabilities have been identified.
Spatial Diversity Gain	Achieve spatial diversity gain with certain densities and uncorrelated observations.	Not able to achieve.
Fading Signals	Higher detection sensitivity under proper density.	Able to achieve detection sensitivity by using feature detection techniques, such as cyclostationary, and covariance-based detection.
Coordination	Sensing and access are fully controlled by the central controller.	May result in disorderly accesses to the same available sub-bands like a swarm of bees.
Reliability	Highly depends on the data fusion scheme as well as the credibility of sensing nodes.	Highly depends on sensing techniques.

Clearly, both cooperative and stand-alone sensing schemes are subject to limitations on the suitability for realizing the proposed CEF framework. For example, due to the strong heterogeneity in modern wireless networks which may accommodate devices of different vendors and wireless techniques, using a central controller to handle spectrum sensing, access and resource allocation processes may result in problems of flexibility, scalability, and interoperability. In addition, the CEF BSs and femtocell users are simple devices, and could be infeasible to serve as a distributed computing platform for realizing complicated cooperative sensing. Conversely, in the event that all the spectrum sensing and information processing processes are performed independently without any information and coordination, though resolved the aforementioned problems, it could lead to significant performance downgrade due to disorderly accesses among secondary femto users.

2.2 Media Access

In general, there are four types of media access approaches for decentralized multichannel ad hoc networks that can be possible candidates for the CR ad hoc networks of interest in the study: i)dedicated control channel, ii) reserved time slots, iii) channel hopping, iv)cluster-based coordination.

2.2.1 Dedicated control channel

To our best of our knowledge, most of the reported studies on CR multi-channel networks have taken a common assumption on the presence of one or multiple frequency bands as dedicated control channels [10, 11, 39, 43–52]. In [43], a cross-layer opportunistic multi-channel MAC protocol integrated with spectrum sensing at the physical layer and packet scheduling at the MAC layer was proposed. Two collaborative channel spectrum-sensing policies were proposed, in which the channel selection information is exchanged via a dedicated control channel to support the agreement during the channel access process between transmission pairs. In [39], constraints on sensing and transmission were considered in designing a stopping algorithm to realize opportunistic media access with the aid of the dedicated control channel to exchange control messages. In [48], a code-division multiple-access (CDMA) based channel-aware access control (CAAC) algorithm was proposed that adjusted channel access probabilities based on the received SINR and measured interference temperature. The algorithm is then implemented on a Carrier Sense Multiple Access With

Collision Avoidance (CSMA/CA) access method where the channel status information is overheard and exchanged over a common control channel.

While conceptually simple, this approach is mainly subject to two issues when applied to the multi-channel CR ad hoc networks. Firstly, since all channel selection information is exchanged via a dedicated control channel, the dedicated control channel may encounter jamming and saturation [53] in case the CR nodes are densely located. In situations where a large number of data frames are queued for transmission, the reserved resources become saturated from contention [54], which leads to failed channel allocation and potentially poor performance. Secondly, such an approach may be subject to information staleness due to the fact that each CR node has to listen to and process all transmissions along the dedicated control channel to ensure informational accuracy. Thirdly, the future CR ad hoc networks are envisioned to demonstrate very high heterogeneity and dynamics. This makes the assumption of using static dedicated control channels at each CR node of different vendors and technologies not always true.

2.2.2 Reserved time slots

This approach involves the use of reserved time slots [55–58], where time is sub-divided into beacon intervals, and channel negotiation is performed at the beginning of each beacon interval. The exchanged channel selection information during the beacon intervals is then used to facilitate the channel negotiation process between the transmission pairs. To improve efficiency, numerous methods were introduced to adapt the time window size according to network traffic [56, 57] and signal-to-interference plus noise ratio (SINR) at the receiver [58]. Although effective, the using reserved time slots is subject to a number of problems. Similar to the first type that relies on a dedicated control channel, the second type is vulnerable to jamming and channel saturation when performing channel negotiation during reserved time slots. Furthermore, this type of approaches requires accurate time synchronization, which could be difficult to achieve in highly distributed and heterogeneous environments such as multi-channel CR ad hoc networks.

2.2.3 Channel hopping

In a traditional multichannel network, some MAC protocols apply channel hopping [59–61] as an alternative, where each node follows a set of pre-defined multi-channel hopping sequences in an attempt to access channels with any intended receiver without the need for

a dedicated control channel. While channel hopping holds a great potential in alleviating the need of dedicated control channels, it is subject to a critical limitation when applied in a CR network.

Currently existing channel hopping schemes are based on fixed and static sequences, which are either generated from simple hashing functions [60] or pseudo-random hopping sequences [59]. Without considering the underlying channel availabilities of the network environment, the channel hopping schemes do not account for the highly dynamic wireless channels and user behaviours, which serve as the most important and unique features of CR networks. This will certainly lead to poor performance of CR systems as transmission pairs may not be able to identify commonly available channels in a timely manner due to poor hopping sequences.

2.2.4 Cluster-based coordination

There are only a few related works on media access without a predefined dedicated control channel. The study in [53] focused on developing a cluster-based coordination scheme, where coordination channels are selected as common control channels in CR network via a recursive distributed voting process. In this approach, the channels providing the highest neighborhood connectivity are selected as the coordination channels for users within a neighborhood, and this process continues until all users are connected to its neighbors. As such, unlike predefined dedicated control channel approaches, a set of control channels are determined dynamically based on the neighborhood characteristics. Since the cluster-based coordination scheme proposed by Zhao *et al.* attempts to minimize the number of clusters used, the number of common channels within each neighborhood is also reduced. As such, the change of primary user activities can result in the disconnection of users from their neighbors, hence leading to the need for frequent reclustering to ensure full neighborhood connectivity [62].

To alleviate this problem, Lazos *et al.* proposed a spectrum-opportunity clustering algorithm [62], where the CR nodes are clustered based on similar channel availabilities. This allows the CRs to choose a control channel from a large group of idle channels, as well as enables the CRs to migrate to another control channel without the need for reclustering if the current control channel becomes occupied due to primary user activities. The cluster-based coordination schemes are reported to yield similar performance as that by the dedicated control channel scheme. However, the overhead in the reclustering and neighbor discovery processes imposes a barrier in the deployment of the schemes.

2.2.5 Other approaches

There are a few MAC protocols designed for CR networks that try to dance around the need for pre-defined dedicated control channels, but with implicit assumptions on common resources, such as channels, time slots, as well as codes, which can be used to facilitate the media access. In [63], based on an assumption that bidirectional communication links exist between communication pairs enabling coordination and selection of common channels to communicate, the problem of media access is then studied in a two-tier media access game composed of a channel allocation and a multiple access sub-games. In [64], a slotted beaconing period is defined in each MAC super-frame to exchange information and negotiate channel usage. A beacon is signed when a node detects an available channel where no other beacon is present, and other nodes can join the beacon group by sending its own beacon. In this way, a dynamic rendezvous channel is selected by the beacon group, where these nodes can communicate with each other. In [47], an analytical framework for opportunistic spectrum access based on a Partially Observable Markov Decision Process is developed. A simplified suboptimal algorithm that greedily maximizes each-slot throughput is proposed for spectrum sensing and access, and the idea of receiver oriented code assignment is used to facilitate the initial handshake.

2.3 Interference Mitigation

In the limited literature available, several interference management approaches have been proposed, and can be categorized into three classes in terms of the spectrum deployment methods. The first class of interference avoidance are those with universal frequency reuse in the two-tier networks, such as a power control strategy for femtocell users [65–68], time hopped CDMA (TH-CDMA) combined with sectoring antenna [69], and signal-to-interference-plus-noise based component carrier selection [70]. In [71], a near-Gaussian nature of per-subcarrier interference analysis is used to estimate signal-to-interference ratio, which is fed to the Viterbi decoder as the weight of branch metrics to suppress the interference effects.

Moreover, according to the most recent development in the 3G Partnership Project (3GPP) LTE/LTE-Advanced standardization progress, 3GPP LTE BSs (including macrocells and femtocells) had been capable of measuring the Received Interference Power (RIP) in uplink [72] to avoid interference from users without appropriate control. To avoid interferences from the macrocell, measuring the RIP in downlink for femtocell BSs have recently

received considerable attention [73], where periodic channel measurement on RIP is performed at femtocell BSs to identify which resource block is occupied by the macrocell in a subframe. In subframes not performing measurement, the femtocell BS can perform data transmission based on the resource block availability obtained in the previous measurement period.

The second class of interference mitigation is achieved by a dedicated universal physical channel, where global real-time information of difference radio access technologies with regards to available spectrum bands, services, network policies, interference condition etc. are provided. Wireless users calibrate with the information and reconfigure themselves in order to connect to all these different radio access technologies on various frequency bands accordingly depending on their needs [74–76]. Although the dedicated channel deployment can avoid cross-tier interferences, the limited bandwidth of both femtocells and macrocell could seriously impair the performance. It is particularly not feasible under dense deployment of femtocells since each femtocell can only access very limited bandwidth. In the co-channel and partial co-channel deployment, on the other hand, a global scheduling scheme is needed for channel allocation; otherwise both the femtocells and the macrocell may suffer from terrible interference with each other. This becomes a major challenge in adopting these schemes.

The third class of approach shares part of the total spectrum band, and the rest of the band is used exclusively by macro or femto cells to minimizing the interference. In [77], difference algorithms to minimize the interference such as frequency sharing with hopping sequence, frequency sharing with cost function, time sharing with hopping sequence and time/requency sharing are investigated. In [78], CR sensing techniques are applied to identify resource block (which is an LTE term and corresponds to the smallest time frequency resource that can be allocated to a user) at the femto BSs, and the resource blocks that are sensed not occupied are assigned to femto users in a centralized manner to mitigate the interference. Meanwhile, the optimal sensing period is obtained to guarantee the statistic access delay of the femto users. In [79], a location-aware cooperative resource management protocol is designed within a cognitive WiMAX [80] with femtocell architecture, where both macro BS and secondary users are equipped with ultra-sensitive cognitive radios, and primary users communicate with femto BSs via dedicated channels while secondary users communicated with macro BSs by considering interference avoidance.

However, if the design of femtocell devices adheres to the principle of simplicity and no modifications on existing macrocell base stations, these interference management approaches may not be efficient and scalable. Note that the coverage of a macrocell could be over thousands of femtocells. Therefore, it is not a scalable solution to jointly consider

those femtocell users in the design of macrocell resource allocation and scheduling schemes.

Chapter 3

Cognitive-Empowered Femtocell Framework

This chapter describes in detail the proposed CEF framework. The operation and cognitive functionality of each component in the framework is described.

3.1 Framework Overview

The introduced CEF framework contains two functional components: sensing coordination modules installed on the CEF BS, and end user modules added on the femto user handsets. The operation of each sensing coordination module is comprised of three main processing phases: i) proactive sensing phase, ii) sensing coordination phase, and iii) acknowledge (ACK) information adjustment phase. The operation of each end user modules is comprised of two main processing phases: i) knowledge-based estimation phase, ii) sensing under reasoning phase, iii)gossip enabled stochastic medium access phase.

The interactions between these phases are shown in Fig 3.1, where the proactive sensing phase continuously monitor reusable spectrum to collect immediate information for the sensing coordination phase. Based on the preliminary sensing results, the CEF BS instruct the femto users on which sub-band to sense in a stochastic manner so as to avoid serious interference caused by disorderly accesses to the same set of available sub-bands, as well as inner-tier interference. At the femto users, the end user modules takes advantage of both extrinsic and intrinsic knowledge about the network environments to estimate the optimal number of stand-alone sensing for feature detection based on the CEF device

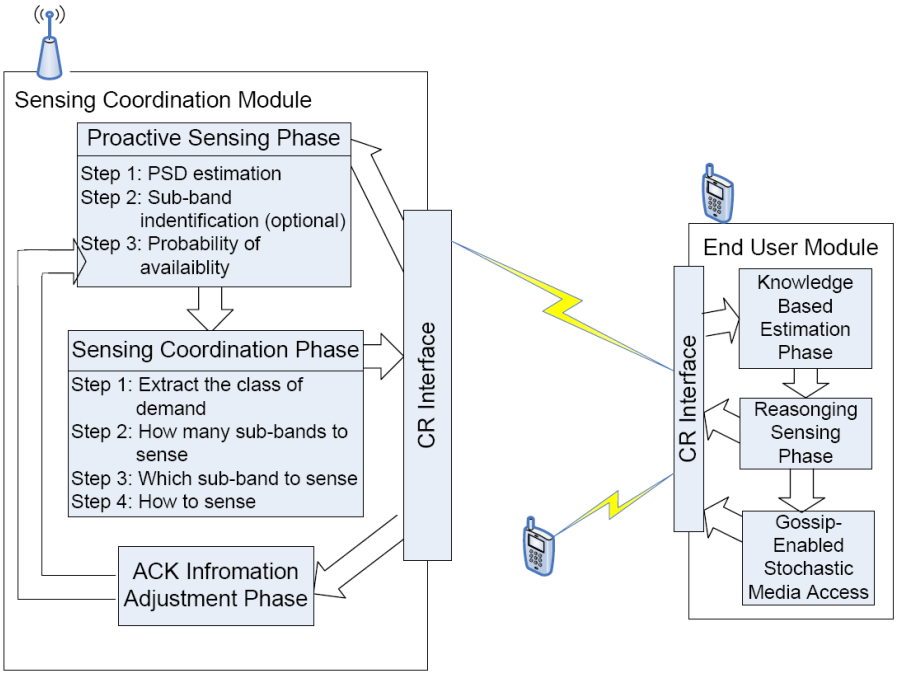

Figure 3.1: An overview of CEF framework.

instruction. An Extended Knowledge-Based Reasoning (EKBR) [18] approach is applied to sense the instructed sub-bands to further mitigate the cross- and inner-tier inference in their own communication range. The end user modules first estimate the maximum number of sensing iterations based on the received instructions and finally goes through a reasoning process to determine when to stop the sensing process and start media access. Media access process is started with gossip-enabled channel negotiation, where a set of common available channel between femto communication pairs are obtained without involving a dedicated control channel. A power controlled media access control protocol as well as build-in interference mitigation features of packet segmentation and contention resolution are applied to the femto users to achieve the media access with limited interference. As such, the network intelligence can be expanded from controlling the intelligence paradigm to better understand the satisfy femto user needs [81, 82]. Once the access to a specific set of sub-bands is commenced by the femto user, the femto user acknowledges the usage of the sub-bands. This ACK information assists the sensing coordination module to continuously monitor the spectrum to identify the macrocell user signals coming back to those sub-bands used by secondary users and reacts accordingly to instruct femto users to evacuate from those sub-bands immediately.

The detailed descriptions on each of functional components, as well as the corresponding phases are elaborated in following Chapters.

3.2 System Model

3.2.1 Network Architecture

An illustrative example of a femtocell underlay and a macrocell two-tier network architecture is shown in Fig 3.2, where different femto users operating under various wireless techniques (e.g., WiMAX, UMTS, TV broadcast, etc.) in macrocell networks may coexist within the same area, with femto BS acting as wireless service consumers installed in building complexes and densely populated neighborhoods. The femto BS are connected to the wired backhaul through a broadband gateway, such as digital subscriber line (DSL), cable, and Ethernet over the Internet to the macrocell operator network. In this two-tier network, the femto users can be viewed as the "secondary" users to the "primary" macrocell users or/and other incumbent users. Therefore, the network formed by primary users is called primary users network, while the network formed by the secondary users is called secondary users network. From this point on, secondary users and femto users will be used alternately.

3.2.2 Channel Model

In the CEF framework, femto users are allowed to access the spectrum licensed for its corresponding macrocell, named as licensed spectrum for femto users. Moreover, femto users are equipped with CR and thus can opportunistically access spectrum bands licensed for other macrocell, such as Very/Ultra High Frequency (VHF/UHF) TV bands, which will be available in the near future by CRs [83]. These spectrum are not licensed for the femtocell are named as unlicensed spectrum in this dissertation. Both licensed and unlicensed spectrum are named as reusable spectrum for femto users.

Over the reusable spectrum, there are K non-overlapping channels $\{\mathbf{C}|C_i, i = 1, 2, ..., K\}$ centered at $\{f_c^i\}_{i=1}^K$. Note that the channels $C_i, i = 1, 2, ..., K$ are not necessarily equally spaced; instead, the CR system should support channel spacings of $6, 7$ and 8 MHz, and be capable of adapting to these channel spacings accordingly [6]. Furthermore, the femtocell network has a coordination channel C_0 within the licensed spectrum, which is used

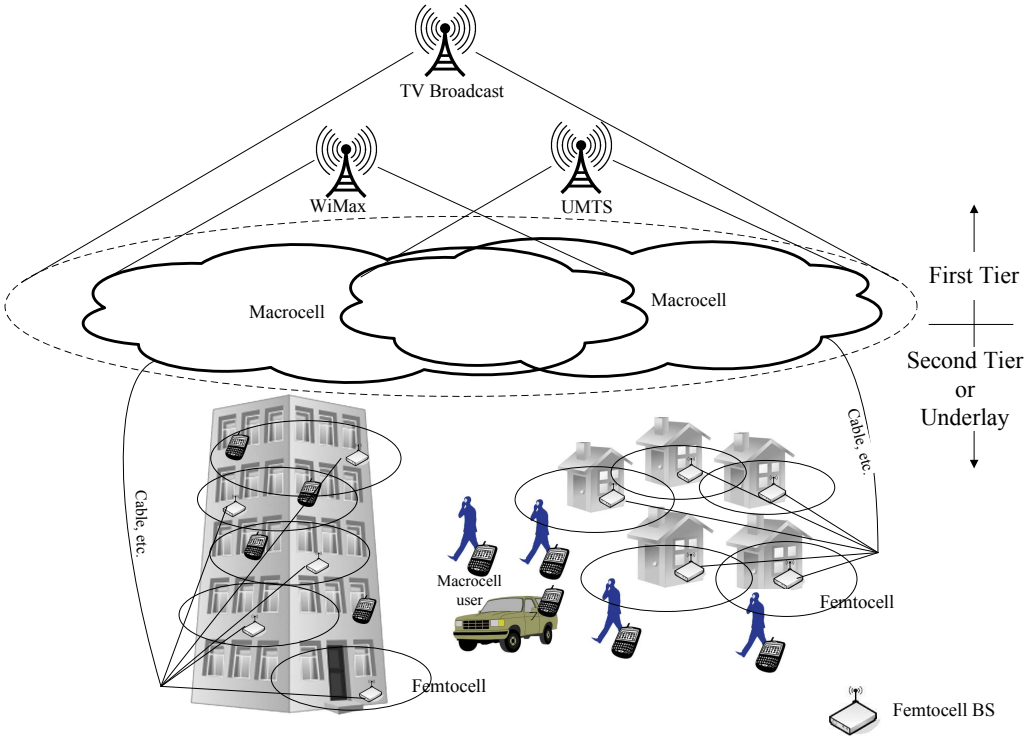

Figure 3.2: Macrocell-femtocells/primary-secondary two-tier network architecture.

to transmit control information when the secondary users require more spectrum resources (i.e., $C_i, i = 1, 2, ..., K$) beyond the capacity of their own networks.

3.2.3 Spectrum Sensing Model

Spectrum sensing in the CEF network is a key step in the interference avoidance with the primary user network. In this study, two-stage sensing that involves fast sensing and fine sensing processes are adopted. In the fast sensing, three types of primary signals over the unlicensed spectrum of the femtocell being sensed are Digital TV (DTV), Analog TV (ATV), and wireless microphone, while the primary signals over the licensed spectrum being sensed by the femto users are the their corresponding macrocell users. The DTV signals show narrow-band features on the pilot carrier f_p^i, which is located at approximately 310 kHz above the lower edge of the channel and contains about 7% of the total signal power according to Advanced Television Systems Committee (ATSC) standard. The narrow-band features of ATV signals exhibit on the video carrier f_v^i, which is located at 1.25 MHz above the lower edge of the channel and contains about half of the total signal power according to National Television System Committee (NTSC) standard. Therefore, the presence of DTV/ATV signals can be effectively identified via energy detection using a binary hypothesis test [84], where H_1 and H_0 indicate the presence and absence of primary signals, respectively. Under these two hypotheses, the received bandpass waveform on C_i at the secondary user can be represented using the model proposed in [85] as,

$$x_i(t) = \begin{cases} Re\{[h_c S_{\mathrm{LP}}(t) + w_{\mathrm{LP}}(t)]e^{j2\pi f_*^i}\}, & H_1 \\ Re\{w_{\mathrm{LP}}(t)e^{j2\pi f_*^i}\}, & H_0 \end{cases}, \tag{3.1}$$

where $i = 1, ..., K$, and $Re\{\cdot\}$ indicates the real part of a complex value, h_c is the channel impulse response, f_*^i is the feature carrier frequency, and $*$ indicates different signals. For example, $* = p$, f_p^i is the pilot carrier frequency of DTV signal on C_i; $* = v$, f_v^i is the video carrier frequency of ATV signals on C_i; $* = m$, f_m^i is the wireless microphone operational frequencies; and $* = (2)$, $f_{(2)}^i$ is the secondary user signal pilot carrier frequency if a secondary user pilot signal is used for energy detection. $S_{LP}(t)$ and $w_{LP}(t)$ refers to an equivalent low-pass representation of the DTV/ATV signal and an additive white Gaussian noise (AWGN) with zero mean and a known power spectral density (PSD) N_0, respectively. Using a band-pass filter, given the observed signal $x_i(t)$ on C_i, for $0 \leq t \leq T$, the test statistics can be expressed as

$$u_i \cong \frac{2}{N_0} \int_T x_i^2(t)dt, \tag{3.2}$$

which is a random variable with a chi-square (χ^2) distribution. Therefore, the probability density function (PDF) of u_i can be expressed as [85]

$$f(u_i) = \begin{cases} \frac{1}{2^{k_\Gamma/2}\Gamma(k_\Gamma/2)} u_i^{(k_\Gamma/2)-1} e^{-u_i/2}, & H_0 \\ \frac{1}{2} e^{-(u_i/2+\omega)} (\frac{u_i}{2\omega})^{k_\Gamma/4-0.5} J_{(k_\Gamma/2)-1}(\sqrt{2\omega u_i}), & H_1 \end{cases}, \tag{3.3}$$

where k_Γ is the degrees of freedom, ω is the instantaneous signal-to-noise ratio (SNR), Γ denotes the Gamma function, and J denotes a modified Bessel function.

For spectrum sensing under situations characterized by low SNR, it is very difficult to distinguish between a faded DTV/ATV signal and white noise. Moreover, wireless microphone signals exhibit no stable and common features due to the fact that design parameters such as operational frequencies and transmission power can vary from different wireless microphone manufacturers [84]. As shown in laboratory tests conducted by Shellhammer et al. [84], the presence of wireless microphone signals can be confused by other unknown narrow-band spikes. Therefore, the binary hypothesis may not be suitable for identifying spurious emission interferences from wireless microphone signals. This fact should be taken into consideration of the fine sensing technique design for a CR system [16], which is nonetheless beyond the scope of the study.

3.2.4 Primary User Dynamics

Due to primary user dynamics, a collision or interference occurs when a primary user signal returns to the channel that was originally identified as idle and is still being accessed by the femto user. To account for the impact of collisions or interference to the primary users, we assume the primary user's dynamics follow a M/G/1 queue model [86], where the primary users arrive on channel i according to Poisson process with rate $\lambda_i^{(1)}$, and the busy period of usage which is with an arbitrary distribution. Thus the probability of the earliest returning primary user on channel i during the transmission period of femto users can be evaluated as

$$P_{i,re} = \frac{\mathbb{I}_i^{(1)}}{\bar{t}_i} \int_0^{T_\Sigma} (1 - e^{-t/\mathbb{I}_i^{(1)}}) f_{t_i}(t) dt, \tag{3.4}$$

where $\mathbb{I}_i^{(1)}$ is the average idle period in macrocell network, $f_{t_i}(t)$ is the probability density function of femtocell user transmission time, $\bar{t}_i$ and T_Σ are the average and maximum transmission time of femtocell user, respectively.

3.2.5 Spectrum Request Arrival Model

In the secondary network, we assume that each user may issue a request to finely sense X number of channels, where X is a discrete random variable in the range $[1, \varrho]$. In other words, there are a total of ϱ classes of request that could be issued by a secondary user. In the study, the inter-arrival time of the requests in class X, denoted as T_X, is statistically modeled as a hyper-exponential distribution [87], and the PDF of T_X is given by

$$f_{T_X}(t_X) = \sum_{X=1} \varrho \lambda_X^{(2)} e^{-\lambda_X^{(2)} t_X} p_X, \tag{3.5}$$

where $\lambda_X^{(2)}$ is the mean arrival rate of class $X, m = 1, 2, ..., \varrho$, and p_X is the probability of class X. Furthermore, we assume that each class of request can be statistically modeled using a Pareto distribution, and the PDF of class of request X is given by

$$f_X(x) = \frac{k^x \{\chi^x\}^{k^x}}{x^{k^x+1}}, \tag{3.6}$$

where χ^x is a positive minimum possible value of x, and k^x is a positive parameter known as the Pareto index. What Eq. (3.6) indicates is that the probability decreases with increasing the class of requests, i.e., there is usually fewer high class of requests, which is representative of real network conditions.

3.2.6 Access Model

An Orthogonal Frequency Division Multiple Access (OFDMA) system is utilized as the underlying multiple access technique for data transmission across multiple free channels in the spectrum, as shown in Fig. 3.3. This access model is well-suited for time-slotted primary user systems, such as WiMAX, UMTS system and digital TV system. Thus, channels that are successfully identified as available will be used by the secondary users in the remaining time of the primary time slot. Furthermore, the state of channel availability is assumed to be constant within each time slot. This assumption is practical since most digital systems such as WiMAX, UMTS, and digital TV system are time-slotted systems and is widely used in sensing-based MAC protocols such in those presented in [12, 39, 64]. Moreover, in the access system, a channel is a sub-carrier in the OFDMA system and is categorized into γ different modulation schemes with corresponding data transmission rates based on the perceived signal to interference plus noise ratio (SINR) of the channel obtained through fine sensing process. A secondary collision occurs when two or more femto users within the

transmission range launch Ready-to-Send (RTS) packets in the vulnerable time, and such an event can be captured by the femto transmitters. The vulnerable time is defined as the duration in which an emitted signal can not be detected, i.e., the one-way propagation delay plus detection delay.

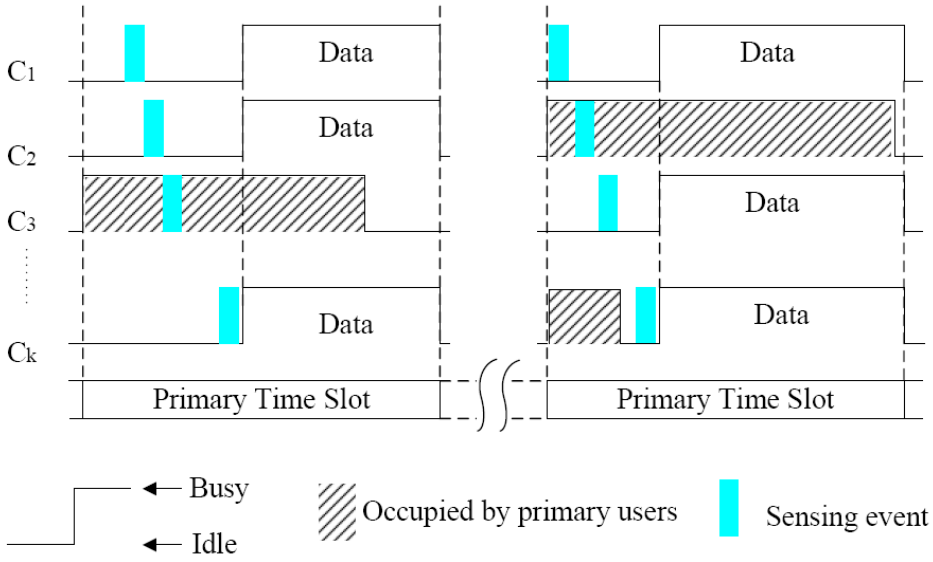

Figure 3.3: Access model.

3.2.7 Interference Model

In the interference model, any secondary transmitter must ensure that its interference power on a particular channel i added to the existing interference power $P^{I}_{i,(1)}$ at a primary receiver must not exceed the interference power limit. By assuming that the secondary transmitters operate with average power $P_{i,(2)}$, the maximum interference power at the primary receiver $P^{I,\max}_{i,(1)}$ on channel i should be satisfied by [88],

$$P^{I}_{i,(1)} + \varepsilon_i P_{i,(2)} \leq P^{I,\max}_{i,(1)}. \tag{3.7}$$

The selection of ε_i has been shown to be dependent on the distance d on channel i between the closest primary receiver and the femto transmitter, and the distribution of the corresponding minimum distance d_{min} is given by [88, 89]

$$p(d_{\min} < d) = 1 - e^{-\alpha_i \eta_i \pi d^2}, \tag{3.8}$$

where α_i is the probability of primary user transmission, and η_i is the average number of primary users per unit area. Therefore, we can get the ε_i with the interference probability from secondary transmission $\hat{p}$ with distance d under the channel fading model. Accordingly, the maximum allowable transmission power $P_{i,(2)}^{\max}$ at the femto transmitter is given by

$$P_{i,(2)}^{\max} = \frac{P_{i,(1)}^{I,\max} - P_{i,(1)}^{I}}{\varepsilon_i}. \tag{3.9}$$

Chapter 4

Sensing Coordination

The sensing coordination module equipped on the femto BS, denoted as $\aleph_c$, keeps track of *a priori* information such as feature carriers, transmission power of primary users, and the channel spacings of the frequency bands that have been deregulated by the radio regulations. To improve coordination performance over time, the sensing coordination module updates the stored *a priori* information whenever new frequency bands are deregulated and more secondary user design constraints are released. As shown in Fig. 4, the coordination node $\aleph_c$ senses the channels $C_i, i = 1, 2, ..., K$ sequentially and repeatedly in a proactive manner through the use of energy detection on feature carriers f_*^i, which is a fast and effective method for identifying the presence of the primary user signals. Upon an arrival of request X, femto user $\aleph_j$ sends a request to femto BS $\aleph_c$ on coordination channel C_0. Once $\aleph_c$ receives the request, it responds to $\aleph_j$ with coordination instructions, such as $(\mathbf{C}^*, \mathbf{\Gamma})$, which can help $\aleph_j$ to perform stand-alone fine sensing. Based on the coordination instructions, $\aleph_j$ can select the channels to be finely sensed as well as which fine sensing technique to use (e.g., energy detection or any other fine sensing technique). When $\aleph_j$ identifies an available channel(s), and decides to access this channel(s), it turns on its own pilot signal on the carrier $f_{(2)}^i$ according to the instructions. The feature signals that $\aleph_c$ sensed belongs to both primary users and femto users, but the channel usage of primary users can be differentiated from that of femto users based on differing feature carriers.

4.0.8 Proactive sensing phase

To collect information with regards to primary signal presence on channels $C_i, i = 1, 2, ..., K$, the coordination node $\aleph_c$ enters the proactive sensing phase, where fast sensing is performed

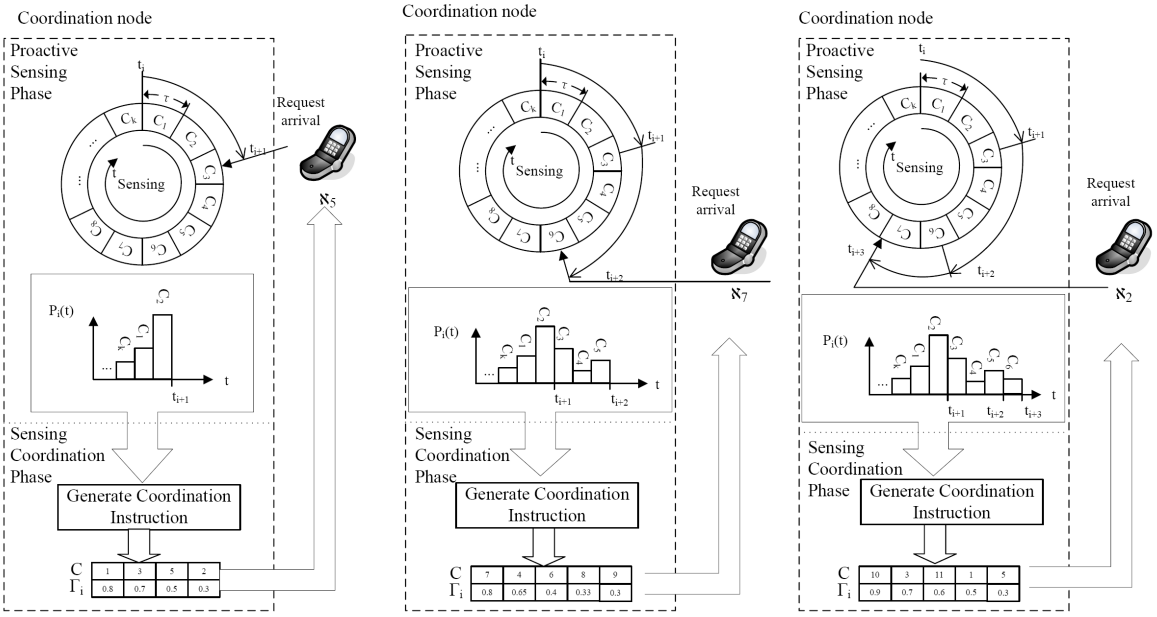

Figure 4.1: The femto BS performs proactive sensing and sensing coordination upon the request of femto users $\aleph_5$, $\aleph_7$, and $\aleph_2$ at times t_{i+1}, t_{i+2}, and t_{i+3}, respectively, the coordination nodes generates sensing coordination instructions based on sensing results up to time t_{i+1}, t_{i+2}, and t_{i+3} and sends a response containing the sensing instructions $(\mathbf{C}^*, \mathbf{\Gamma})$ back to $\aleph_5$, $\aleph_7$, and $\aleph_2$, respectively.

via energy detection. This fast sensing is effective at detecting the presence of primary user signals while remaining efficient to reduce the likelihood of interference. At $\aleph_c$, each iteration of energy detection on channel C_i provides sensing results in terms of the likelihood of channel availability, $p_i(t), i = 1, 2, ..., K$. The signals present in the channels can be issued either by primary users or secondary users. Since the feature signals of primary users are on fixed frequency carriers, the pilot signals of secondary users should be added on different carriers with enough separation such that the sensing coordination module can better distinguish whether the signal is from a primary user or a secondary user. According to the system model, there are two hypotheses H_1 and H_0, which stands for signal presence and signal absence, respectively. The probability of detecting the user presence is defined as $p_d^* = prob(u_i > \gamma_* | H_1)$ and the probability of false alarm is defined as $p_f^* = prob(u_i > \gamma_* | H_0)$, where $* = p, v, m, (2)$ indicates different signals. By comparing u_i to threshold γ_*, the sensing coordination module can estimate the likelihood of user presence. Generally, the threshold γ_* determines how sensitive the energy detection is in a fading channel environment. In other words, given a certain probability of false alarm, the probability density function of the test statistics u_i from Eq. (3.3), the user signal sampled at its Nyquist rate, and a given noise PSD model N_0, the detection threshold is given by

$$\gamma_* = N_0 B_* (1 + \frac{Q^{-1}(p_f^*)}{\sqrt{M}}), \tag{4.1}$$

where M is the number of samples, B_* is the signal bandwidth of different signals, and $Q(\cdot)$ is the Q function. The probability of detection p_d^* of different user signals can be evaluated as

$$p_{d|N_0}^* = prob(u_i > \gamma_* | H_1, N_0) = \int_{\gamma_*}^{\infty} f(u_i) du_i. \tag{4.2}$$

In a Rayleigh fading channel model, the average detection probability (i.e. the likelihood of channel availability $p_i(t)$) can be evaluated as

$$p_i(t) = p_d^* = \frac{1}{\bar{\omega}_*} \int_0^{\infty} \int_{\gamma_*}^{\infty} f(u_i) \exp(-\frac{\omega_*}{\bar{\omega}_*}) du_i d\omega_*, \tag{4.3}$$

where $\bar{\omega}_*$ is the average SNR of different signals. This result is consistent with that obtained in [85].

The sensing coordination module identifies the likely available channels and then stores the proactive sensing results for a period of time with the design constraints of system memory. In other words, the new observation results will overwrite the oldest ones as time goes by for $C_i, i = 1, 2, ..., K$. Furthermore, the observation results will be used to learn the characteristics of user behavior used in the sensing coordination phase.

4.1 Sensing coordination phase

In the sensing coordination phase, the femto BS provides instructions to femtocell users on how many channels, which sub-bands, as well as how to sense these sub-bands, in order to mitigate interference and improve the likelihood of meeting the bandwidth and tolerable sensing delay requirements, while leaving the decision on transmission rate and modulation to the femtocell users to satisfy their own requirements. This is accomplished as follows:

- **Step 1:** Based on the data transmission request of a femto user, extract the associated class X of demand, such as best effort, real-time, etc.
- **Step 2:** Stochastically determine the number of sub-bands, denoted as N^X, for femto users to sense with a probability θ^X according to a distribution $f_X(\bar{N}^X, \sigma^X)$ with mean $\bar{N}^X$ and standard deviation σ^X. Note this distribution is predetermined by the manufacturer.
- **Step 3:** Stochastically select a set of N^X sub-bands for femto users to sense and access according to the probability of sub-band availability determined in the proactive sensing phase. As such, the femto users are instructed on the most likely available sub-bands.
- **Step 4:** Amongst the set of selected sub-bands, instruct the femto users to perform only energy detection prior to access on sub-bands associated with the sensing results within the channel detection time (CDT), which is specified in IEEE 802.22 [6]. Energy detection is sufficient for these cases due to the freshness of the sensing results. For sub-bands with sensing results older than CDT, instruct the femto users to perform feature detection prior to access given the staleness of the sensing results.

It is important to note that determining the number of sub-bands in stochastic manner allows for improved fairness, thus better achieving welfare or equilibrium. Moreover, the stochastic selection of N^X sub-bands is also aimed at mitigating the inner-tier interference since the probability of femto users selecting the same sub-bands in the same order to sense is low, which is demonstrated in simulations.

4.1.1 Sensing Coordination Design

Upon a request by $\aleph_j$, the coordination node $\aleph_c$ sends the fast sensing results of instructed channels to $\aleph_j$. With the sensing results, $\aleph_j$ further identifies the presence of primary user

signals and tries to access the available channels. To account for the dynamic nature of the two-tier network, the following three environment states should be considered and included in the sensing results.

Presence/Absence of User Signals

It is intuitive that if a certain amount of energy has been detected on a feature carrier, the presence of primary and/or secondary user signals is identified with probability p_d^* given the design constraints of p_f^*. While the energy detection scheme may mistakenly observe interference as the presence of primary user signals, it is acceptable for $\aleph_c$ to set these channels as lower priority to in the sensing result distribution because the possible interference to the other secondary users should still be avoided even if the subsequent fine sensing process shows availability at those channels.

Number of Channels for Fine Sensing

In the sensing coordination phase, $\aleph_c$ provides instructions to secondary user $\aleph_j$ on how many channels, which channels, as well as how to sense these channels, in order to improve the likelihood of meeting the bandwidth and tolerable sensing delay requirements, while leaving the decisions on transmission rate and modulation to $\aleph_j$ to satisfy its own requirements. This is accomplished as follows. Based on the class X of demands, the coordination node $\aleph_c$ instructs $\aleph_j$ to sense N^X channels, where N^X is the maximum number of likely available channels that $\aleph_c$ recommends based on the X demands. Intuitively, one approach to determining number of channels for $\aleph_j, \forall j$ is to assign N^X on a first-come first-serve (FCFS) basis until all likely available channels detected by $\aleph_c$ have been distributed. This kind of greedy method has been demonstrated as an efficient way in terms of resource utilization but lacks any fairness constraints and thus makes it difficult to achieve welfare or equilibrium [90]. To achieve fairness while avoiding complexity in channel selection, $\aleph_c$ statistically assigns a number of $\{N_j^X | N_j^X \leq N^X\}$ channels with a probability θ^X. In other words, N_j^X is assigned according to a distribution $f_X(\bar{N}^X, \sigma^X)$ with mean $\bar{N}^X$ and standard deviation σ^X, where $\bar{N}_j^X$ is a function of number of channel K.

Credibility of Sensing Results due to Timeliness

The credibility of energy detection is determined by the energy detection scheme itself as well as the *timeliness* of the sensing results. The following discussion will be on the

timeliness issue only because the design of energy detection schemes is far beyond the scope of the study.

As $\aleph_c$ continuously performs energy detection on each channel $C_i, i = 1, 2, ..., K$, a sensing period is defined as $K \times \tau_d$, where τ_d is the time consumed for each energy detection. In this case, *sensing precision* could be different for each channel due to stale channel states. To characterize the problem, the study defines that the previous η set of channel states (i.e., the channels of $C_{(i-\eta) \ mod \ K}$) in the sensing result is considered reliable for $\eta = \lfloor CDT/\tau_d \rfloor$, where CDT refers to the channel detection time, and is defined as the maximum required detection time specified in IEEE 802.22 functional requirements [6] for all primary signals on TV bands.

The CDT can also be implicitly interpreted as the maximum detection delay tolerable to a primary user when secondary users are operating below the allowable Effective Isotropic Radiate Power (EIRP) on TV bands. Therefore, we suggest to take CDT as an indicator on how fresh the sensing results are, in which any sensing result falling within the window of CDT will be referred to as *CDT-fresh*. On the other hand, the sensing results outside of the CDT window are taken as *stale*. Thus, the problem of assigning channels with stale sensing results can be formulated as a prediction problem. To capture the high heterogeneity of user behavior, a two-stage hyper exponential distribution is assumed for the PDF of inter-arrival time of primary users. Denoted as $T_i^{(1)}$ on channel C_i with mean $1/\lambda_i^{(1)}$, the PDF is given by

$$f_{T_i^{(1)}}(t) = \frac{\alpha}{\alpha+1}\alpha\lambda_i^{(1)}e^{-a\lambda_i^{(1)}t} + \frac{1}{\alpha+1} \cdot \frac{\lambda_i^{(1)}}{\alpha}e^{-\frac{\lambda_i^{(1)}}{\alpha}t}, \tag{4.4}$$

where α corresponds to the user behavior with a high variability.

The reliability of the sensing results is defined as the probability that no arrival of the primary user signals within time period t can be estimated as

$$p_i^{(1)}(t) = \frac{\alpha}{\alpha+1}e^{-a\lambda_i^{(1)}t} + \frac{1}{\alpha+1}e^{-\frac{\lambda_i^{(1)}}{\alpha}t}. \tag{4.5}$$

With Eq. (4.5), $\aleph_c$ prioritizes the channels with better CDT-freshness in the sensing result distribution phase. Once all channels with CDT-fresh sensing results have been consumed, $\aleph_c$ estimates the reliability of stale sensing results associated with the remaining likely available channels based on Eq. (4.5). Considering both detection error and the reliability of stale results, the probability of selecting a channel C_i given stale results is

given by

$$\Gamma_i = \frac{w_i p_i(t) + (1 - w_i) p_i^{(1)}(t)}{\sum_{i=1}^{K} w_i p_i(t) + (1 - w_i) p_i^{(1)}(t)}, \tag{4.6}$$

where weights ω_i can be configured based on the relative importance of these two factors. Finally, the channel C_i with higher Γ_i is likely to be selected by the coordination node to the secondary user $\aleph_j$ to fine sense.

Sensing Coordination Algorithm

The sensing coordination phase is presented as follows.

if A data traffic sending request from $\aleph_j$ **then**
  Extract the class of demand;
  Find N_j^X with a probability θ_j^X following a distribution $f_X(\bar{N}^X, \sigma^X)$ with mean $\bar{N}^X$ and standard deviation σ^X. ;
  if N_j^X <=the number of channels considered to be associated with CDT-fresh sensing results **then**
    Assign N_j^X to $\aleph_j$;
  else
    Assign the number of channels considered to be associated with CDT-fresh sensing results;
    Assign the remaining requested channels according to Eq. (4.6);
  end if
end if

4.1.2 ACK information adjustment phase

In the ACK information adjustment phase, the ACK messages that are sent back to the CEF femto BS provides information with regards to which sub-bands have been used by the femto users. Therefore, based on this information, the femto BS can use the estimated signal energy of the femto users to adjust the original detection threshold to better estimate the activity of the primary users. If the primary user signal is identified on those sub-bands, the femto BS instructs the femtocell users to evacuate the sub-bands immediately to mitigate the cross-tier interference.

4.2 Performance Analysis

Performance analysis is conducted on the upper bound of the average time consumed at each femto user on sensing, denoted as $\bar{T}_s$. We focus on the analysis of upper bound of sensing overhead instead of an exact derivation of the sensing overhead because the sensing time is specific to the adopted sensing strategy, which is not applicable in this scheme. It is important to note that the actual sensing overhead relies heavily on the order in which available channels are obtained and thus is difficult to present using a theoretical model.

Given the success rate of spectrum sensing p_s, the upper bound of sensing overhead can be approximated by

$$\bar{o}^{\star} = (1 - p_s)\bar{T}_s. \tag{4.7}$$

For a femto user $\aleph_j$, the upper bound on the number of channels to sense is the number of channels N_j^X assigned according to distribution $f_X(\bar{N}^X, \sigma^X)$ by the femto BS upon each class of request, while the actual number of channels to be sensed at the femto user is not defined by any sensing strategies, as they may consider transmission rate or/and modulation to satisfy its own requirements, which will be discussed in next chapter. The assigned number of channels N_j^X consists of N_{CDT} available channels with CDT-fresh sensing results and $N_j^X - N_{CDT}$ channels selected with probability Γ_i. Therefore, for a particular class X of requests, the upper bound on the average time consumed on sensing $\bar{T}_s^X$ can be expressed as

$$\bar{T}_s^X = \tau_d \bar{N}_{CDT} + \tau_f \max\{0, \bar{N}^X - \bar{N}_{CDT}\}, \tag{4.8}$$

where τ_f are the time consumed on fine sensing, and $\bar{N}^X$ is a function of the number of channels K, $\bar{N}_j^X \sim f(K)$. The probability $p(N_{CDT} = n)$ of obtaining N_{CDT} number of channels is dependent on how many channels have been fast sensed within CDT by the coordination node during the inter-arrival time of requests. Therefore, for a particular class X of requests, the probability of obtaining number of N_{CDT} channels $p^X(N_{CDT} = n)$ can be determined as

$$\begin{aligned} & p^X(N_{CDT} = n) \\ & = \begin{cases} e^{-n\tau_d\lambda_X^{(2)}} - e^{-(n+1)\tau_d\lambda_X^{(2)}}, & 0 \le n \le \min\{\eta, K\} - 1 \\ e^{-n\tau_d\lambda_X^{(2)}}, & n = \min\{\eta, K\} \end{cases}, \end{aligned} \tag{4.9}$$

where $\eta = \lfloor CDT/\tau \rfloor$. The average number $\bar{N}_{CDT}$ is thus given by

$$\begin{aligned} \bar{N}_{CDT} \quad = & \sum_{n=0}^{\min\{\eta,K\}-1} n(e^{-n\tau_d\lambda_X^{(2)}} - e^{-(n+1)\tau_d\lambda_X^{(2)}}) \\ & + \min\{\eta, K\} e^{-\min\{\eta,K\}\tau_d\lambda_X^{(2)}}. \end{aligned} \tag{4.10}$$

Substituting Eq. (4.10) into Eq. (4.8), we obtain the complete expression of the upper bound of average time consumed on sensing for a particular class X of requests. Since it is a function of K, by removing the condition on a particular X class, the approximated upper bound of sensing time is given by

$$\bar{T}_s(K) = \sum_X p_X \bar{T}_s^X, \tag{4.11}$$

where p_X is probability of class X with distribution given by Eq. (3.6)Therefore, we can obtain the upper bound of sensing overhead by applying Eq. (4.7). This approximation will be verified through simulations.

4.3 Performance Evaluation

Simulations were conducted to evaluate the effectiveness of the proposed sensing coordination scheme in order to evaluate its sensing accuracy, network-wide efficiency, and fairness. Quantitative comparisons were made between the proposed coordination scheme, stand-alone, as well as cooperative spectrum sensing approaches. The following four performance metrics are taken into consideration as they provide direct indication of spectrum sensing performance:

- Success rate of spectrum sensing, p_s.
- Sensing overhead, o.
- Probability of sensing conflict, Υ.
- Temporal usage rate, R_u.

4.3.1 Success Rate

In this set of simulations, we compared the success rate of spectrum sensing, p_s, achieved by the proposed sensing coordination scheme with a state-of-the-art stand-alone stochastic channel prioritization approach [35], as well as statistical cooperative approach [32]. The success rate of spectrum sensing of each secondary node $\aleph_j, j = 1, 2, ...$ associated with the proposed coordination scheme was measured and is expected to provide a clear indication of spectrum sensing accuracy and fairness. The success rate of spectrum sensing, p_s, can

be defined as the ratio between the number of successfully identified channels n_{ava} and the number of actual sensed channels N_s, which is designed to capture the sensing accuracy of a spectrum sensing at each individual secondary user.

$$p_s = \frac{n_{ava}}{N_s}. \tag{4.12}$$

We compare the sensing accuracy of proposed coordination scheme with the stand-alone sensing approach by observing arbitrary $N_{(2)} = 5$ number of femto users, with $\varrho = 5$ different classes of requests and associated different secondary user signal arrival rates $\lambda_X^{(2)} = \{10^{-2}, 10^{-1}, 10^0, 10^1, 10^2\}$, as well as different primary user signal arrival rates $\lambda_i^{(1)} = \{10^{-3}, 10^{-2}, 10^{-1}, 10^0, 10^1, 10^2, 10^3\}$ randomly assigned over the K channels with primary user behavior variability factor $\alpha = 2$. The average success rates of spectrum sensing $\bar{p}_s$ of each observed individual secondary user $\aleph_j$ are shown in Fig. 4.2. It can be observed that the proposed coordination scheme outperforms the stand-alone approach in terms of the success rate of spectrum sensing. It thanks to the *a priori* information used in the coordination process.

Moreover, it can be observed that each node in the network has almost consistent success rates of spectrum sensing while those utilizing the stand-alone approach have a relatively large deviation in comparison. The reason for this is that, in the stand-alone approach, a femto user with a poor statistical understanding of the network environment, due to factors such as not having enough timely observations, would result in a poor channel selection for spectrum sensing.

The impact of average speed is shown in Fig. 4.3 with $K = 5$. It can be observed that the average success rate by the proposed sensing coordination scheme slightly decreases as $\bar{v}$ increases in the scenarios. Nevertheless, the average success rates of the proposed sensing coordination scheme in are noticeably higher than that by the non-coordination approach and the statistical cooperative scheme.

4.3.2 Sensing overhead

The second set of simulations evaluates the sensing overhead associated with the proposed sensing coordination scheme, which is defined as the total time the femto users $\aleph_j$ spent on sensing unavailable channels based on the obtained sensing instructions:

$$o = \bar{\Sigma}_d + \bar{\Sigma}_f \tag{4.13}$$

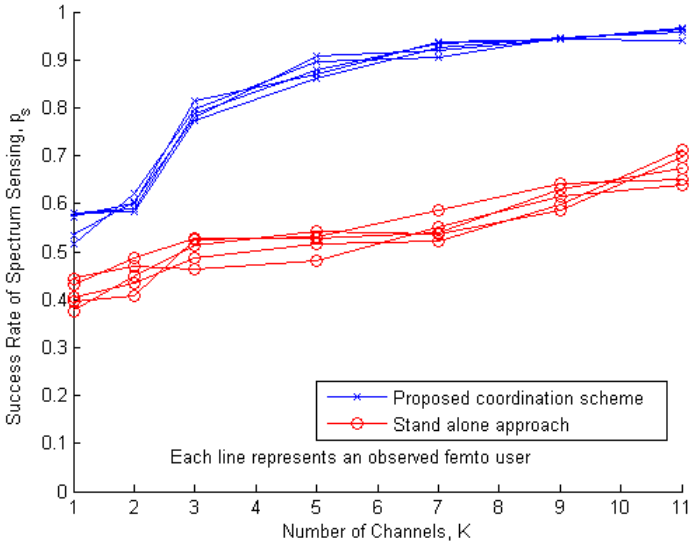

Figure 4.2: Success rate of spectrum sensing with different number of channels.

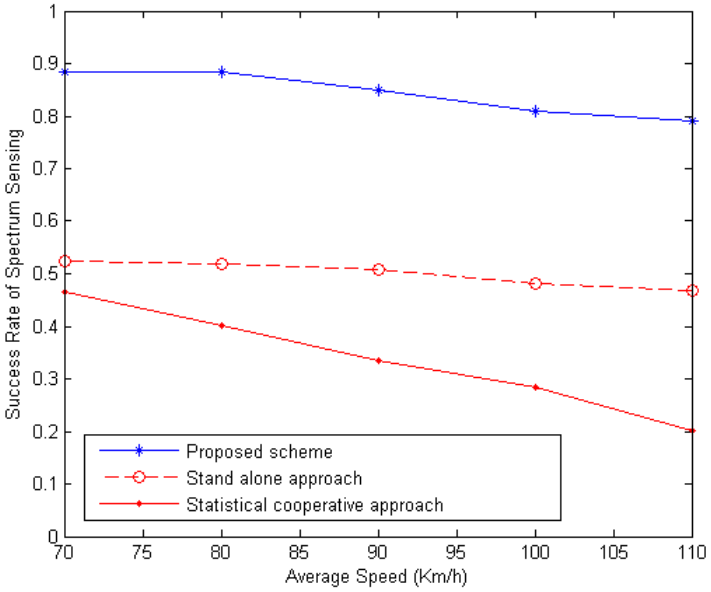

Figure 4.3: Average success rate vs. different average speed.

where $\bar{\Sigma}_d$, and $\bar{\Sigma}_f$ are the total time consumed on energy detection and fine sensing at the femto users, respectively. In Fig. 4.4, the average sensing overhead o of the proposed sensing coordination scheme is compared with the one in [35] and the state-of-the-art cooperative approach [32]. A peak of sensing overhead occurs at $K = 2$. This peak is due to the fact that, the above mechanism does not noticeably show improvement under situations characterized by very limited resources, since all channels are required to sense for every node. Therefore, going from one channel to two channels result in an increase in overhead. However, as the number of channels increases beyond this point, there are more opportunities for the femto BS to assign different channels with higher probability getting CDT-fresh available channels. As expected, the sensing overhead associated with the proposed sensing coordination scheme is noticeably lower than both the stand-alone and cooperative non-coordination approaches. This is due to the fact that the femto users in the proposed sensing coordination scheme only need to fast or/and finely sense a smaller number of channels based on the coordination instructions from the coordination node.

Finally, we validate the developed analytical model by making a comparison between the simulation and analytical results, as shown in Fig. 4.4. It can be observed that the simulation results are lower than that obtained by the developed analytical upper bound of average sensing overhead. This is due to the fact that the sensing process stops when the required number of available channels are identified in the simulation, while in the analytical model the sensing order of available channels is unknown. The difficulty in modeling the order of available channels is also the reason that the gap between analytical results and simulation results increases when K increases. However, this analytical upper bound is lower than other approaches, and more importantly its shape is very close to that by simulation, thus validating the developed analytical model.

4.3.3 Probability of Sensing Conflict

The third set of simulations evaluates the probability of sensing conflict in the proposed coordination scheme, which is the probability of having more than one femto user that identify the same available channels. In such a circumstance, competition for medium access could arise, which leads to interference among equal-tier femto users. The probability of sensing conflict, denoted as Υ, is also a direct performance measure on the proposed sensing coordination scheme, which can be defined as the ratio of the number of available common channels n_{com} sensed by more than one femto user in the secondary network to

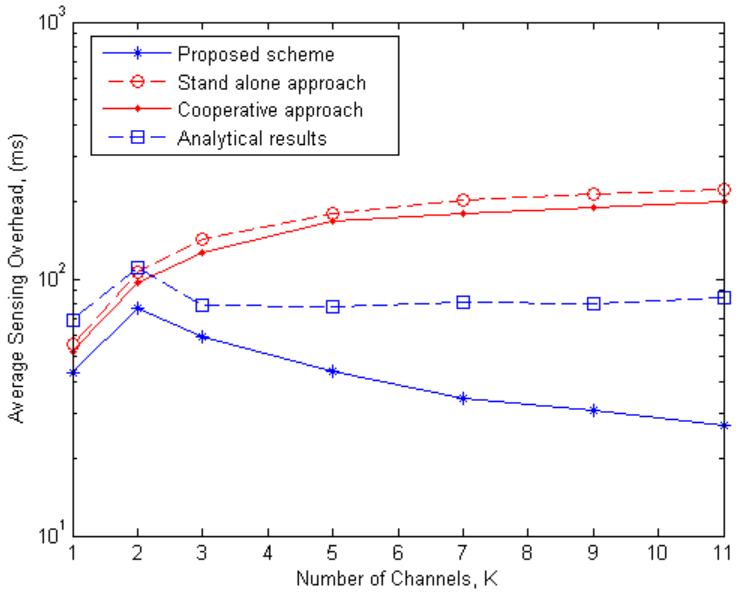

Figure 4.4: Average sensing overhead vs. different number of channels, K.

the total number of different channels Σ_s sensed by the same set of femto users,

$$\Upsilon = \frac{n_{com}}{\Sigma_s} \tag{4.14}$$

In Fig. 4.5, the probability of sensing conflict Υ in proposed coordination scheme and the stand-alone sensing approach in [35] is compared with the number of channels being set to $K = 5$. As expected, the proposed sensing coordination scheme yields smaller Υ, which is slowly increased as the number of secondary users $N_{(2)}$ increases. The results demonstrate the improved sensing efficiency that can be achieved through the use of the proposed coordination scheme.

4.3.4 Temporal Usage Rate

In this set of simulations, we investigate the scenario where homogeneous class of request is set, such that each channel has the same statistical characteristics (e.g., the primary user arrival rate $\lambda_i^{(1)}$ for each channel is identical), and the primary user behavior with low variability $\alpha = 1$. Such scenario settings facilitate the evaluation on how Λ, $\lambda^{(2)}$, as well as the number of femto users impact on the network-wide performance. We are interested in the temporal usage rate R_u, which is defined as the percentage of unoccupied time on

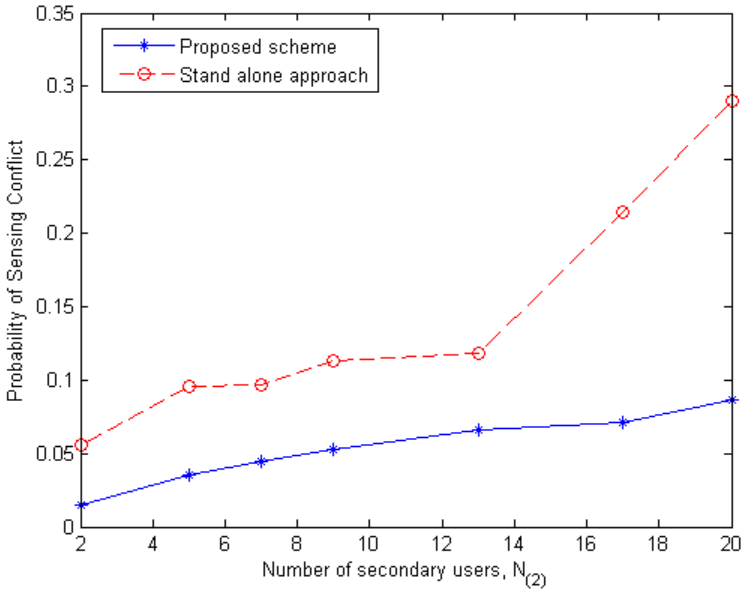

Figure 4.5: Probability of sensing conflict vs. different number of secondary users, $N_{(2)}$.

channels used by the secondary users $\aleph_j, j = 1, 2, ...$ The temporal usage rate R_u can be expressed as

$$R_u = \sum_{i=1}^{K} T_i \Big/ \sum_{i=1}^{K} T_i^{ava}, \tag{4.15}$$

where T_i is the time used on available channel C_i, T_i^{ava} is the available time on channel C_i.

Although mainly focusing on spectrum sensing, this work implements a channel access mechanism in the set of simulations to examine the temporal usage rate metrics. In order to reduce the impact of channel access mechanism, small message sizes are considered so that RTS/CTS handshake is not involved, which is similar to the access mechanism in IEEE 802.11 specification for small message sizes. Fig. 4.6 shows the temporal usage rate R_u in the proposed coordination scheme with different femto user signal arrival rate $\lambda^{(2)}$, primary user signal arrival rate Λ, as well as different numbers of femto users in a single channel primary user network. It can be observed that the temporal usage rate R_u is not sensitive to Λ but increases with the increase of both $\lambda^{(2)}$ and the number of femto users. The relative independency of R_u from Λ is a promising feature that demonstrates scalability of the proposed sensing coordination scheme.

To further evaluate the network-wide temporal efficiency, we compare the proposed scheme with one of the stand-alone spectrum sensing approaches in [35] in terms of the

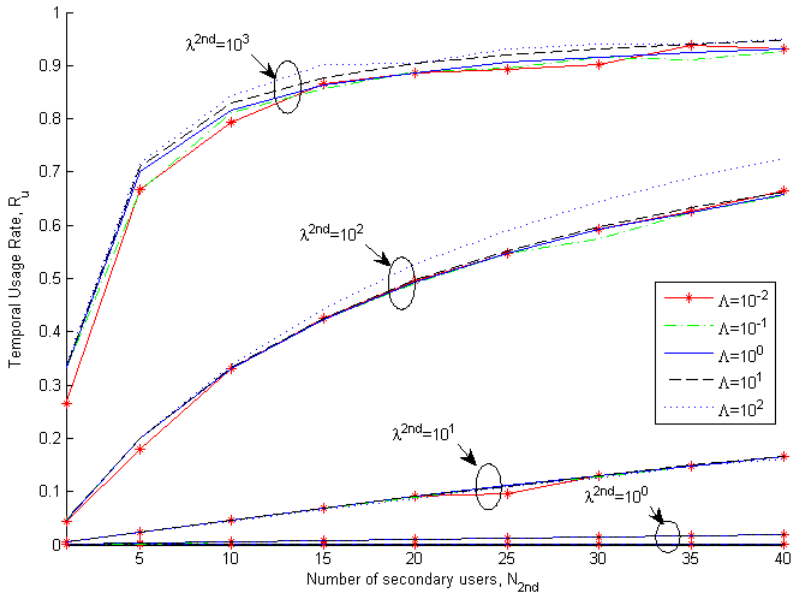

Figure 4.6: Temporal usage rate of the proposed coordination scheme with different femto user signal arrival rate $\lambda^{(2)}$, primary users signal arrival rate Λ, as well as different number of femto users $N_{(2)}$ in a single channel primary users network.

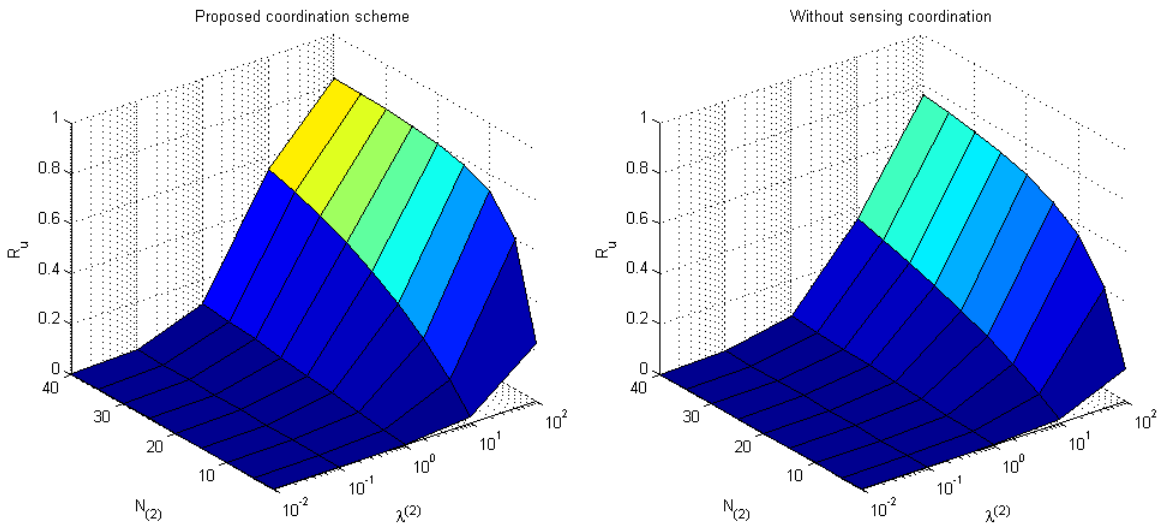

Figure 4.7: Network-wide temporal usage rate with fixed $\Lambda = 10^0$, and different $\lambda^{(2)}$ and $N_{(2)}$.

temporal usage, which is shown in Fig. 4.7. It can be observed that the temporal efficiency in the proposed scheme is noticeably higher due to the improved sensing accuracy. The femto BS $\aleph_c$ instructs the most likely available channels for femto users $\aleph_j$ based on *a priori* channel information obtained from its fast sensing results given in Eq. (4.3) and reliability given in Eq. (4.5). Moreover, we further consider a multichannel scenario with fixed $N_{(2)} = 40$, and the simulation results are plotted in Fig. 4.8. These results demonstrate the effectiveness of the proposed scheme at providing improved spectrum sensing accuracy and efficiency.

4.4 Summary

In this chapter, a novel information-adaptive sensing coordination scheme is proposed for CEF femto BS. The proposed scheme takes the best of the two conventional spectrum sensing architecture (i.e., stand-alone and cooperative), while mitigating their respective disadvantages, which aims to achieve better sensing accuracy, efficiency and fairness than the conventional approaches. By utilizing *a priori* information such as feature carriers, channel spacing of frequency bands, proactive fast sensing information, as well as user-based class information, the proposed coordination scheme provides intelligence in channel selection of spectrum fine sensing for secondary users. Experiment results show that the

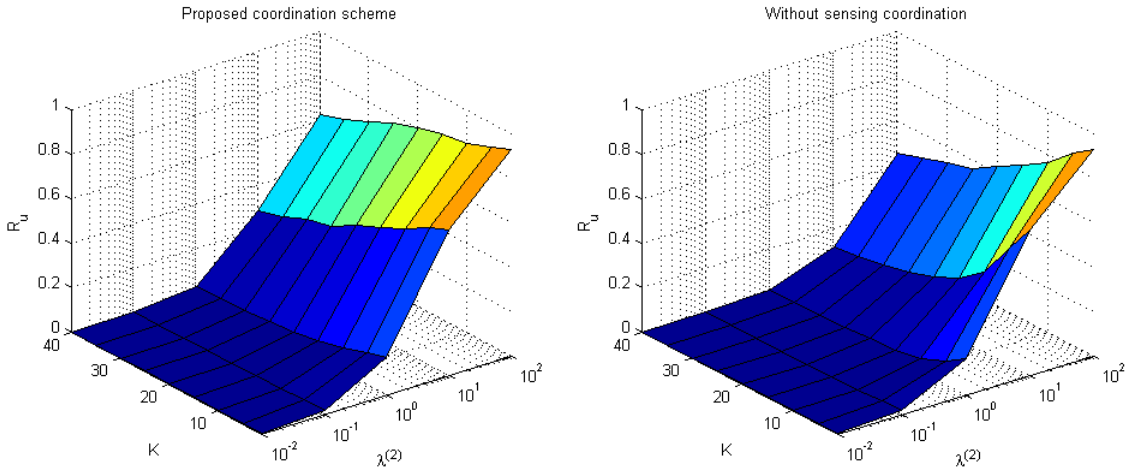

Figure 4.8: Network-wide temporal usage rate with fixed $N_{(2)} = 40$, and different number of channels K and $\lambda^{(2)}$.

proposed coordination scheme for spectrum sensing can solidly outperform the previously reported stand-alone and cooperative sensing approaches in terms of a number of important performance metrics under the highly dynamic environments.

Chapter 5

Sensing with Extended Knowledge-Based Reasoning

In this chapter, a spectrum sensing in MAC layer for CEF end user module applied on femto users, called Extended Knowledge-Based Reasoning (EKBR) [18], is proposed to answer some of the critical questions, such as when to start and stop the spectrum sensing and what strategy to take in the data transmission and rate selection so that an individual CR can get the channels that optimally fit its desired performance requirements.

The EKBR scheme takes advantage of both intrinsic and extrinsic knowledge about network states and environments to both prioritize channels and estimate the optimal range of radio spectrum to finely sense as well as dynamically refine the amount of fine sensing to achieve the desired performance requirements of the users while minimizing service processing time. The new features of the proposed EKBR scheme are summarized as follows. First, the EKBR scheme jointly considers short-term statistical information, data transmission rate information, and contention characteristics as priors to facilitate the estimation of optimal range of channels for fine sensing. Second, the EKBR scheme takes advantages of a knowledge-based channel prioritization strategy based on short-term statistical information and fast sensing results to further enhance spectrum sensing efficiency.

Performance analysis is conducted on the proposed EKBR scheme using a multi-dimensional absorbing Markov chain to evaluate various performance metrics of interest, such as average sensing delay, and average data transmission rate. Numerical results show that the proposed EKBR scheme achieves better performance when compared to existing techniques by balancing trade-offs between performance and complexity.

5.1 Proposed Spectrum Sensing Scheme

The proposed spectrum sensing scheme can be described as follows. Upon the request of data transmission, a femto user $\aleph_j$ acquires an sensing instruction from femto BS. After the femto user $\aleph_j$ obtain the coordination instruction $(\mathbf{C}^*, \mathbf{\Gamma})$, it retrieves the short-term statistics of channel sequence $(\mathbf{C}^*)$, i.e., $\hat{P}_s(C_1^*)$,$\hat{P}_s(C_2^*)$,...,$\hat{P}_s(C_{N_j^X}^*)$, which are obtained in a short time scale τ_s. The sensing prioritization process is performed for fine sensing based on the statistical likelihood of channel availability by jointly exploiting short-term statistics and instructed information $\mathbf{\Gamma}$. The details of the sensing prioritization process can be found in [32, 35]. Based on results of the sensing prioritization process, $\aleph_j$ estimates the number of prioritized channels for fine sensing by comprehensively considering the short-term statistics, data transmission rate information, and contention characteristics, which is then used as the upper bound of the fine sensing process in order to secure at minimum the slowest required data transmission. Finally, fine sensing is performed according to the prioritized sensing results in a dynamic manner, where the fine sensing process is adaptively terminated based on additional prior knowledge, such as instantaneous channel quality information determined by actual fine sensing process, to satisfy the necessary performance requirements while minimizing sensing overhead. The short-term statistics used in the system, knowledge-based estimation process, as well as the reasoning approach of the proposed EKBR spectrum sensing scheme are further elaborated in the following sections.

5.1.1 Short-term Statistics

The short-term statistics are used to estimate the likelihood of channel availability at time instance ζ based on a short observation window of previous τ_s seconds. The use of short-term statistics of channel behavior is motivated by previous work demonstrating that channel availability demonstrate patterns can be modeled using a statistical approach [91, 92]. In the proposed EKBR scheme, each femto users maintain the observations for channel C_i^* $\Omega_i^{\tau_s} = \{\omega_i(\tau_1), \omega_i(\tau_2), ..., \omega_i(\tau_n)\}$, which represents the observations of primary user channel occupancy as successfully identified by the femto user. Based on Ω_i^{τ}, assuming that the observations are independent and identically distributed (i.i.d.) with a Poisson distribution during previous τ_s as not to lose generality, the arrival rate of primary users $\hat{\lambda}_i^{(1)}$ on C_i^* can be estimated as

$$\hat{\lambda}_i^{(1)} = \sum_{t=\tau_1}^{\tau_n} \omega_i(t)/\tau_s. \tag{5.1}$$

Therefore, based on $\hat{\lambda}_i^{(1)}$, the short-term statistics of availability of the instructed channel $\hat{P}_s(C_i^*)$ based on the observations over previous τ_s can be estimated as

$$\hat{P}_s(C_i^*) = 1 - \int_0^{\tau_s} \hat{\lambda}_i^{(1)} e^{-\hat{\lambda}_i^{(1)} t} dt. \tag{5.2}$$

5.1.2 Knowledge-based Estimation

During the fine sensing process, $\aleph_j$ senses a set of prioritized channels $\Theta = \{C_{(1)}, C_{(2)}, ...\}$ based on the descending order of the short-term statistics obtained in Eq. (5.2) to identify the availability of a channel as well as the underlying channel conditions. $\aleph_j$ continues to perform the fine sensing process from one channel to another until sufficient channels for data transmission are found. It is observed that as the number of channels sensed is increased, the likelihood of obtaining channels with better quantity and quality is increased. This results in an improved data transmission rate and thus higher data throughput. Unfortunately, sensing too many channels during the fine sensing process results in significantly increased overall processing time T_Σ, and consequently decreased throughput ρ, which is defined as $\rho = L_p/T_\Sigma$, where L_p is the length of the data packet (frame). Furthermore, a long fine sensing process increases the likelihood of unsuccessful transmissions within the primary time slot and lost opportunities due to the time-sensitive nature of spectrum sensing. Hence, the optimal number of channels to be finely sensed should be determined in such a way that the total processing time T_Σ is minimized. Furthermore, by minimizing T_Σ, the throughput ρ is effectively maximized. The knowledge-based estimation on n^* for determining the number of channels to be finely sensed can be formulated as

$$n^* = \arg\min_n \{T_\Sigma | T_\Sigma = n\tau_f + \frac{L_p}{\bar{R}} + \Delta t + T_b\} \tag{5.3}$$

where τ_f is the time consumed by each fine sensing iteration, Δt is the processing time of the proposed scheme and other time consumed by the system, T_b is the back-off time determined by back-off mechanism during channel access, and $\bar{R}$ is the expected basic data transmission rate obtained in n iterations fine sensing. The basic data transmission rate R_k can be determined based on the information rate of modulation symbols N_ξ, number of available channels k obtained by $\aleph_j$ after performing the fine sensing process for n iterations, and sample time t_s. We note that N_ξ is dependent on the channel quality, i.e., a bigger SINR suggests a better quality channel so that a faster modulation scheme can be used. However, at this estimation stage, no fine sensing process is involved so that $\aleph_j$ is not able to determine the modulation schemes. If taking Binary Phase Shift Keying

(BPSK) as the slowest modulation scheme at the estimation stage in the OFDMA system, it can be expressed as [93]

$$R_k = \frac{N_1 k}{t_s}, \tag{5.4}$$

where N_1 is the information rate of BPSK. $\aleph_j$ will refine the decision on modulation schemes on the fly at the reasoning stage.

It can be observed that the number of identified available channels k is highly dependent on the channel availability and the estimated n iterations of fine sensing. The channel availability of a channel, which is prioritized as $C_{(i)}$, at time instance ζ is estimated by using Eq. (5.2) during the short-term observation. By using this prior information, the probability representing the short-term likelihood of $C_{(i)}$ being available with respect to the other channels at time instance ζ is normalized as

$$\bar{P}_s(C_{(i)}) = \hat{P}_s(C_{(i)})/n, \tag{5.5}$$

and the aggregate probability that the channel $\{C_{(i)}, \forall i\}$ is not available is normalized as

$$\bar{P}'_s = \frac{1}{n}\sum_{i=1}^{n}[1 - \hat{P}_s(C_{(i)})]. \tag{5.6}$$

With probability $\bar{P}_s(C_{(1)})$, $\bar{P}_s(C_{(2)})$,...,$\bar{P}_s(C_{(n)})$ and $\bar{P}'_s$ so that $\sum_{i=1}^{n}\bar{P}_s(C_{(i)}) + \bar{P}'_s = 1$, the fine sensing of n channels (where each iteration of sensing involves the sensing of a single channel) resulting in k identified available channels follows a multinomial distribution [94]. Since the number of outcomes on $C_{(i)}, i = 1, 2, ..., n$ can be observed at most once over n fine sensing iterations, for the purpose of notation simplification, let the random variable x_i represent the i^{th} identified available channel found over the n iterations based on the channel prioritization results. The probability mass function of $i = k$ with parameters n and $\bar{\mathbf{P}}$, where $\bar{\mathbf{P}} = (\bar{P}_s(C_{(1)}), ..., \bar{P}_s(C_{(n)}), \bar{P}'_s)$, is therefore given by

$$\begin{aligned} &f(k; n, \bar{P}_s(C_{(1)}), ..., \bar{P}_s(C_{(i)}), \bar{P}'_s) \\ &= \tfrac{n!}{(n-k)!}\prod_{i=1}^{n}\bar{P}_s(CH_{s_i})^{I(i)}\bar{P}_s'^{(n-k)} \end{aligned} \tag{5.7}$$

where indication function is defined as

$$I(i) = \begin{cases} 1 & C_{(i)} = x_i \\ 0 & C_{(i)} \neq x_i \end{cases} \tag{5.8}$$

By averaging k, the expected basic data transmission rate of is given by

$$\begin{aligned}\bar{R} &= \int_0^n f(k; n, \bar{P}_s(C_{(1)}), ..., \bar{P}_s(C_{(i)}), \bar{P}'_s) R_k dk \\ &= \sum_{k=0}^{n} \left[\frac{N_1 k}{t_s} \cdot \frac{n!}{(n-k)!} \prod_{i=1}^{n} \bar{P}_s(C_{(i)})^{I(i)} \bar{P}_s'^{(n-k)} \right]\end{aligned} \tag{5.9}$$

Substituting Eq. (5.9) into Eq. (5.3), $\aleph_j$ can then estimate the number of channels that should be finely sensed.

5.1.3 Fine Sensing Under Reasoning

Although the estimated number of channels n^* to be finely sensed is estimated, simply performing fine sensing n^* iterations on the channels given by the channel prioritization process could still be an expensive process. Note that a lengthy sensing process could lead to unsuccessful channel access due to the dynamic nature of channel conditions. To improve sensing efficiency while maintaining the desired transmission rate, the EKBR scheme introduces an extended knowledge-based reasoning approach that takes advantage of additional prior knowledge such as instantaneous channel quality information to dynamically terminate the fine sensing process. With the proposed reasoning approach, the $\aleph_j$ has the intelligence and knowledge necessary to determine whether the fine sensing process should be terminated.

The proposed reasoning approach under EKBR can be explained using a "seashell collection" analogy described as follows. Suppose that a person walks along a beach, looking for seashells to collect. When the person comes upon a seashell, he or she can either collect the seashell or not. For any seashell that is not collected, it will never be considered again. Further, the person knows little about the type of seashell he or she will come upon next nor does he or she knows how far to walk to come upon the next seashell as the tide may either wash a seashell ashore or away at any time. Hence, the person needs to decide whether to pick up and collect an encountered seashell based on limited observations and knowledge after each step.

In the case of EKBR, the person is analogous to $\aleph_j$, the seashells are taken as spectrum resources, and the tide is analogous to the dynamic nature of channel availability. To decide whether the next channel is finely sensed, $\aleph_j$ evaluates the possible outcomes prior to the next fine sensing iteration. Each spectrum fine sensing iteration will either find an available channel or not. Either of the outcomes imposes a profound influence on the subsequent fine sensing iterations. If $\aleph_j$ decides to sense the next channel and find an

available channel, the aggregate data transmission rate is increased based on Eq. (5.4), which may increase the success probability in data transmission within the remaining time in the primary time slot. However, if the $\aleph_j$ decides to proceed the next iteration and, unfortunately, fails in finding any available channel, the time spent in the iteration is totally wasted, which decreases the success probability in data transmission within the remaining time. Therefore, the reasoning approach should be designed at each iteration of fine sensing based on whether or not $\aleph_j$ can gain better success probability of data transmission by continuing finely sensing the next channel. If there is no any marginal return by performing the next iteration of fine sensing, the fine sensing process should be terminated, and $\aleph_j$ should immediately start the channel access and subsequent data transmission by using the currently collected channels.

Mathematically, X_i is denoted as a spectrum offer at the i^{th} fine sensing, which is a set of identical and independent random variables with a cumulative distribution function (CDF) F, which is known as the *profile function* of the spectrum. The net spectrum offer return $Y_{(i)}$ at the i^{th} fine sensing step is given by

$$Y_{(i)} = \sum_{i=1}^{i} X_i - iC \qquad 0 < i < n^*, \tag{5.10}$$

C is the cost associated with each fine sensing. Therefore, the expected return of the next move $Y_{(i+1)}$ is given by

$$\begin{aligned} E[Y_{(i+1)}] &= \hat{P}_s(C_{(i)}) \left[\sum_{i=1}^{i+1} X_i - (i+1)C \right] \\ &+(1 - \hat{P}_s(C_{(i)})) \left[\sum_{i=1}^{i} X_i - (i+1)C \right] \qquad 0 < i < n^*. \end{aligned} \tag{5.11}$$

$\aleph_j$ continues finely sensing the next channel as long as the following condition is satisfied:

$$E[Y_{(i+1)}] > Y_{(i)} \qquad 0 < i < n^*. \tag{5.12}$$

Eq. (5.12) is equivalent to

$$\hat{P}_s(C_{(i)})X_{i+1} - C > 0 \qquad 0 < i < n. \tag{5.13}$$

What Eq. (5.13) means is that any additional fine sensing should provide a certain desired marginal return. If the required return cannot be obtained, the reasoning process of EKBR

terminates the fine sensing process. One possible definition of the cost is the time consumed on each fine sensing iteration, i.e., τ_f, and the spectrum offer, X_i, is the saved time through increased data transmission rate, i.e., $(L_p/R_{(i)} - \tau_f)N_1/t_s/R_{(i)}$. Therefore, Eq. (5.13) can be rewritten with respect to time as

$$\frac{L_p}{R_{(i)}} > \frac{L_p}{R_{(i)} + \frac{N_1}{t_s}\hat{P}_s(C_{(i)})} + \tau_f \quad 0 < i < n^*. \tag{5.14}$$

where $R_{(i)}$ is the aggregate data transmission rate after i^{th} fine sensing, and it is determined adaptively on channel quality by $\aleph_j$ based on SINR level through fine sensing. This channel quality information is taken into account by classifying the individual channels into γ modulation class with corresponding spectrum sensing thresholds to further aid in the decision-making process. This prior knowledge of network states can further aid $\aleph_j$ determine whether to continue fine sensing on the next channel by comparing the expected throughput gained in the next move with present throughput; therefore, $R_{(i)}$ can be rewritten as $R_{(i)} = \sum_i N_\xi^{(i)}/t_s$, where $N_\xi^{(i)}$ is the i^{th} N_ξ. Eq. (5.14) can be interpreted as that any additional fine sensing should only be performed if it can compensate for the additional fine sensing time cost τ_f through increased data transmission rates by taking the slowest modulation. Eq. (5.14) serves as the 'reasoning' process, by which $\aleph_j$ determines whether to proceed with additional fine sensing efforts in an attempt to achieve the desired throughput.

5.2 Performance Analysis

For the purpose of performance analysis, the proposed EKBR scheme is modeled as a multi-dimensional absorbing finite Markov chain process [95], where the average transmission delay and resultant average data transmission rate are evaluated by solving the formulated Markov chain. Because each fine sensing iteration only scans one channel, there is at most one channel that could possibly be identified as available and labeled with a certain class ξ among γ classes according to SINR level when $\aleph_j$ decides to proceed to the next fine sensing iteration. Once a channel is labeled, the channel state will not be changed during the remaining time in the primary user time slot. In such primary systems, the secondary users can either detect and then use the time slots that are not assigned to the primary users or use up the remaining time in the time slot that have already been assigned to the primary users but is not being used up by the primary users. We denote $\eta_\xi, (\xi = 1, 2, ..., \gamma)$ as the number of available channels of class ξ collected at the i^{th} fine sensing. Hence, the

transition state space S consists of a set of integers $\{\eta_1, \eta_2, ..., \eta_\gamma\} : \sum_{\xi=1}^{\gamma} \eta_\xi = k$, and the number of mutually exclusive states is denoted as $\Phi = \sum_{k=0}^{k} \begin{pmatrix} k+\gamma-1 \\ k \end{pmatrix}$. Furthermore, there are Φ absorbing states $\Re$ associated with all the transition states. This is due to the fact that the fine sensing process could terminate at any state and then enter the corresponding absorbing state if $\aleph_j$ decides not to proceed. Hence, both transition state space S and absorbing state space $\Re$ form a γ-dimensional absorbing Markov chain with a finite set of 2Φ mutually exclusive states. The probability that a process moves from state S_i to S_j is only determined by state S_i.

Based on the above descriptions, the objectives of the performance analysis are formulated as follows:

1. To evaluate the conditional probability that the fine sensing process enters state S_j, given that it is leaving state S_i.

2. To evaluate the average number of transitions that remain in a particular active state before absorption. Using this information, the average number of reasoning iterations required by the fine sensing process before terminated as well as the average overall delay due to the fine sensing process and data transmission can be evaluated, respectively.

3. To estimate the probability that the process is stopped at an absorbing state, which can facilitate the evaluation of average data transmission rate.

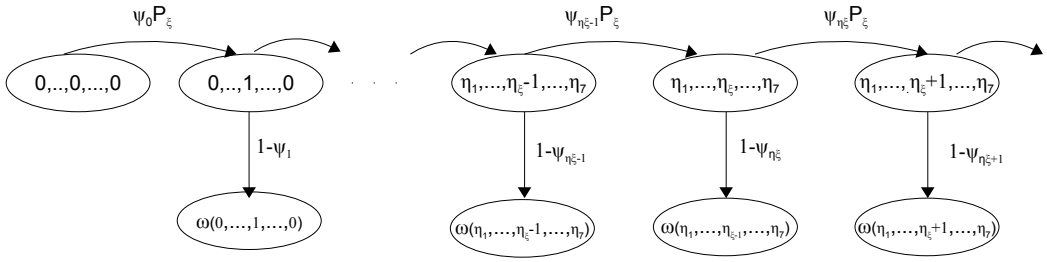

Figure 5.1: A cross-section of multi-dimensional absorbing Markov chain.

A cross-section of the γ-dimensional Markov chain is shown in Fig. 5.1. For ease of presentation, we will first describe a one-dimensional Markov chain case. Each reasoning

iteration of fine sensing will result in either: i) an increment on η_ξ, or ii) no available channel. We have the transition probabilities $P_{(\eta_1,\eta_2,...,\eta_\xi,...,\eta_\gamma)(\eta_1,\eta_2,...,\eta_\xi+1,...,\eta_\gamma)}$ that represent the cases of gaining channel, $P_{(\eta_1,\eta_2,...,\eta_\xi,...,\eta_\gamma)(\eta_1,\eta_2,...,\eta_\xi,...,\eta_\gamma)}$ that represent the cases of getting no channel, and $P_{(\eta_1,\eta_2,...,\eta_\xi,...,\eta_\gamma)(\varpi(\bullet))}$ that represent the cases of stopping fine sensing to enter the corresponding absorbing state $\varpi(\bullet) = \varpi(\eta_1, \eta_2, ..., \eta_\xi, ..., \eta_\gamma)$. Upon each reasoning iteration, the CR decides whether or not to continue the fine sensing toward the next iteration. If it decides to continue, there is a probability that an available channel of certain quality is obtained. Therefore, the transition probability $P_{(\eta_1,\eta_2,...,\eta_\xi,...,\eta_\gamma)(\eta_1,\eta_2,...,\eta_\xi+1,...,\eta_\gamma)}$ and $P_{(\eta_1,\eta_2,...,\eta_\xi,...,\eta_\gamma)(\eta_1,\eta_2,...,\eta_\xi,...,\eta_\gamma)}$ are determined by two factors: i) the probability ψ_{η_ξ} that the femto user decides to continue the fine sensing process based on the proposed reasoning approach, and ii) the probability P_ξ of getting channels of class ξ. Therefore, we have the following expression:

$$P_{(\eta_1,...,\eta_\xi,...,\eta_\gamma)(\eta_1,...,\eta_\xi+1,...,\eta_\gamma)} = \psi_{\eta_\xi} P_\xi \tag{5.15}$$

where ψ_{η_ξ} is determined by how likely the inequality (5.14) holds, which can be expressed as

$$\begin{aligned} \psi_{\eta_\xi} &= P\left(\frac{L_p}{R_{(i)}} > \frac{L_p}{R_{(i)} + \frac{N_1}{t_s}\hat{P}_s(C(i))} + \tau_f\right) \\ &= P\left(R_{(i)} < \sqrt{\frac{N_1 L_p}{\tau_f t_s}\hat{P}_s(C_{(i)}) - \left[\frac{N_1}{2t_s}\hat{P}_s(C_{(i)})\right]^2} - \frac{N_1}{\varrho}\hat{P}_s(C(i))\right) \end{aligned} \tag{5.16}$$

Then, the probability of entering the absorbing state is

$$P_{(\eta_1,...,\eta_\xi,...,\eta_\gamma)(\varpi(\bullet))} = 1 - \psi_{\eta_\xi}. \tag{5.17}$$

The probability P_ξ of getting channels of class ξ is determined by SINR level. The probability that the femto user decides to continue for the next reasoning iteration but eventually gets no available channel, is formulated as

$$P_{(\eta_1,...,\eta_\xi,...,\eta_\gamma)(\eta_1,...,\eta_\xi,...,\eta_\gamma)} = \psi_{\eta_\xi} P_{-\xi}, \tag{5.18}$$

where $P_{-\xi}$ is the probability of the noise that is not in any range of class ξ, which means the channel is not available.

While the description of the one-dimensional Markov chain case is useful for illustrative purposes, it is insufficient for modeling the proposed scheme because there are γ possible classes for channel quality. Therefore, to consider all the γ classes of channel qualities in the performance analysis, a γ-dimensional Markov chain is developed as follows. The

transition probabilities as listed in objective (1) are as follows:

$$
\begin{aligned}
&P_{(\eta_1,\eta_2,...,\eta_\xi,...,\eta_\gamma)(\eta_1+1,\eta_2,...,\eta_\xi,...,\eta_\gamma)} = \psi_{\eta_1,\eta_2,...,\eta_\xi,...,\eta_\gamma} P_1 \\
&P_{(\eta_1,\eta_2,...,\eta_\xi,...,\eta_\gamma)(\eta_1,\eta_2+1,...,\eta_\xi,...,\eta_\gamma)} = \psi_{\eta_1,\eta_2,...,\eta_\xi,...,\eta_\gamma} P_2 \\
&... \\
&P_{(\eta_1,\eta_2,...,\eta_\xi,...,\eta_\gamma)(\eta_1,\eta_2,...,\eta_\xi+1,...,\eta_\gamma)} = \psi_{\eta_1,\eta_2,...,\eta_\xi,...,\eta_\gamma} P_\xi \\
&... \\
&P_{(\eta_1,\eta_2,...,\eta_\xi,...,\eta_\gamma)(\eta_1,\eta_2,...,\eta_\xi,...,\eta_\gamma+1)} = \psi_{\eta_1,\eta_2,...,\eta_\xi,...,\eta_\gamma} P_\gamma \\
&P_{(\eta_1,\eta_2,...,\eta_\xi,...,\eta_\gamma)(\eta_1,\eta_2,...,\eta_\xi,...,\eta_\gamma)} = \psi_{\eta_1,\eta_2,...,\eta_\xi,...,\eta_\gamma} P_{-\xi} \\
&P_{(\eta_1,\eta_2,...,\eta_\xi,...,\eta_\gamma)(\varpi(\bullet))} = 1 - \psi_{\eta_1,\eta_2,...,\eta_\xi,...,\eta_\gamma} \\
&\text{where} \\
&\psi_{\eta_1,\eta_2,...,\eta_\xi,...,\eta_\gamma} = P\left(R_{(i)} < \sqrt{\tfrac{N_1 L_p}{\tau_f t_s}\hat{P}_s(C_{(i)}) - \left[\tfrac{N_1}{2t_s}\hat{P}_s(C_{(i)})\right]^2} - \tfrac{N_1}{t_s}\hat{P}_s(C_{(i)}) \right)
\end{aligned}
\qquad . \tag{5.19}
$$

One possible approach in solving the γ-dimension Markov chain is to project it into 2-dimensional space so as to allow the problem to be solved using a wider range of approaches. In this study, we put all possible γ-dimension states into a canonical form, and the resultant transition probability $\mathbf{P}$ can be arranged as follows:

$$
\mathbf{P} = \begin{array}{c} \\ TR. \\ ABS. \end{array} \begin{array}{c} \begin{array}{cc} TR. & ABS. \end{array} \\ \begin{pmatrix} \mathbf{Q} & \mathbf{R} \\ \mathbf{0} & \mathbf{I} \end{pmatrix} \end{array} \tag{5.20}
$$

where

1. $\mathbf{Q}$ is a $\Phi \times \Phi$ matrix, whose elements are the transitional probabilities between non-absorbing states;
2. $\mathbf{R}$ is a $\Phi \times \Phi$ matrix, whose elements are the probabilities from transient state S_i to the absorbing states;
3. $\mathbf{0}$ is a $\Phi \times \Phi$ zero matrix;
4. $\mathbf{I}$ is a $\Phi \times \Phi$ identity matrix.

The fundamental matrix $\mathbf{N}$ for $\mathbf{P}$ can be defined as follows:

$$
\mathbf{N} = (\mathbf{I} - \mathbf{Q})^{-1}, \tag{5.21}
$$

The entry n_{ij} of $\mathbf{N}$ gives the expected number of times that the process enters the transient state S_j if it starts in the transient state S_i. The fundamental matrix $\mathbf{N}$ possesses many interesting properties, with which we can obtain the results listed in the objectives. The following theoretical results are thus obtained to fulfill the objectives of the performance analysis:

1. The conditional probabilities of objective (1) are given by Eq. (5.19).

2. The average number of iterations that the sensing process is in state S_j given that it starts in state S_i is given by the elements of the fundamental matrix $\mathbf{N}$. The expected steps to absorption given that the chain starts in state S_i is given by

$$\vec{\Delta} = \mathbf{N}\vec{c}, \tag{5.22}$$

   where $\vec{c}$ is an all "1" column vector. Here, the first element Δ_0 is of particular interest since it represents the average number of steps taken before the fine sensing being terminated. Using this information, we can estimate the average sensing delay as

$$\bar{T}_s = t\Delta_0. \tag{5.23}$$

3. Let $\mathbf{B}$ be the absorption probabilities with entries b_{ij}, which states an absorbing chain will be absorbed if it starts in the transient state S_i. Then the $\Phi \times \Phi$ matrix can be defined as

$$\mathbf{B} = \mathbf{NR}, \tag{5.24}$$

   The probabilities b_{0j} of absorption in state S_j, starting from the initial state, can be obtained from the first row of matrix $\mathbf{B}$. The average data transmission rate is then determined as

$$\bar{R}^* = \sum_{(\eta_1,\eta_2,\ldots,\eta_\gamma)\in S} [b_{(0)(\eta_1,\eta_2,\ldots,\eta_\gamma)} \sum_{\xi=\gamma}^{\gamma} \frac{\eta_\xi N_\xi}{t_s}]. \tag{5.25}$$

5.3 Numerical Results

A series of simulations were conducted to evaluate the efficiency of the proposed EKBR scheme, where the performance of the proposed scheme was compared with a number of previously reported schemes, such as the spectrum sensing approach without the use of reasoning, as well as the state-of-the-art stopping algorithm proposed in [39].

Table 5.1: Relationship between SINR and information rate of different modulation schemes.

SINR (dB)	Information rate of different modulation Scheme, N_s , (bits/channel)
<0	0[1]
0-5	0.5
5-8	1
8-12	1.5
12-15	2
15-18	3
18-23	4
>23	4.5

[1] This channel cannot be used to carry data signals.

The simulations of the proposed EKBR scheme, along with the other sensing schemes under consideration, were evaluated via an event-driven simulation program written in C++. The Distributed Coordination Function (DCF) was used as the underlying MAC protocol in a multichannel environment to achieve channel access. Each spectrum sensing event is triggered by the arrival of a femto user data transmission request. Observations are made at randomly selected femto users placed over the network. The analytical results were calculated using MATLAB. The parameters adopted in the simulation is summarized as follows. The symbol size t_s of the OFDMA system is set as 0.31 ms [64], and the fine sensing time for each channel is set as 92.5 ms [96]. The time window for obtaining the short-term statistics was set to $\tau_s = 1000\ ms$. The data length is assumed to be uniformly distributed from 0 to 2048 bytes based on IEEE 802.16-2001 and IEEE 802.11 specifications. The individual channels are classified into γ channel quality classes along with the corresponding spectrum sensing thresholds. Each of the γ SINR levels is obtained by assuming the maximum transmitting power for each transmission, where a femto user can select an appropriate modulation scheme corresponding to the SINR level. The transmission rates in terms of bits per symbols and the corresponding SINR taken in the numerical analysis are summarized in Table 5.1 [93, 97]. The relationship may vary according to the underlying specification or modulation technology.

The performance measurements are defined as follows:

- Data transmission rate, R_j: the aggregate data transmission rate when fine sensing process terminated at j^{th} iteration.
- Percentage of missed spectrum opportunities, θ_m: the ratio between the number of missed available channels and the number of actual available channels to be finely sense.
- Sensing overhead, o: the ratio of total time consumed on spectrum sensing to the data transmission time.
- Throughput, ρ: the ratio of data packet (frame) length to the overall process time, i.e., the amount of data bits transmitted every second.

5.3.1 Data Transmission Rate

In this set of simulations, we compare the performance of the proposed EKBR scheme with the other schemes under consideration in the study using the data transmission rate, R_j. The statistical results pertaining to the simulated data transmission rate with the proposed EKBR scheme, where Eq. (5.14) is used, and the non-reasoning approach, where the fine sensing process is statically performed for all n^* channels, as well as the stopping algorithm are showed in Fig. 5.2. The statistical results consists of the minimum (min), mean, median, maximum (max), and standard deviation (std) of the data transmission rate. It can be observed that the non-reasoning approach is able to achieve higher overall data transmission rates than that achieved by both the EKBR scheme and the stopping algorithm. This is due to the fact that the femto user perform lengthy sensing so that it has higher probability of getting more available channels. It can be also observed that the overall data transmission rate, R_j, achieved using EKBR is comparable to that obtained by using the stopping algorithm. The data transmission rate is an important measurement for evaluating the performance of EKBR; however, it is important not to jump to a conclusion based on a single measurement of performance.

5.3.2 Percentage of Missed Spectrum Opportunities

To provide a good indication of spectrum sensing efficiency, we evaluate the percentage of missed spectrum opportunities θ_m associated with the proposed EKBR scheme in this set of simulations. Comparison are made with the non-reasoning approach and the stopping algorithm in Fig. 6.7. It can be observed that the EKBR scheme is in general subject

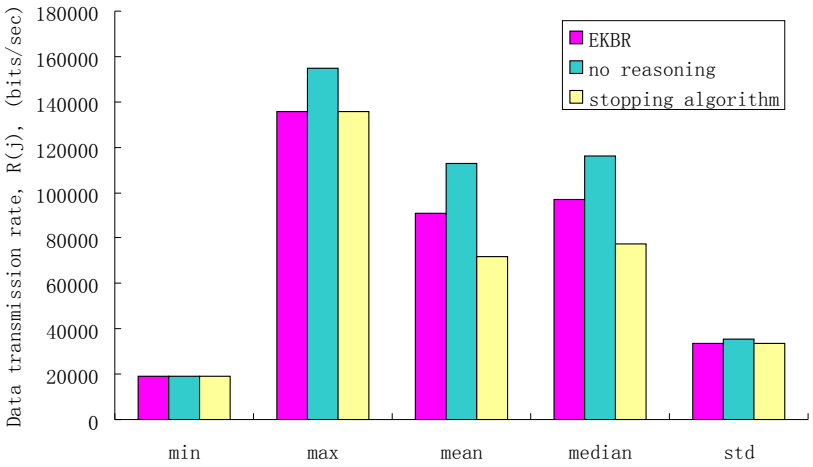

Figure 5.2: Statistics pertaining to data transmission rate comparison between EKBR, non-reasoning approach, and the stopping algorithm.

to lowest missed spectrum opportunities when compared to the other tested spectrum sensing schemes. In Fig. 5.4, the statistics pertaining to the percentage of missed spectrum opportunities show that the proposed EKBR scheme showed improvements of 42% and 34% in terms of missed spectrum opportunity reduction when compared to the non-reasoning approach and the stopping algorithm respectively. This reduction in the missed spectrum opportunities can be contributed to the fact that the EKBR scheme jointly considers fast sensing results obtained from coordination instruction. and short-term statistical information to further enhance the selection of optimal range of channels for fine sensing. These experimental results demonstrate the effectiveness of the proposed EKBR scheme in providing improved spectrum sensing accuracy and efficiency.

5.3.3 Sensing Overhead

To investigate the tradeoff between the projected data transmission rate and sensing time, we compare the sensing overhead of the proposed EKBR scheme with the sensing overhead of the non-reasoning approach. The reason for not comparing the stopping algorithm is that EKBR has a fundamental difference with the stopping algorithm, where fine sensing process is artificially and statically truncating to K stages. Therefore, it is difficult to compare the sensing overhead between these schemes in this set of simulations.

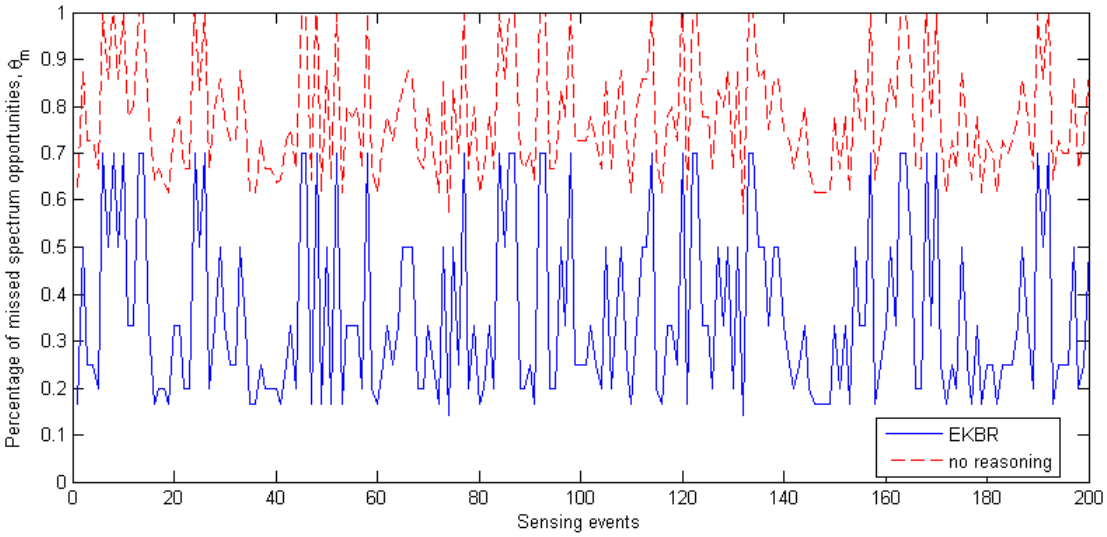

(a) EKBR vs. no reasoning.

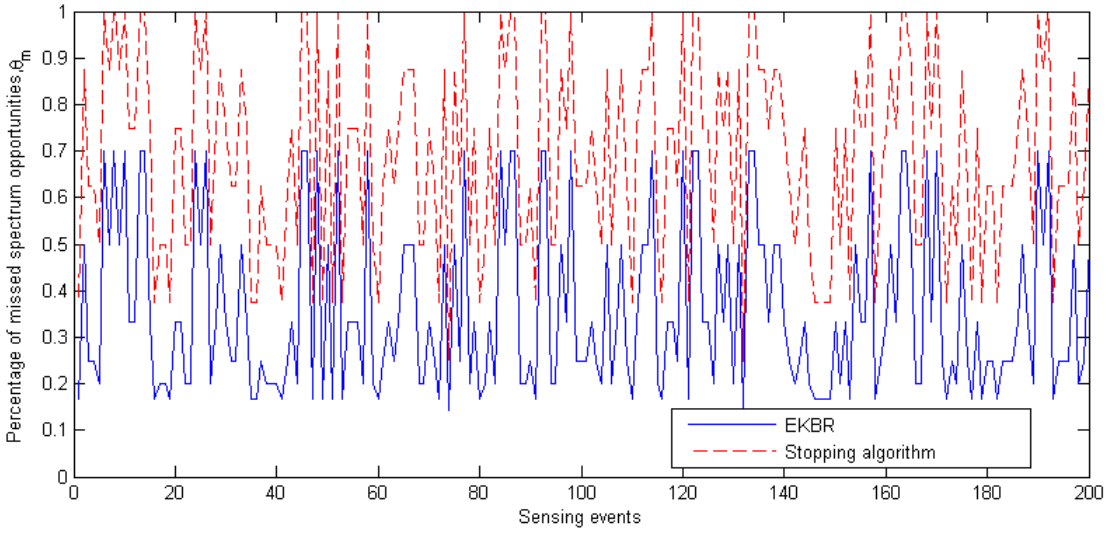

(b) EKBR vs. stopping algorithm.

Figure 5.3: Simulation results of percentage of missed spectrum opportunities in comparison.

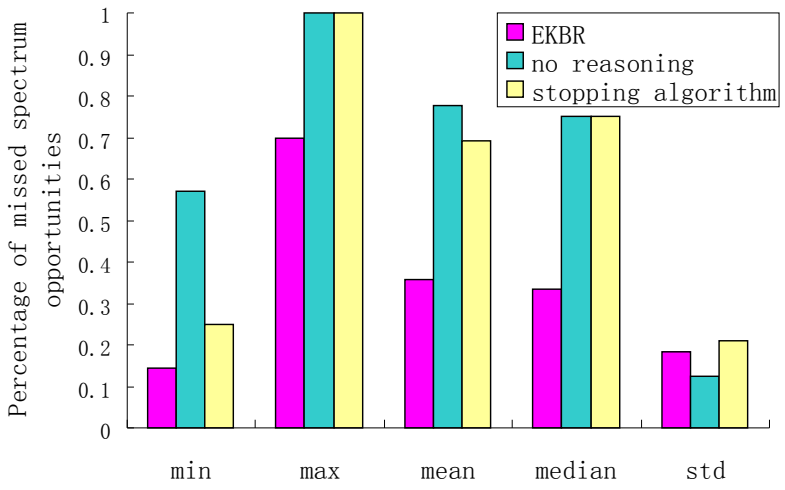

Figure 5.4: Statistics pertaining to percentage of missed spectrum opportunities between EKBR, non-reasoning approach, and the stopping algorithm.

In Fig. 5.5, the statistics pertaining to the sensing overhead o for both the EKBR scheme and the non-reasoning approach are plotted. It can be observed that EKBR has significantly reduced overall sensing overhead when compared with the non-reasoning approach. Furthermore, Fig. 5.6 shows the simulation results on the estimated iterations of fine sensing under different channel conditions as determined by short-term statistics in Eq. (5.2). It can be observed that the estimated iterations of fine sensing is significantly reduced as the channel condition improves. This is because the femto user only needs to finely sense a small number of channels until the transmission requirement is satisfied. Therefore, by intelligently reducing the number of channels for being finely sensed, the proposed EKBR scheme can achieve lower overhead by better saving sensing time and consumed energy. In addition, as the data length for transmission is increased, the femto user has to finely sense more channels so as to improve the likelihood of getting better channels in terms of quantity and quality, and in turn to ensure successful data transmission.

5.3.4 Throughput

In this set of simulations, we further compare the performance of the proposed scheme with other sensing approaches under consideration in the study using throughput, ρ, as shown in

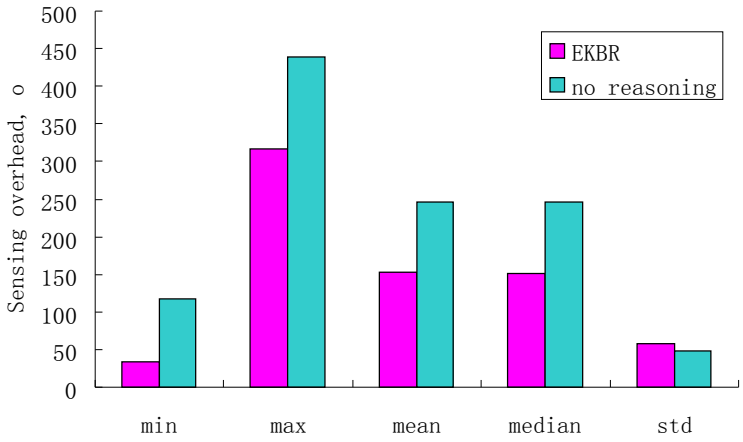

Figure 5.5: Statistics pertaining to sensing overhead comparison between EKBR and the non-reasoning approach.

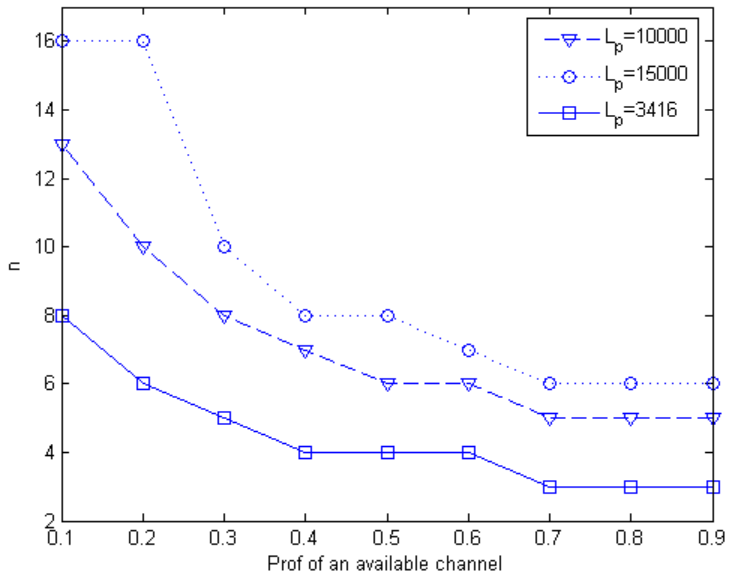

Figure 5.6: Relationship between estimated fine sensing number and the channel condition.

Fig. 5.7. It can be observed that while the data transmission rate, Rj, of the non-reasoning approach is higher than EKBR, the overall throughput is significantly higher for EKBR than the non-reasoning approach, as demonstrated in Fig. 5.7(a). This is because finely sensing all the n^* channels takes more than twice as much time in fine sensing as that by EKBR. The much longer fine sensing time for each data transmission dramatically impairs the throughput although the data transmission rate of identified channels could be higher. In Fig. 5.7(b), it can be observed that the data transmission rate of EKBR is also noticeably improved when compared to that obtained by using the stopping algorithm, while performing fine sensing on much fewer channels. This is because EKBR takes advantage of prior knowledge of network states to intelligently prioritize channels and locate a spectrum range for fine sensing that can help the femto user capture the pattern of channel variation. Therefore, in spite of comparable data transmission rates, the proposed EKBR scheme has achieved better throughput than the stopping algorithm as shown in Fig. 5.7. Without using any prior knowledge of channel states, on the other hand, the stopping algorithm can less likely ensure that the qualities of channels identified in the fine sensing process will stay static and realizable in the subsequent data transmission stage.

To further compare EKBR with the other sensing approach, Fig. 5.8 shows the simulation results on the average throughput of these schemes with respect to the increasing primary traffic volume Λ in the whole network (measured in packet arrival rate). First of all, we found that the sensing efficiency of each scheme in terms of average throughput is sensitive to the network load. It can be observed that the average throughput of EKBR decreases much slower than that by the stopping algorithm of $K = 5, 10$, and that by the non-reasoning approach, when the traffic volume Λ of the network increases.

5.3.5 Average Data Transmission Rate & Average Sensing Delay

In this set of simulations, we validate the developed analytical model in Section 5.2 by making a comparison between the simulation and analytical results in terms of the average data transmission rate $\bar{R}^*$ and the average sensing delay, $\bar{T}_s$. The analytical and simulation results on the average data transmission rate in the case where the EKBR operates in a low traffic volume scenario at $\Lambda = 10^{-1}$ packet/sec and high traffic volume scenario at $\Lambda = 10^3$ packet/sec are shown in Fig. 5.9 with the 93% confidence interval. A number of observations can be made as follows. Firstly, the simulation and analytical results closely match with each other in both of the traffic volume scenarios, which validated the proposed analytical model. Secondly, in the scenario of a higher traffic volume scenario, the average data transmission rate increases until the estimated number of fine sensing (i.e., n^*) reaches

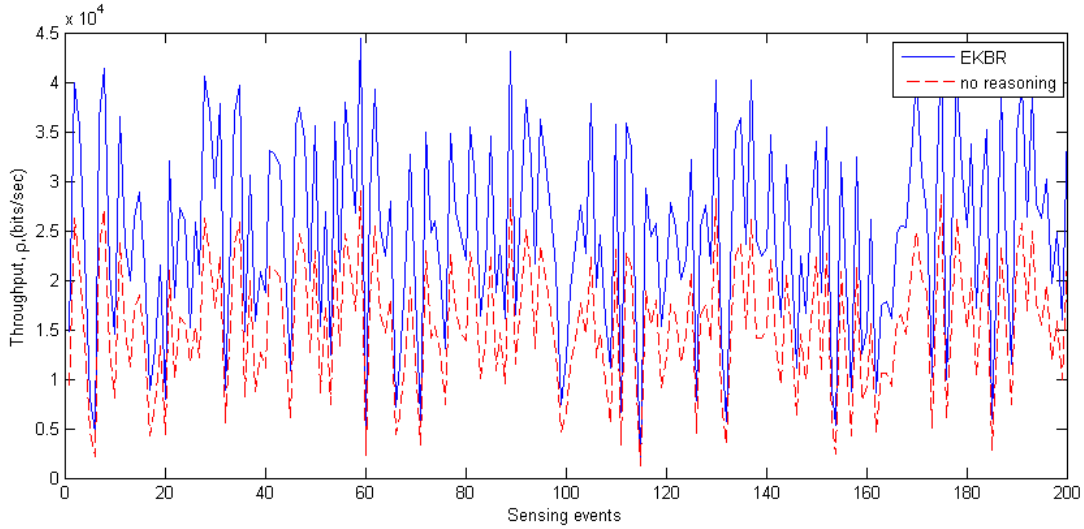

(a) EKBR vs. no reasoning.

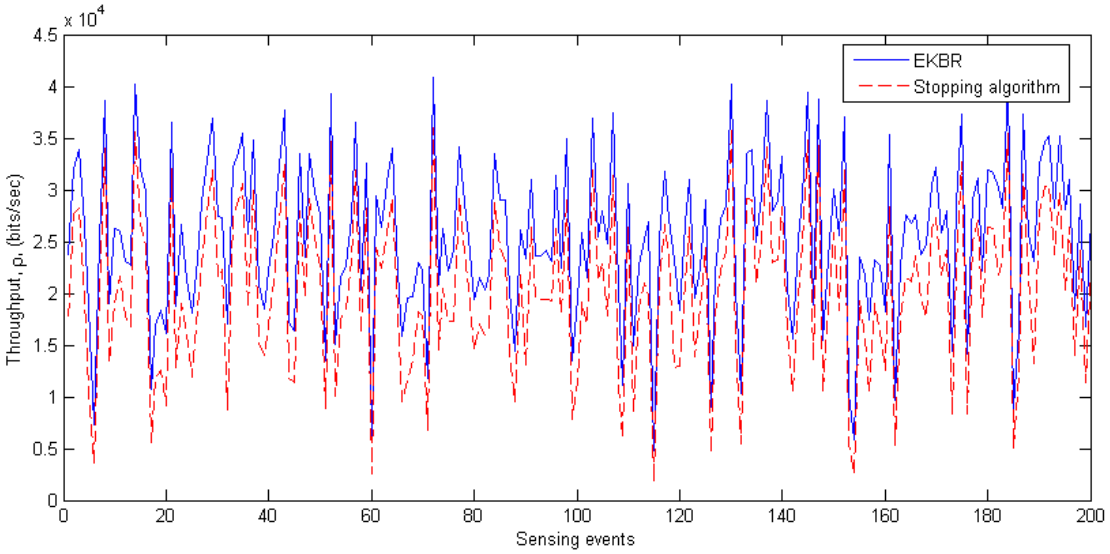

(b) EKBR vs. stopping algorithm.

Figure 5.7: Simulation results of throughput in comparison.

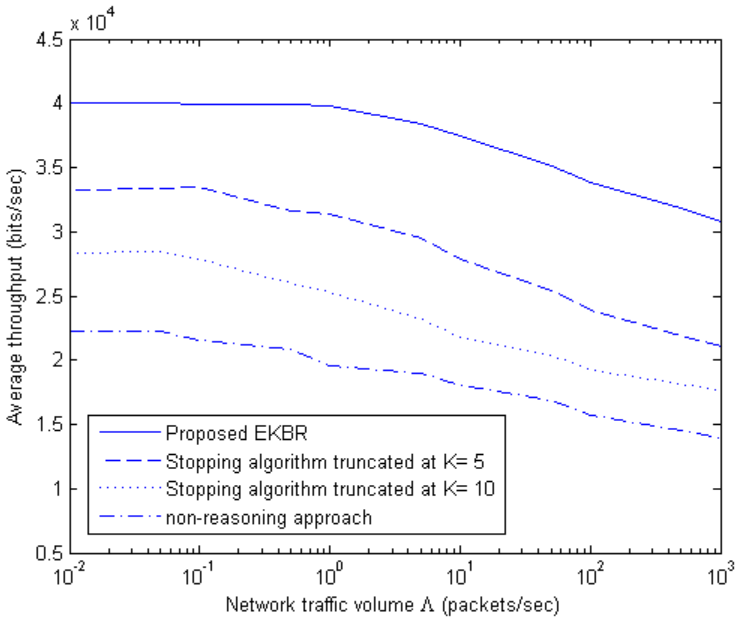

Figure 5.8: Simulation results of average throughput in comparison.

a certain threshold (in this case, $n^* = 4$). The data transmission rate nonetheless stabilizes and decreases slightly as n^* continues to increase. The reason for this decrease is that the number of anticipated fine sensing is directly correlated with network traffic volume, which is in turn determined by the number of nodes in the network and their traffic loads. As such, the increase of n^* potentially increases the number of fine sensing iterations, and thus damages the data transmission rate due to the interference of other nodes.

Fig. 5.10 shows the average sensing delay with different numbers of channels being finely sensed with the 93% confidence interval. We observed that in the case of a low traffic volume in the network, the average sensing delay increases very slowly when using EKBR. On the other hand, when a higher traffic volume in the network, the average sensing delay increases noticeably. This is due to the fact that as the number of anticipated fine sensing increases, the effect of interference increases and as a result the number of available channels decreases. Therefore, more fine sensing iterations are required by the femto under such a scenario in order to satisfy the data transmission quality requirements of the system.

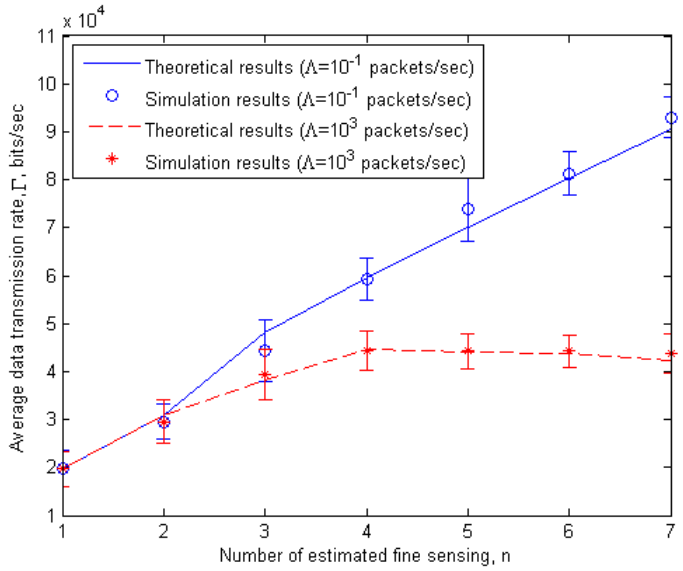

Figure 5.9: Simulation and analytical results for average data transmission rate.

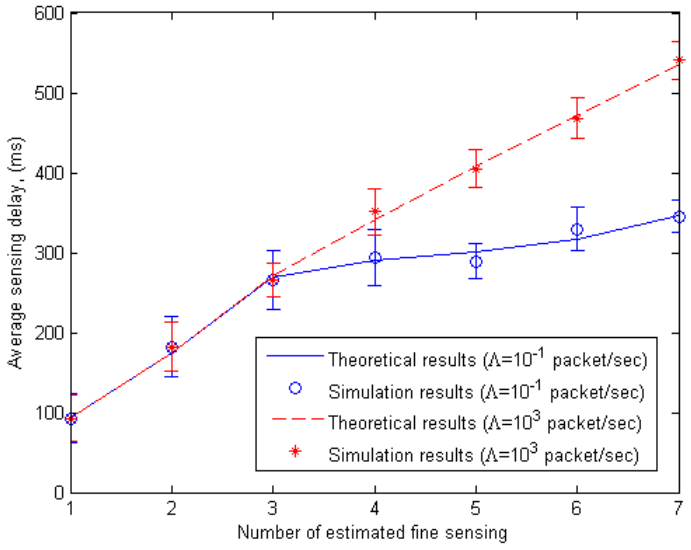

Figure 5.10: Simulation and analytical results for spectrum sensing delay.

5.4 Summary

In this chapter, an extended knowledge-based reasoning (EKBR) scheme is introduced for efficient MAC layer spectrum sensing CEF femto user. By additionally employing prior knowledge of network sates such as coordination instruction, short-term statistics of channel availability/quality, and channel access the proposed EKBR scheme can achieve efficient spectrum sensing by initiating a graceful tradeoff between data transmission rate and sensing overhead. This scheme is considered particularly effective when a rigid upper bound is imposed on the total processing time for each packet (frame). Performance analysis was conducted on EKBR by way of a multi-dimensional absorbing Markov chain. Simulations were conducted to validate the proposed analytical model and compare the proposed scheme with existing state-of-the-art spectrum sensing methods. The simulation results demonstrated that the proposed scheme noticeably outperforms the existing methods in terms of throughput due to the adoption of prior knowledge of network states. Abundant discussions were provided on the observations we made from the simulation results.

Chapter 6

Gossip-Enabled Stochastic Medium Access

In the previous chapters, we have introduced the sensing coordination scheme at the femto BS and EKBR scheme at the femto user to efficient identify spectrum availability in the CEF framework. Based on the identified spectrum availability, the femto user must determine which channels to use for data transmissions in presence of the dynamic and opportunistic nature of wireless environment. In the CEF framework, the coordination channel C_0 is reserved for the femto users communicating with the corresponding femto BS regarding of the instruction of the available channels. The femto users then launch data transmission/reception on these identified available channels to the femto BS, which forwards the data to/from the macrocell network to accomplish the data transmission.

In an ad hoc mode, the femto users communicate with each other without the femto BS forwarding data to/from the macrocell network. This application scenario can be happened for local femto gaming, and peer-to-peer (P2P) real-time file sharing, etc., where the coordination channel may be restricted for P2P control signaling and handshaking in order to protect femto-to-macro data communication performance degrading from contention and jamming on the coordination channel. Moreover, an ad hoc network can also be formed by femto users from different femtocells; therefore, the coordination channels may not always be on the same frequency band due to the strong network dynamics and user diversity, in which devices of different vendors and even different protocol stacks could be accommodated in a common network domain.

In this chapter, a novel gossip-enabled media access scheme via an efficient dynamic stochastic approach is developed by assuming the unavailability of the dedicated control

channel, i.e., coordination channel in CEF. The proposed media access scheme is characterized by achieving probabilistic objectives of minimum interference to the primary users through a power control mechanism, data fragmentation, as well as collision resolution. While the proposed method does not guarantee perfect accuracy, it is very efficient and expected to provide feasible solutions in a highly dynamic environment. The contributions of this work are as follows:

- By assuming the absence of any pre-defined dedicated control channel, a gossip enabled stochastic media access (GESMA) scheme for femto users in ad hoc networks is introduced, in which the problem of channel selection is formulated as an optimization problem for maximizing the probability of channel access.
- The formulated optimization problem is solved via an adaptive Markov-Chain Monte-Carlo (MCMC) approach [98], given the partial knowledge of channel availability such as gossip information. The dynamic MCMC method is incorporated with the proposed GESMA scheme for channel access in order to achieve high success rates and short delay of data transmission.
- We develop a power-controlled distributed Request-to-Send and Clear-to-Send (RTS/CTS) exchange mechanism, along with the incorporating collision resolution and data fragmentation strategies, that can best fit into the outlined CEF network design premises with an ultimate goal for effectively minimizing the interference on the primary user network.

Performance analysis is conducted on the proposed GESMA scheme in terms of throughput. Numerical results demonstrate that the proposed scheme can achieve similar performance to that using a dedicated control channel, while achieving noticeable improvement to the existing channel hopping approaches. The tradeoff between the proposed GESMA and that with a dedicated control channel in terms of overhead is further investigated. Finally, we expect that the proposed GESMA scheme serves as a value-added feature for not only the CEF framework but also future CR ad hoc networks with very high channel availability dynamics and protocol heterogeneity.

6.1 Problem Formulation

In the scenario without pre-defined control channels, a fundamental question is how to dynamically and adaptively find commonly available channels between femto communication

pairs. Specifically, our goal is to identify the optimal channel sequence for a femto transmitter to negotiate with the intended femto receiver given the limited number of channel negotiation attempts n_{max} that can be performed within a limited time period, such that the probability of successful channel negotiation of the selected channels is maximized.

Let S be a random variable taking on a channel $i, i = 1, 2, ..., K$, and s be the realization of S. Let Y_s be a binary indicator on the results of channel negotiation on s (i.e., a channel $i, i = 1, 2, ..., K$), where $Y_s = 0$ and $Y_s = 1$ indicates a failed and successful channel negotiation, respectively. The problem of selecting channels for negotiation can be formulated as the determination of an optimal sequence of channels, denoted as $\hat{s}_1, \hat{s}_2, ..., \hat{s}_j$, such that the joint probability of successful negotiations on the selected channels is maximized given the limited number of attempts n_{max}. Moreover, the transmission power for channel negotiation at the secondary transmitter should be under the power constraint given by Eq. (3.9) to limit the interference to the primary user signals. In order to increase the probability of reaching the intended femto receiver whose position may be unknown to the femto transmitter, it is also important to select the channels with the highest allowable transmission power. The higher the allowable transmission power, the farther the secondary user can be communicated. Therefore, the problem of determining the optimal sequence of channels for negotiation while meeting the interference power limitation can be formulated as [98]

$$\{\hat{s}_1, ..., \hat{s}_j\} = \arg\max_{s_1,...,s_j} \{p(Y_{s_1} = 1, ..., Y_{s_j} = 1)\}, \tag{6.1}$$

subject to:

$$P_{s_k} \leq \max\{P^{\max}_{s_k,(2)}\} \tag{6.2}$$

where $k = 1, 2, ..., j$ and $j \leq n_{max}$. Based on the widely accepted assumption that activities on each channel are independent [39, 40, 43, 99–102], the right-hand side of Eq. (6.1) can be re-written as $\arg\max_{s_1,...,s_j} \prod_{i=0}^{j} p(Y_{s_i} = 1)$.

A straightforward approach to solving this optimization problem is to identify a sequence of channels sorted according to both channel availability and SINR, and have the system negotiate on channels with higher availability and SINRs first in order to increase the likelihood of successful channel negotiation. However, it is extremely hard, if not impossible, to have sufficient knowledge on the availability of each channel at the intended femto receiver in order to determine an optimal sequence of channels.

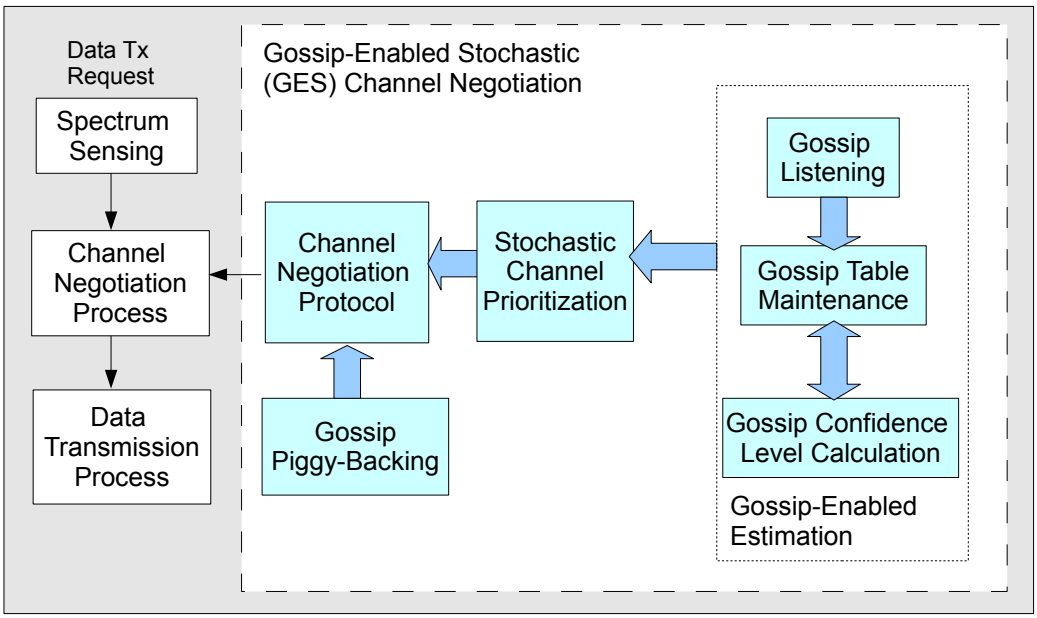

Figure 6.1: Gossip-Enabled Stochastic Media Access Functional Diagram

6.2 Proposed Gossip-Enabled Stochastic Media Access Scheme

The sequence of $\{\hat{s}_1, ..., \hat{s}_j\}$ is obtained by the proposed GESMA scheme to solving Eq. (6.1) via a meta heuristic approach [103]. For this purpose, a Markov-Chain Monte-Carlo (MCMC) Method is adopted to select a set of channel follows a target distribution $p(S)$ in a stochastic manner. As a key process of the proposed approach, the function $p(S)$ at the intended femto receiver is estimated based on *gossip* information such that the most preferred channels can be treated with higher priority in the channel negotiation process to increase the likelihood of successful channel access. The functional diagram of the proposed GESMA scheme is shown in Fig. 6.1 and the functions including an estimation process using the gossip information, MCMC method for channel selection, as well as the associated media access strategies are presented in details in the following sections.

6.2.1 Gossip-Enabled Estimation

In the proposed scheme, a gossip-based estimation mechanism is introduced to enable a femto transmitter in estimating channel availability at the intended femto receiver. The gossip-based estimation mechanism is composed of the following three functional blocks: i) *gossip listening*, ii) *gossip table maintenance*, and iii) *Gossip Confidence Level (GCL) calculation*.

Gossip Model

The concept of *gossip* [104] was reported to enable network-wide consensus in a distributed system. The proposed scheme manipulates the gossip mechanism for the identification of commonly available channels. With GESMA, every femto user obtains gossips by overhearing the other femto users' channel negotiation processes, which contain channel status information, channel usage map, as well as channel preference of other femto users. To consider the fact that the accuracy of obtained channel status fades as time goes by, *Gossip confidence level* (GCL) is defined to quantify how reliable a specific gossip is. All this information will be constantly updated in a *gossip table* maintained at each femto node. Then, a femto transmitter will be able to identify channels that can be used to negotiate with its intended femto receiver according to the real-time channel information in the gossip table. With the channel information obtained from the received gossips, the femto node will have a better chance to achieve successful channel access with the intended femto receiver.

Gossip Listening

Gossips at a femto user in this study are referred to as the signaling messages exchanged among other femto users that support their data transmissions, such as their channel usage map and channel preferences. With the proposed scheme, every femto user listens to a dynamically selected channel (termed *residing channel* and will be specifically defined in Section 6.2.3). Gossip listening is simply the process that a femto user periodically listens to the medium of its *residing channel* with a customized listening period[1], and reads the RTS/CTS messages of surrounding femto users that are on the same residing channel in the transmission range. Note that channel available information of a femto user is attached in its RTS/CTS messages that are further overheard by its neighbouring femto users.

[1]The channel listening interval can be simply defined according to the IEEE 802.11n standard.

A femto user $\aleph_j$ extracts the channel status information from the overheard RTS/CTS messages and stores the information in the gossip table with the corresponding time stamp. The gossip table is updated whenever channel access is accomplished or when another femto user's gossip message is overheard. With the gossip table, a graphical model $G = (V, E_i)$ can be built, which further forms a channel usage map. In $G = (V, E_i)$, the set of vertices $V(|V| \leq N_{(2)})$ represents the number of femto users that are known to $\aleph_j$, and the set of edges $E_i(|E_i| \leq N)$ represents the possible data transmission on C_i between two vertices. The set of edges $E_i(|E_i| \leq N)$ varies with time and provides channel status information.

Gossip Confidence Level

Note that the gossip table is simply a snapshot of the channel usage of the other femto users based on the collected gossip information. Thus, simply using the graphical model mentioned above could lead to inaccurate decision on the channel availability due to the followings. First, the interpretation of gossip information at the gossip source and receiver may be different, which leads to incorrect channel usage maps. For example, each RTS/CTS message only contains the source and destination MAC addresses and the duration of data transmission. As such, it is difficult to capture the exact start time and termination time of the data transmission. Note that the effectiveness of a piece of gossip information fades as time elapses. Second, it is necessary to deal with empty entries in the gossip table, which cannot be properly interpreted and handled using a simple graphical model.

To jointly consider the validity of gossip information, *gossip confidence level* is introduced in order to improve the accuracy of channel usage maps. With the gossip confidence level, a new *confidence-weighted graphic model* $G' = (V, E_i, W(E_i, t))$ is formed as an extension of the original graphical model $G = (V, E_i)$. The positive-valued weight $W(E_i, t)$ associated with each channel $C_i, i = 1, 2, ..., K$ represents the confidence level of the edge E_i and is correlated with the time difference δt between the current time instance t and time stamp associated with E_i.

The proposed confidence-weighted graph can take the high network dynamics into consideration by specifying how confident the channel usage map is based on a time-sensitive confidence weighting function. The problem due to empty entries can be resolved, too, which is described as follows. Since an empty entry means that the corresponding channels are not being used, the confidence-weighted graphical model $G' = (V, E_i, W(E_i, t))$ can be further extended to a confidence-weighted full graphical model $G'' = (V, E_i, E'_i, W(\forall E_i, t))$, where $\forall E_i = E_i \bigcup E'_i$, with two sets of edges E_i and E'_i representing recorded possible data

transmission and empty entries, respectively. To determine the level of confidence on the channel usage map at a particular edge E_i, a Butterworth function is employed to weight the gossip information associated with the other femto users $\aleph_k$:

$$W(\forall E_i, t) = \frac{1}{1 + (\delta t / c_i)^{g_{\aleph_k}}}, \tag{6.3}$$

where the parameter c_i is the cutoff point when the value of Butterworth function $W(\forall E_i) = 0.5$ on C_i, and the parameter $g_{\aleph_k}$ represents the decay rate of the reliability of $\aleph_k$. This confidence weighting function is designed such that the reliability of gossip information is not a fixed binary response (e.g., stale or not) based on a hard threshold. This soft thresholding strategy ensures a tighter control without asserting a hard threshold [105].

Estimated Channel Preference Ratio

Based on the confidence-weighted full graphical model $G'' = (V, E_i, E_i', W(\forall E_i, t))$, $\aleph_j$ can obtain a dynamic channel usage map of the secondary ad hoc network as well as a set of observations on C_i of other femto user $\aleph_k$, which is denoted as $\Omega_k^i = \{\omega_k^i(t_1), \omega_k^i(t_2), ..., \omega_k^i(t_n)\}$, where

$$\omega_k^i(t) = \begin{cases} 1 & \text{C}_\text{i} \text{ in use} \\ 0 & \text{C}_\text{i} \text{ not in use} \end{cases} \tag{6.4}$$

and can be used to learn the channel preference behavior of the other secondary users. Ω_k^i are grouped into ϵ sampling time bins $b_1, b_2, ..., b_\epsilon$ each with a number of observations denoted as $u_m(t), m = 1, 2, ...$ The number of observations $u_m(t)$ shows the number of usages on C_i out of the overall observations Ω_k^i at time bin $b_m, m = 1, 2, ..., \epsilon$. The observation window slides as the time elapses, where the oldest observations are removed from the system while the latest observations are being recorded. With the observations, the total volume of usage on C_i can be computed as $U_i(t) = \sum_m u_m(t)$. To identify channels with higher likelihood of mutual availability for negotiation between the femto communication pair, we are interested in those with larger channel preference ratios according to the following preference function:

$$f(U_i, t) = \frac{U_i(t)}{\sum_i^K U_i(t)}. \tag{6.5}$$

6.2.2 Markov-Chain Monte-Carlo Method for Channel Selection

This section introduces the proposed channel selection strategy under the GESMA scheme. Firstly, we assume that the channel preference is addressed according to how frequent the channel has been occupied/used in the previous observation window. Nonetheless, there is a dilemma for choosing preferred channels for negotiation: *A frequently used channel should be the one subject to less interference in the past, so the intended receiver should put high priority to use it for channel negotiation; on the other hand, the frequently used channel is the one subject to a high traffic load, and the intended receiver should avoid to use it any more in the near future.* The dilemma obviously complicates the algorithm design.

To resolve the dilemma, a meta-heuristic approach, MCMC Method for channel selection, is proposed to draw a set of samples that follows a target distribution $p(S)$ in a stochastic manner. When it is applied to solve the problem formulated in Eq. (6.1), the target distribution becomes the real profile of channel availability over the licensed spectrum, and a set of channels for negotiation are drawn based on this target distribution. As discussed in the previous section, it is very challenging to model channel availability accurately in a highly dynamic radio environment with network states rapidly fluctuated. Taking an alternative approach, the channel availability (i.e., the target distribution) may be well approximated using the gossip-enabled estimation in Eq. (6.5) despite of the imperfect channel information. Therefore, the target distribution in this study is defined as

$$p(S) = f(U_s, t) \cdot \mathbf{C}^T, \tag{6.6}$$

where S, and s, (as defined in Chapter 6.1), are a radome variable taking on channel i, and the realization of S, respectively, and $\mathbf{C}^T$ is the transpose of $\mathbf{C}$. The benefits of using the MCMC approach is that it can better account for uncertainties introduced by the system components, such as channel fading effect, preference estimation error, and unpredictable primary user usage.

Note that $p(S)$ is based on estimation of collected gossip information, and could be an arbitrary probability distribution instead of any reported parametric model. It is difficult to sample from an arbitrary probability distribution $p(S)$, particularly given that it can change for each energy detection process over the spectrum. One possible approach to sampling from an arbitrary PDF is to first sample from a uniform distribution and map the samples using its CDF. However, it is too computationally complex given changes in $p(S)$ over time. Therefore, a more effective approach to sampling from $p(S)$ is to use an MCMC approach [106]. The Metropolis-Hastings [107] MCMC scheme, which is used in the

proposed solution, takes advantage of an acceptance-rejection sampling process according to a proposal density function $Q(s'_k|s_{k-1})$. Specifically, $p(S)$ is taken as a dominating function over the target density, and a set of channels $\{s_1, ..., s_j\}$ is randomly drawn from the proposal probability distribution $Q(\cdot)$.

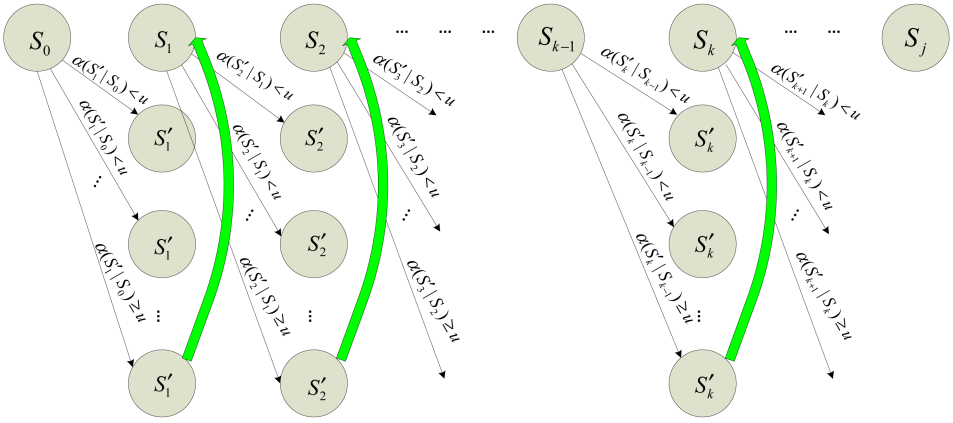

Figure 6.2: An overview of the acceptance-rejection channel selection

An overview is shown in Fig. 6.2, where the k^{th} channel for negotiation is selected through a way where a proposal channel s'_k is first drawn from a proposal probability distribution $Q(s'_k|s_{k-1})$. The probability of the proposal channel s'_k being selected for channel negotiation based on the previous selected channel s_{k-1}, denoted as $\alpha(s'_k|s_{k-1})$, can be defined as

$$\alpha\left(s'_k|s_{k-1}\right) = \min\left\{1, \frac{p(S = s'_k) \cdot Q(s_{k-1}|s'_k)}{p(S = s_{k-1}) \cdot Q(s'_k|s_{k-1})}\right\}. \tag{6.7}$$

Using a symmetric proposal probability distribution such as a Gaussian distribution, where $Q(s'_k|s_{k-1}) = Q(s_{k-1}|s'_k)$, the $Q(\cdot)$ functions cancel each other out on both the numerator and denominator. Thus Eq. (6.7) can be rewritten as

$$\alpha\left(s'_k|s_{k-1}\right) = \min\left\{1, \frac{p(S = s'_k)}{p(S = s_{k-1})}\right\}. \tag{6.8}$$

Based on Eq. (6.8), if the following criteria are satisfied, the proposal channel s'_k is accepted as a channel for negotiation, denoted as s_k:

$$\alpha\left(s'_k|s_{k-1}\right) \geq u, \tag{6.9}$$

where a random number u is drawn from a uniform distribution $U(0,1)$, and

$$s'_k \notin \{s_1, \cdots, s_{k-1}\}. \tag{6.10}$$

This approach generates a Markov chain as shown in Fig. 6.2.

This channel selection process is repeated until the desired set of channels to negotiate on channels $\{s_1, s_2, \cdots, s_j\}$ is determined. Moreover, amongst the selected set of channels, the higher the maximum allowable transmission power, the higher probability of reaching the intended secondary receivers that are located at farther distances. Therefore, by incorporating the power control information, we sort the set of drawn channels based on $P^{\max}_{s_k,(2)}$ to get a set of channels $\{\hat{s}_1, \hat{s}_2, \cdots, \hat{s}_j\}$ denoted as Θ. The pseudo code of the proposed dynamic MCMC channel selection method is shown in Algorithm. 1.

Algorithm 1 Dynamic MCMC Channel Selection

(Upon each data transmission request)
Set an initial channel s_0 as the channel recently negotiated;
for $k = 1; k < n_{max}; k++$ **do**
  Generate a candidate channel s'_k from $Q(\cdot)$ and a value u from $U(0,1)$;
  while $u > \alpha\left(s'_k|s_{k-1}\right)$ and $s'_k \notin \{s_1, \cdots, s_{k-1}\}$ **do**
    Reject the candidate channel s'_k;
    Generate a new candidate channel s'_k from $Q(\cdot)$ and a new value u from $U(0,1)$;
  end while
  Accept the candidate channel $s_k \leftarrow s'_k$;
end for
Obtain the set of channels $\{s_1, s_2, \cdots, s_j\}$.
Sort according to $P^{\max}_{s_k,(2)}$ to obtain $\Theta = \{\hat{s}_1, \hat{s}_2, \cdots, \hat{s}_j\}$.

6.2.3 GESMA Scheme

The proposed GESMA scheme defines a suite of distributed and asynchronous media access mechanisms for CR multi-channel ad hoc networks that enables the CEF femto users to agree on a set of channels for negotiation and access. This mechanism also ensures that with

interference probability from the femto transmission $\hat{p}$, (given in Eq. (3.8)) the secondary transmission will not disturb in the vicinities of primary users.

With GESMA, as soon as the femto user finds possibly available channels, it switches its operating central frequency on these channels to further identify the presence of faded primary signals. After identifying the availability of the channels, the femto user stays on any of these available channels (i.e., residing channel, denoted as s_0) until it either detects any primary user signal or identifies any on-going transmission between other femto users. Fig. 6.3 shows an exemplary state diagram of the proposed GESMA scheme. The detailed explanation is provided in following subsections.

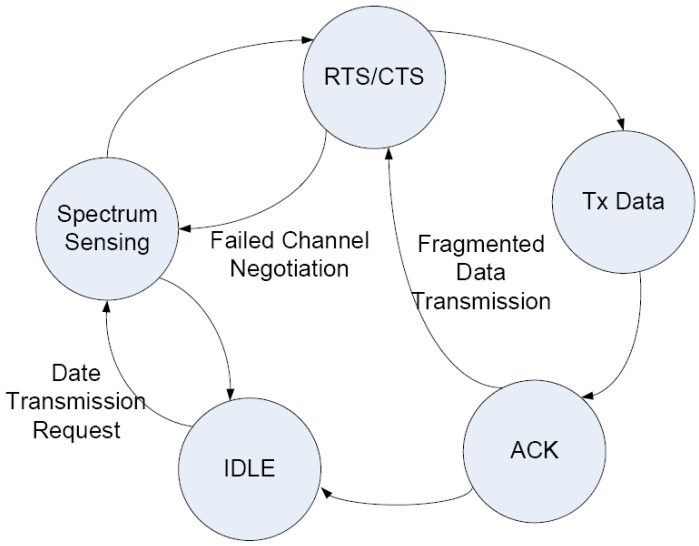

Figure 6.3: State Diagram of GESMA.

RTS/CTS Exchange

Suppose that a femto transmitter A has data to transmit to a femto receiver B. The femto transmitter A performs sensing over the instructed channels and selects a set of channels $\Theta = \{\hat{s}_1, \hat{s}_2, \cdots, \hat{s}_j\}$ based on the gossip information and proposed dynamic MCMC approach with power constraints described in Eq. (6.2). The femto transmitter A attempts to find a set of channels among Θ where the femto receiver B can possibly be reached.

An overview of the RTS/CTS exchange procedure is shown in Fig 6.4. Femto transmitter A sends a RTS message at the basic rate R_1 on its residing channel s_0 at the maximum allowable transmission power $P_{s_0,A}^{\max}$ (computed according to Eq. (3.9)). The RTS message not only includes the MAC address of the femto transmitter, intended femto receiver, and the duration value required to transmit the pending data transmission at the basic rate, but also piggy-backs the channel sequence Θ and maximum allowable transmission power $P_{s_0,A}^{\max}, P_{\hat{s}_1,A}^{\max}, ..., P_{s_j,A}^{\max}$, which can be used to aid femto receiver B in determining better common available channels. Note that the channel sequence indicates a set of available channels at the femto transmitter side, while the maximum allowable transmission power information indicates the closest primary user locations with probability $\hat{p}$.

If the femto receiver B is not on channel s_0, it is unable to receive the RTS message so that no CTS message will be responded. Therefore, A tunes to channels $\hat{s}_1, \hat{s}_2, ..., \hat{s}_j$ one by one after each timeout and repeats sending the same RTS message. If the femto receiver B is reached via channel s_k, it performs fast scans on the set of channels Θ upon receiving the RTS message, and determines the feasible set of common available channels $\Theta' \in \Theta$ as well as the noise level on those selected channels. Consequently, the femto receiver B responds the RTS by launching a CTS message back to A on all of its selected common available channels Θ', which contains the duration and corresponding noise level for intending data transmission. The CTS message implicitly instructs the femto transmitter A to meet the maximum allowable transmission power constraint, as well as instructs the intending data transmission on the channels Θ' to the other secondary neighbors.

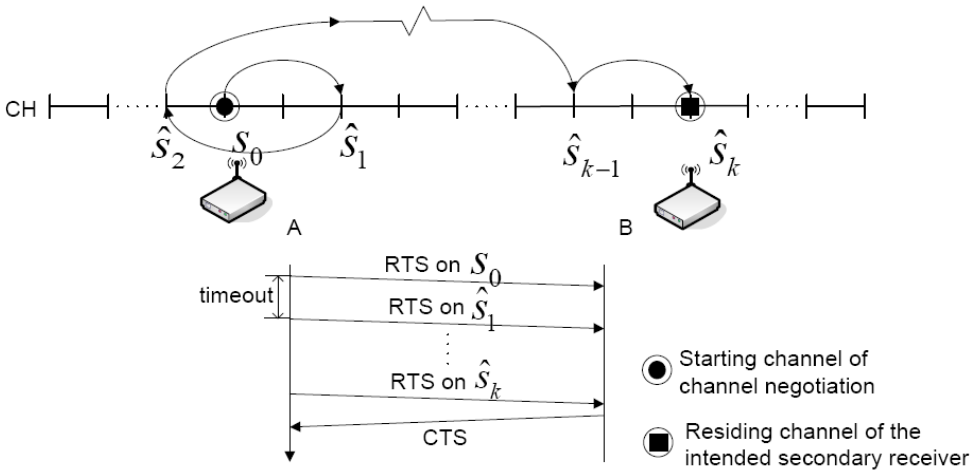

Figure 6.4: Overview of RTS/CTS exchange.

The proposed stochastic approach of channel selection can alleviate serious collisions amongst the secondary users by stochastically distributing access attempts on different channels even if these femto users identify similar sets of available channels at the same time. Moreover, a classical issue that needs to be dealt with in the design of a media access scheme is the hidden terminal problem, which can be mitigated by applying state-of-the-art strategies such as inserting busy tones [108, 109]. In this study, the major effort and focus is on the minimization of interference to the primary user transmission, and not on solving the hidden terminal problem, which is beyond the scope of this study.

Data Packet Fragmentation and Transmission

After completing the RTS/CTS exchange, the data transmission from A to B takes place on the agreed common available channel set $\Theta' \in \Theta$. For transmission of a long data packet, fragmentation is necessary to improve the performance due to the following reasons. First, a longer data packet takes longer transmission time, during which the transmission may more likely be subject to loss of channel availability and spectrum opportunity. Second, a user launching a longer data packet will likely occupy the channel for a longer period of time and prevent other users from fairly accessing the same media, which raises an issue on temporal fairness [110]. The above two situations become critical in the dynamic environment of secondary networks.

To address the problem, the proposed scheme defines segmentation of long data packets, and imposes a parameter on the maximum length on data fragment, denoted as L_{fr}. Here, $L_{fr} = R_1 \cdot CMT$, where R_1 is the basic transmission rate, and CMT is the channel move time defined in IEEE 802.22 [6]. Note that CMT can be interpreted as the longest allowable time period that the secondary system can possibly stay on a channel that has just been identified as occupied by any primary user.

The data transmission rates in the proposed scheme are determined based on the channel condition obtained from RTS/CTS message exchange. This allows a higher quality channel to achieve a higher rate of data transmission, which in turn can deliver more data packets within T_Σ. Fig 6.5 illustrates the proposed mechanism in transmitting fragmented data packets. In the case where the transmission of a packet at A is less than L_{fr}, B sends an ACK message to acknowledge a successful reception at the channel where B was originally found. On the other hand, in the case where a data fragment (DF) is transmitted at a high data transmission rate, additional DFs may be transmitted within T_Σ, and an ACK message is returned by B after each transmission of a DF, which acts as a virtual RTS

message. Upon receiving this ACK message from B, the secondary receiver A performs the same process as if it had received a real RTS message.

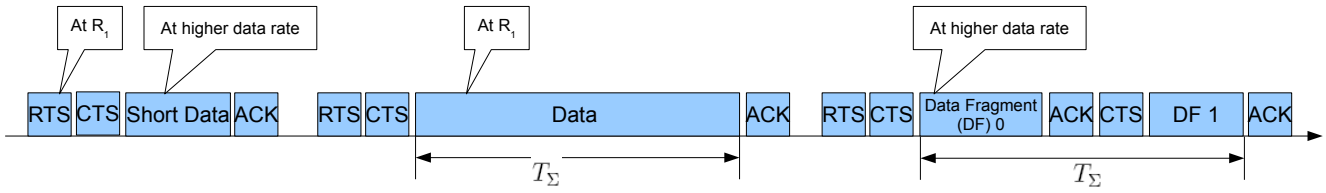

Figure 6.5: Illustration of data fragmentation time line.

Gossip Information Message

A gossip contains the full or partial gossip table, which is piggy-backed by a RTS/CTS message. Obviously, the longer piggy-back gossip information attached at the channel negotiation packet can yield a better chance in successfully finding a common channel for negotiation, while at the expense of larger opportunity of collision with the primary user signals. Therefore, the packet length of channel negotiation packet plus piggy-backed gossip information should be within a single DF.

6.2.4 Collision Solution

With access efficiency and interference reduction in mind when designing a media access scheme for secondary network, we realize that the characteristics and behavior of the spectrum resources in the secondary user network are significantly distinguished from that in the primary user network. In the proposed GESMA scheme, the collision resolution mechanism, which is one of the most important functions in a MAC protocol, will be substantially different from that in current IEEE 802.11 in order to fit into the dynamic environment.

Instead of employing the popular random backoff algorithm, the proposed GESMA simply retransmits a collided packet so as to minimize the interference on the primary network. Note that the imprecision of primary user identification is the main cause of interference from secondary users, which can be much more frequently encountered if there is possibly a long backoff delay in sending each packet. The problem due to imprecision of

primary user identification certainly becomes more serious when the period of backoff for each packet is getting longer. The retransmission of collided packets instead of backoff is expected to effectively solve this problem at the expense of increased secondary network access overhead. Our proposed design is based on the theorem provided as follows.

Theorem 6.2.1. *An increase of backoff time of the secondary users results in an increase in the probability of interference to the primary user networks.*

Proof. Let the backoff time of secondary users be denoted as $\tilde{T}_b$, which is a random variable with a probability density function $f_{\tilde{T}_b}(t)$. Let the probability distribution of primary traffic arrival be denoted as $F(T_i^{(1)}; \lambda_i^{(1)})$ with an arrival rate $\lambda_i^{(1)})$ on each channel. The probability of no primary traffic arrival during $T_i^{(1)} < T_b$ on channel i can be determined as $p_i(T_i^{(1)} > T_b)$, thus the probability of any primary traffic arrival during a given backoff period of the secondary users is given by

$$1 - p_i(T_i^{(1)} > T_b) = F(T_b; \lambda_i^{(1)}). \tag{6.11}$$

In other words, $F(T_b; \lambda_i^{(1)})$ is the probability of the interference to the primary user on each channel given the backoff period T_b. The average probability of interference $I(\lambda_i^{(1)})$ to the primary user using a backoff scheme on each channel is given by

$$I(\lambda_i^{(1)}) = \int_0^{T_{b,max}} F(T_b; \lambda_i^{(1)}) f_{\tilde{T}_b}(T_b) dT_b, \tag{6.12}$$

where $T_{b,max}$ is the maximum backoff time. Therefore, amongst $|\Theta'|$ number of selected channels, the probability of interference is determined by the first arrival of primary traffic, i.e., the earliest interference from the secondary user introduced by the backoff scheme, which can be given according to order statistics analysis [111] as

$$I_{\Theta'} = \sum_{k=1}^{|\Theta'|} \left(\begin{array}{c} |\Theta'| \\ k \end{array} \right) (I(\lambda_i^{(1)}))^k (1 - I(\lambda_i^{(1)}))^{|\Theta'|-k}. \tag{6.13}$$

For example, if we assume $f_{\tilde{T}_b}(t) = 1/T_{b,max}$ to be uniformly distributed within time window $[0, T_{b,max}]$, as well as $F(t; \lambda_p) = 1 - e^{-\lambda_i^{(1)} t}$, Eq. (6.13) can be written as

$$I_{\Theta'} = \sum_{k=1}^{|\Theta'|} \left(\begin{array}{c} |\Theta'| \\ k \end{array} \right) (1 + \frac{1}{\lambda_i^{(1)} T_{b,\max}} (e^{-\lambda_i^{(1)} T_{b,\max}} - 1))^k (\frac{1}{\lambda_i^{(1)} T_{b,\max}} (e^{-\lambda_i^{(1)} T_{b,\max}} - 1))^{|\Theta'|-k} \tag{6.14}$$

The plot of Eq. (6.14) for different $T_{b,max}$ and different primary traffic arrival volumes is shown in Fig. 6.6. As we can see, the probability of interference increases rapidly as $T_{b,max}$ increases under heavier primary traffic volumes. □

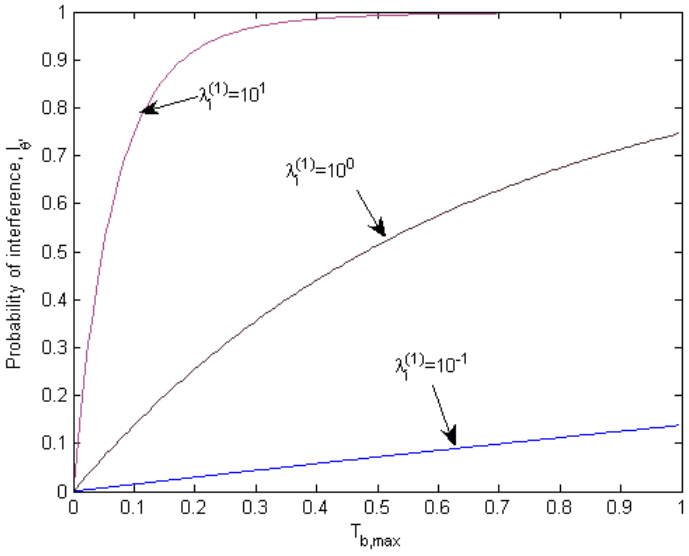

Figure 6.6: Probability of interference increases with increasing of $T_{b,max}$ vs. difference primary traffic arrival rate $\lambda_i^{(1)}$, given $|\Theta'| = 3$.

In the retransmission of a collided packet, the proposed GESMA has to conduct a new round of spectrum sensing and RTS/CTS exchange, which results in additional access overhead and serves as the expense on the reduced interference on primary users. Such a tradeoff between primary user interference and access overhead will be justified in the simulations.

6.3 Performance Analysis

In this section, we present a performance analysis of the proposed scheme in terms of throughput. In the situation where primary and secondary user networks coexist in the area of interest, the status of a single channel alternates between idle and busy, where the busy period can be occupied by primary users or/and secondary users. We assume the primary user network and the secondary user network are independent to simplify the analysis for the secondary user network as the primary user network does not change its behavior according to the secondary access. Based on this assumption, the secondary transmission cycle consists of a busy period (its expectation is denoted as $\bar{B}_i$) plus the following idle period (its expectation is denoted as $\bar{I}_i$), and underlays the idle period of the

primary user network on channel i. Therefore, the channel utilization on channel i for the secondary user network can be given using renewal theory as [108]

$$\rho_i = \frac{\bar{U}_i}{\bar{B}_i + \bar{I}_i}, \tag{6.15}$$

where $\bar{U}_i$ is the average utilization time for successful data transmission. The average duration of an idle period is

$$\bar{I}_i = 1/(\lambda_i^{(1)} + \lambda_i^{(2)}), \tag{6.16}$$

where $\lambda_i^{(1)}$, and $\lambda_i^{(2)}$ denotes the arrival rate of new and rescheduled primary, and secondary packets on channel i, respectively.

A successful data transmission is established by a successful RTS/CTS exchange. A RTS message generated from any secondary transmitter (e.g., femto user A) is successfully transmitted after the channel is sensed idle. Any other messages that are transmitted during the vulnerable period τ cause collision due to that fact that the channel is still sensed as unused. Therefore, the probability of a successful transmission of the RTS message is given by

$$p_{rts,i} = (1 - p_f)e^{-\tau\lambda_i^{(1)}}. \tag{6.17}$$

When the RTS message is received at the intended secondary receiver (e.g., femto user B), the channel negotiation succeeds. Therefore, a successful channel negotiation process consists of $t-1$ number of failed channel negotiation attempts and one successful channel negotiation attempt, which follows an absorbing finite Markov chain [95] with transition states $\{\hat{s}_1, ..., \hat{s}_j\}$ and absorbing state $\hat{s}_t$. Assume each secondary user has a probability of residing on channel i with a probability mass function as $p(i)$; the resultant transition probability $\mathbf{P}$ is formulated as

$$\mathbf{P} = \begin{array}{c} \\ s_0 \\ \vdots \\ s_j \\ \Re_1 \\ \vdots \\ \Re_j \end{array} \begin{array}{c} \overbrace{\hphantom{s_0 \quad p_{0,1} \cdots 0}}^{\text{Transient States}} \quad \overbrace{\hphantom{\Re_1 \cdots \Re_j}}^{\text{Absorbing States}} \\ \begin{array}{cccccc} s_0 & \cdots & s_j & \Re_1 & \cdots & \Re_j \end{array} \\ \begin{pmatrix} 0 & p_{0,1} & \cdots & 0 & p_{1,1^{\Re}} & & 0 \\ & \ddots & & p_{j-1,j} & & \ddots & \\ 0 & & & 0 & 0 & & p_{j,j^{\Re}} \\ 0 & & & 0 & 1 & & 0 \\ & \ddots & & & & \ddots & \\ 0 & & & 0 & 0 & & 1 \end{pmatrix} \end{array} \tag{6.18}$$

Therefore, the probability of a successful channel negotiation, which is also the absorbing

probability, can be estimated as

$$p_{cn} \triangleq p_{rts,s_t} p(i = s_t) \prod_{i=1}^{t-1} [1 - p_{rts,i} p(i)]. \tag{6.19}$$

The successful channel negotiation process is generally followed by successful data transmissions in the cases that hidden problem has been mitigated by applying start-of-the-arts strategies [108, 109, 112], as well as the lack of returning primary users. The probability of the earliest returning primary users on channel i is given by Eq. (3.4). Therefore, the probability of successful data transmission can be estimated as

$$p_{tx,i} \triangleq p_{cn}(1 - p_{i,re}), \tag{6.20}$$

and the average lower bound utilization time, which is estimated based on the basic rate R_0, can be determined as

$$\bar{U}_i \triangleq p_{tx,i} L_{fr}/R_1. \tag{6.21}$$

Hence, the channel utilization we obtain is a lower bound.

To find the average busy period in the secondary network, we adopt the method proposed in [113], where the busy period is considered as the time the channel is sensed as busy due to a successful transmission on channel or due to collision. The average duration of a successful transmission on the residing channel of the intended receiver, which contains RTS/CTS exchange, is determined by

$$T_s^{rts} \triangleq 3\delta + 4\tau + L_{fr}/R_1, \tag{6.22}$$

where δ is the transmission time of control message, i.e., RTS, CTS, and ACK, τ is the radio propagation delay. The average duration of a successful transmission on other commonly available channel, which does not involve addition RTS/CTS exchange, is determined by

$$T_s^{bas} \triangleq L_{fr}/R_1 + \tau. \tag{6.23}$$

Since a secondary user resides on channel i with probability $p(i)$, the average successful busy period can be estimated as

$$\bar{T}_{s,i} \triangleq T_s^{rts} p(i) + T_s^{bas}[1 - p(i)]. \tag{6.24}$$

The failed busy period in the multichannel environment may consist of: 1) one RTS message on a channel that is not the residing channel of the intended secondary receiver, which

then times out due to not reaching the intended secondary receiver; 2) more than one RTS message which arrives during the vulnerable period. Therefore, the average failed busy period of the two cases can be estimated as:

$$\begin{cases} T_{f,i}^{rts} \triangleq \delta + \tau \\ T_{f,i}^{c} \triangleq (\tau + 1/\lambda_i^{(2)})e^{-\lambda_i^{(2)}\tau} - 1/\lambda_i^{(2)} + \delta + \tau \end{cases}, \tag{6.25}$$

where the second equation in Eq. (6.25) accounts for the average time of the arrival RTS messages during the vulnerable period and a RTS transmission time. Since the first case happens on the channel that is not the residing channel of the intended receiver, while the second case can happen on any channel, the average failed busy period can be estimated as

$$\bar{T}_{f,i} \triangleq T_{f,i}^{rts}[1 - p(i)] + T_{f,i}^{c}. \tag{6.26}$$

Therefore, we can obtain the average busy period as

$$\bar{B}_i \triangleq p_{tx,i}\bar{T}_{s,i} + (1 - p_{tx,i})\bar{T}_{f,i}. \tag{6.27}$$

Finally, the channel utilization lower bound of a single channel i can be estimated as

$$\rho_i \triangleq \frac{p_{cn}(1 - p_{i,re})L_{fr}/R_1}{1/(\lambda_i^{(1)} + \lambda_i^{(2)}) + p_{tx,i}\bar{T}_{s,i} + (1 - p_{tx,i})\bar{T}_{f,i}}, \tag{6.28}$$

and thus the network wide normalized throughput lower bound can be estimated as

$$\rho \triangleq \frac{1}{K}\sum_{i}^{K}\rho_i \tag{6.29}$$

6.4 Performance Evaluation

In this section, we present simulation results for the GESMA scheme to evaluate its efficiency and effectiveness. An object-oriented modular discrete event-driven simulation model using OMNeT++ [114] is developed, where a $300m \times 300m$ network area uniformly distributed with different number of primary users and $N(2)s$ number of femto users is considered. We assume the approximated throughput of the primary user network as 0.4 [108]. The size of a primary user packet is uniformly distributed within the range of 0 to 2048 bits. In the secondary network, each femto user has a radio transmission range radius of $R = 200m$ forming a non fully-connected topology, where not all

femto users are within the transmission range of each other. According to IEEE 802.22, for each attempt of media access, the energy detection time for each channel is set as $0.05ms$, the time elapsed for tuning channels is $1\mu s$ [115], and the basic transmission rate is $1Mbps$. The CMT is set to $0.5ms$ instead of $2ms$ in [6] to further limit the interference caused by collision, which results in a collision window with double the transmission time. Therefore, the maximum length of data packet fragmentation is $L_{fr} = 0.5Kbits$ with regarding of the basic transmission rate. The other available transmission rates are set to $2Mbps, 6Mbps, 12Mbps, 36Mbps, 54Mbps$ [115]. For each transmission, a sender is randomly chosen and then the intended receiver is selected randomly among its neighbors. We conducted the simulation for $t_{sim} = 5000s$ for each trial.

In the simulation, we first study the channel negotiation procedure that will fundamentally affect the performance of GESMA. In the second set of simulations, we look into the performance of GESMA and study its effects on the performance of the primary and secondary user networks. The performance measurements are defined as follows:

- Access failure rate: the ratio of the number of failed channel accesses to the number of attempts.
- Access overhead: the time consumed on access attempts for a data transmission (ms).
- Throughput: the fraction of time the channels are used to successfully transmit payload bits [113].
- Packet delay: the average time duration before a successful data transmission.

6.4.1 Failure Rate of Channel Negotiation

The impact of using the proposed channel negotiation scheme on the performance of GESMA is studied and compared with a number of previously reported approaches, such as the dedicated control channel approach and the channel hopping approach [59]. The access failure rate of each short data transmission event are shown in Fig. 6.7 with aggregate secondary arrival rate $\lambda^{(2)} = \sum_{i}^{K} \lambda_i^{(2)} = 0.1$ packets per second, $K = 10$ channels over the licensed spectrum, and different available channels are identified by each femto users. It is observed that the failure rate of the proposed scheme achieves either a similar or a lower failure rate when compared with that by the dedicated control channel approach. Moreover, as expected, the failure rate of the channel hopping approach is significantly

higher than the proposed scheme and the dedicated control channel approach. The poor performance of the conventional channel hopping approach is due to the fact that it does not utilize any channel usage information. Therefore, the channel hopping approach may be more suitable to a static multi-channel environment, while yielding unacceptable performance under high network dynamics such as the CR ad hoc networks where the primary network resources are accessed in an opportunistic and secondary manner.

To further study the performance, Fig. 6.8 shows the simulation results on the average failure rate with respect to different aggregate primary traffic volumes Λ. It can be seen that under a lower primary traffic volume, the proposed GESMA is able to achieve similar performance with that by a dedicated control channel, but becomes outperformed under higher primary traffic volumes. This is due to the lack of dedicated control channel to coordinate the secondary transmission pairs, which increases the overall failure rates; and it becomes a more serious problem when the primary traffic volume is large. Fig. 6.9 shows the impact on the performance due to changes of secondary traffic volumes given a fixed aggregate primary traffic volume $\Lambda = 10^{-1}$. As expected, the proposed scheme achieves comparable performance as the dedicated control channel approach. This is due to the fact that the gossip information compensates for the lack of dedicated control channel in the proposed scheme, as well as that the dedicated control channel approach experiences degraded performance as a result of jamming problem, which accounts for around 75% of these failures. In Fig. 6.10, the average failure rate with a difference number of channels K is shown, with fixed secondary traffic volume $\lambda^{(2)} = 10^1$ and fixed aggregate primary traffic volume $\Lambda = 10^{-1}$. We observed that the proposed scheme and the dedicated control channel approach provide lower failure rates that are insensitive to K, while that of channel hopping approach is noticeably high in general.

6.4.2 Access Overhead

To provide a good indication of media access efficiency, we evaluate the access overhead associated with the proposed GESMA. The comparison results are shown in Fig. 6.11 with $K = 20$, where the secondary traffic volume $\lambda^{(2)}$ is set as low as 10^{-1} so that the impact of the primary traffic can be clearly observed. It can be seen that under low primary traffic volume the proposed scheme is able to outperform the other two approaches, while yielding comparable performance with that by the dedicated control channel approach under medium primary traffic volumes. This is due to the fact that the gossip information helps enhance the performance of the channel negotiation as well as avoid all control messages being jammed on a single dedicated control channel. As the primary traffic

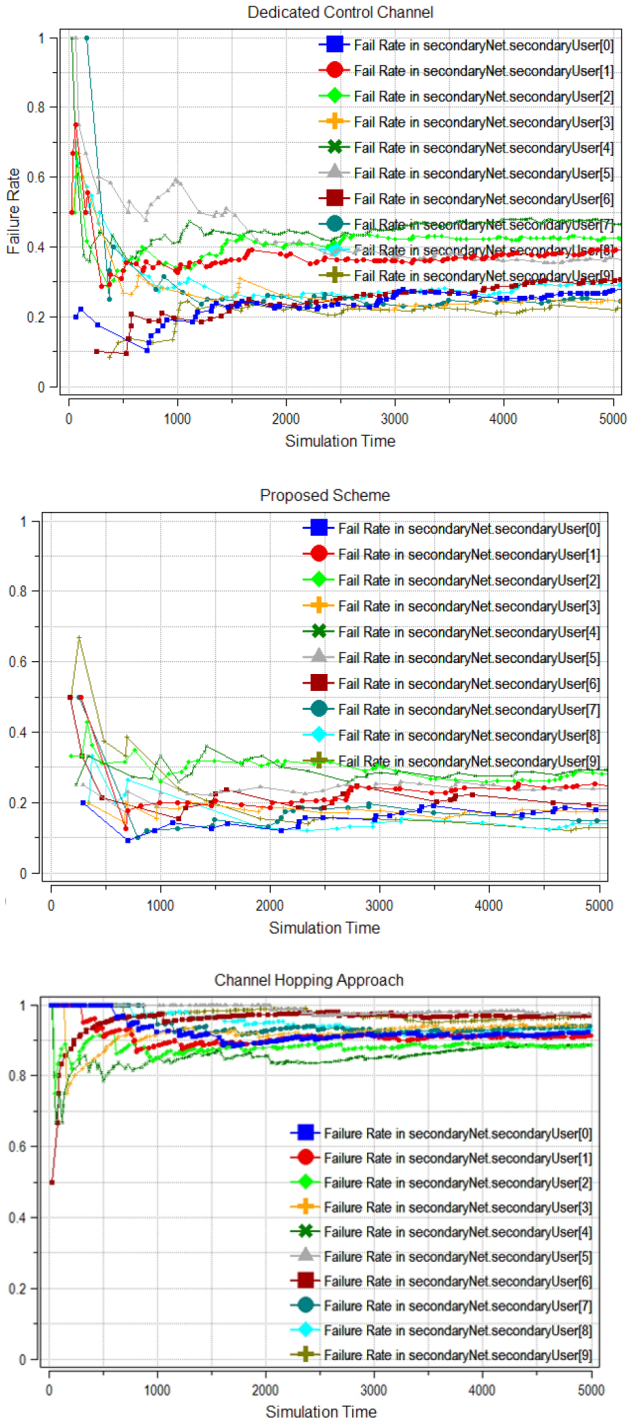

Figure 6.7: Failure rate of the proposed scheme and other approaches with 10 femto users in the primary user network with 15 primary users, and there are $K = 10$ channels over the licensed spectrum.

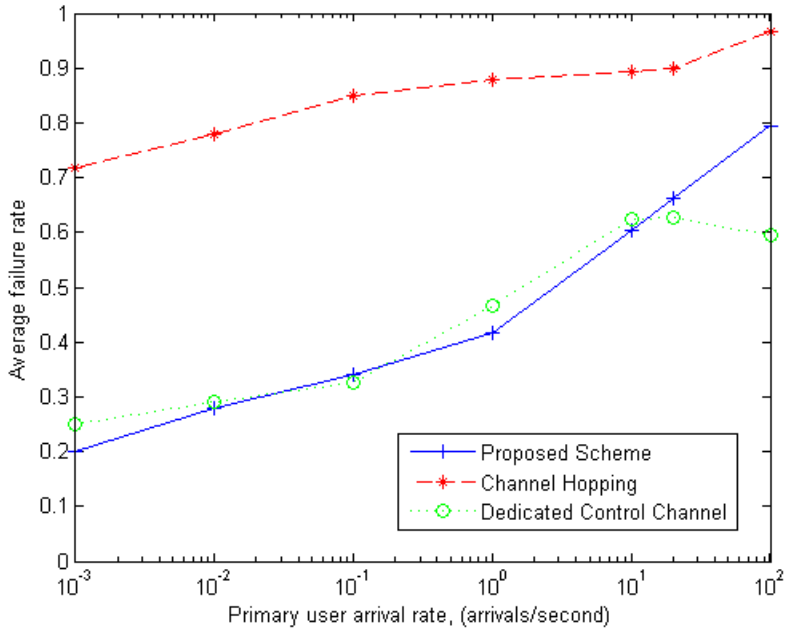

Figure 6.8: Average failure rate versus primary traffic volumes Λ.

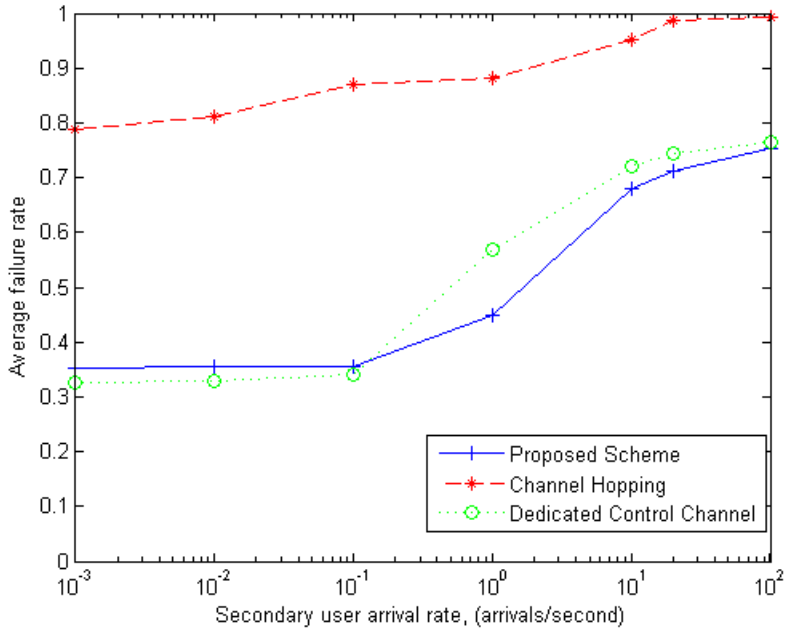

Figure 6.9: Average failure rate versus secondary traffic volumes.

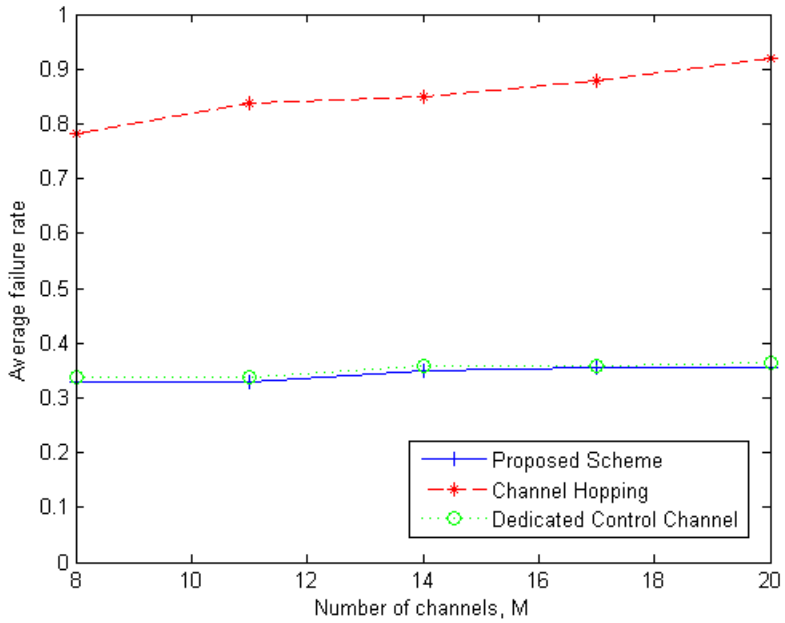

Figure 6.10: Average failure rate versus the number of channels.

volume increases, the average overhead of the proposed scheme is outperformed by the dedicated control channel approach but still outperforms the channel hopping approach. It can be observed that by not performing channel negotiation on dedicated control channel, there is a fundamental tradeoff between extra spectrum resources and increased overhead under high primary traffic volumes. However, it can also be observed that the tradeoff is reasonable. Therefore, we have identified that the proposed GESMA scheme can work quite well by yielding comparable performance with that of using a dedicated channel in CEF ad hoc networks when the primary traffic load is low or medium, which is exactly the situation of current TV bands envisioned in the future CEF applications.

In Fig. 6.12, we have increasing secondary traffic volumes under low primary traffic Λ as 10^{-1} so that the impact of the changes of secondary traffic can be clearly observed. We observe that in terms of the channel negotiation overhead, the proposed scheme is able to achieve comparable performance and outperform the dedicated control channel approach as the secondary traffic volume increases. This is mainly due to the channel negotiation message traffic jamming problem, which results in significant degradation to the performance of the dedicated control channel approach. On the other hand, the proposed scheme diversifies the channel negotiation attempts among the whole spectrum based on

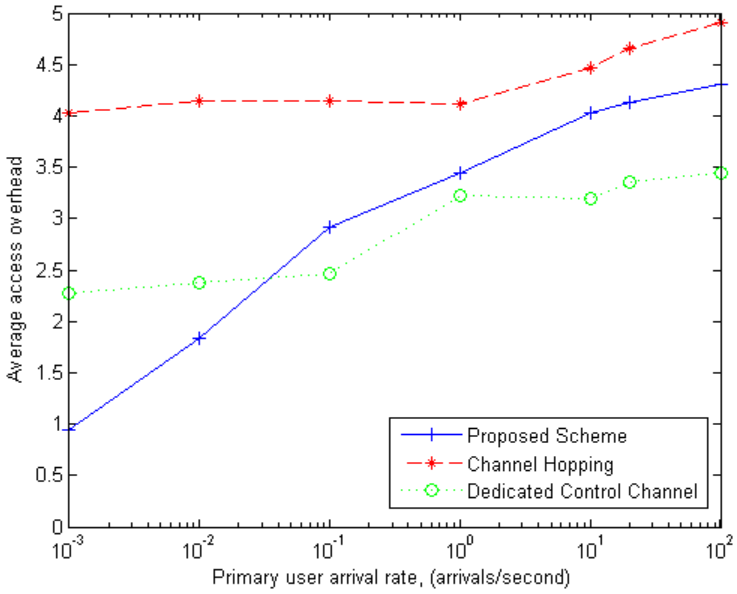

Figure 6.11: Average overhead of the proposed scheme and other approaches with different primary traffic volume λ.

the dynamic environment information, and as such does not suffer from this issue.

In Fig. 6.13, the impact due to different numbers of channels (i.e., K) is studied with low primary traffic volumes Λ and secondary traffic volumes $\lambda^{(2)}$, which were both 10^{-1}. It can be observed that the performance of GESMA and the dedicated control channel approach are insensitive to the variation of K. The result attests again that the dedicated control channel approach is more favourable in terms of overhead and success rate when the primary traffic volumes are low, due to little channel negotiation jamming. We have also seen that the proposed GESMA scheme yields significantly less overhead than that by channel hopping, regardless of the primary traffic.

6.4.3 Throughput of GESMA

Now we investigate the throughput of proposed scheme in terms of average throughput, as well as validate the proposed analytical model. Fig. 6.14 plots the average throughput lower bound $\bar{\rho}$ of secondary user network with primary arrival rate $\Lambda = 10$ arrivals/second versus different number of channel negotiation attempts t associated with normalized $\hat{p}(s_t) = 0.5/K$. All results are within 95% confidence interval. It can be seen that there are high

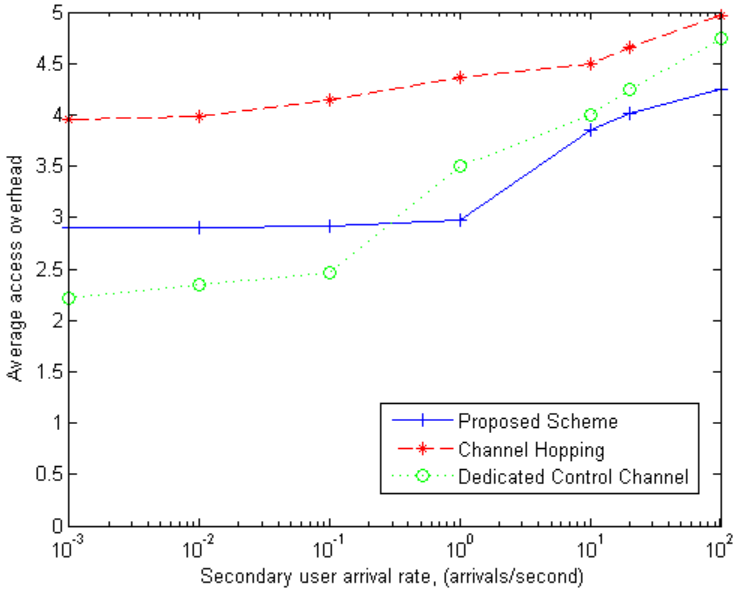

Figure 6.12: Average overhead of the proposed scheme and other approaches with different secondary traffic volume.

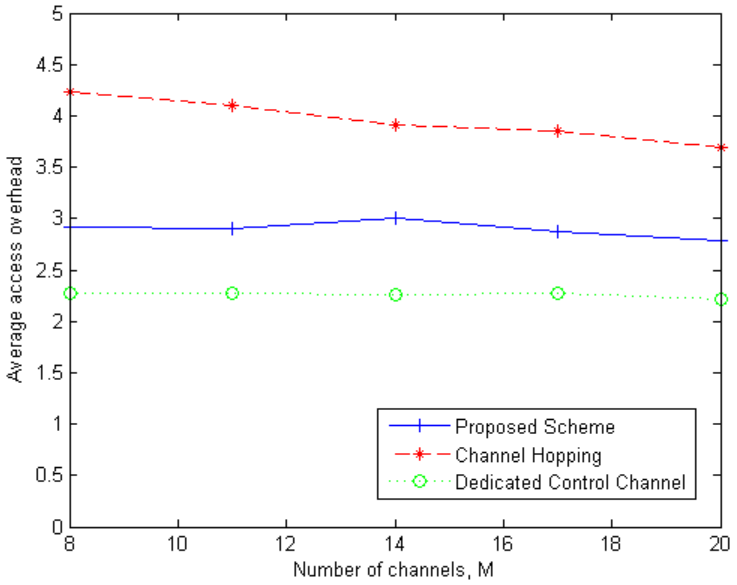

Figure 6.13: Average overhead the proposed scheme and other approaches with different number of channels K.

peaks as secondary user arrival rate reaches 10^1, which indicates more collisions in the secondary user network occurring after this point. Note that this situation is in line with the results of most MAC setups. In Fig. 6.15, the secondary user arrival rate is fixed at the saturation point, and the average throughput lower bound of the secondary user network in the low traffic volume scenario with $\Lambda = 10^{-2}$ arrivals/second as well as the high traffic volume scenario with $\Lambda = 10^2$ arrivals/second versus different normalized $p(s_t)$ are shown. A number of observations can be made. Firstly, with a low primary traffic volume, the average throughput lower bound decreases with the increasing of channel negotiation attempts t due to the fact that the failed channel negotiation has a noticeable impact on the average busy period. Secondly, under a light primary traffic volume, the performance is stable due to the fact that the average throughput of secondary user network is saturated and dominated by the secondary traffic volume. Finally, as expected, a higher primary traffic volume results in lower average throughput lower bound of secondary users.

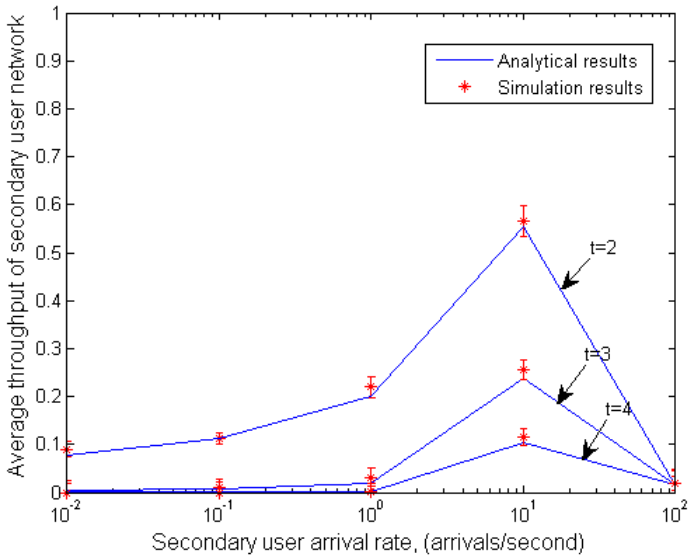

Figure 6.14: Average throughput lower bound of secondary users network with different number of channel negotiation attempts t vs. different secondary arrival rates of the proposed GESMA.

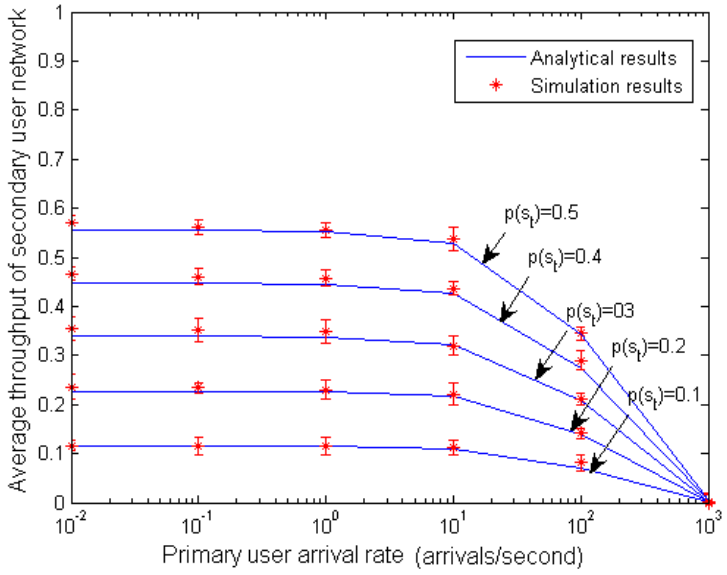

Figure 6.15: Average throughput lower bound of secondary users network with different $p(s_t)$ vs. different primary traffic arrival rates Λ of the proposed GESMA.

6.4.4 Packet Delay of GESMA

We analyzed packet delay of the proposed GESMA scheme with different primary traffic volumes. As shown in Fig. 6.16, the average packet delay of femto users increases as the traffic volume increases. The increased packet delay is mainly contributed by the collisions that occur due to the secondary traffic. Moreover, when taking the same secondary traffic volume, the average packet delay of femto users increases with the increasing primary traffic volume. It is clear that a higher primary traffic volume results in a longer process time on channel sensing and negotiation.

6.5 Summary

This work has presented a gossip-enabled stochastic media access (GESMA) scheme for secondary femto transmitters to efficiently find intended secondary receivers without the presence of dedicated control channel. The obtained gossip knowledge can be used to adaptively select channels with high likelihood of mutual availability between the secondary

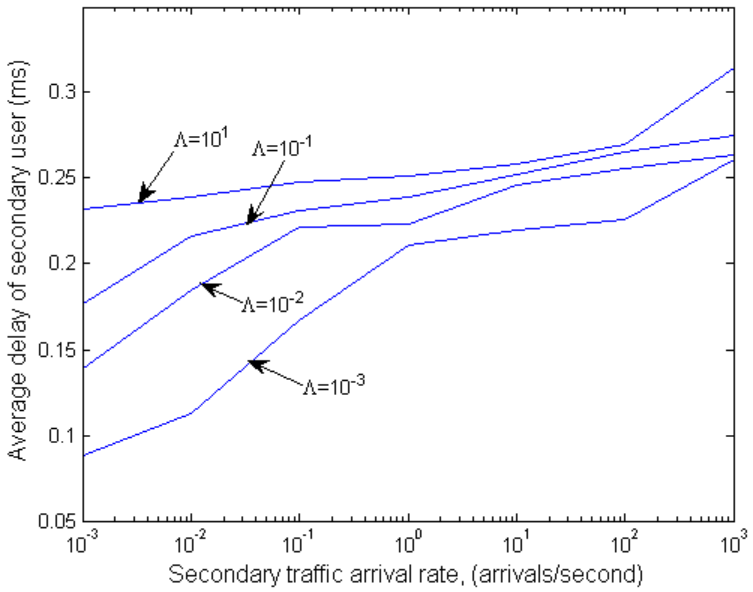

Figure 6.16: Average delay of secondary users with different secondary traffic arrival rate vs. different primary traffic arrival rate.

communication pair. The RTS/CTS exchange is then performed on the selected channel for channel negotiation. The lengthy data fragmentation issue is also addressed by taking into account the interference from miscalculated transmission power and false access attempts to the primary user network. The collision in the secondary user network is simply resolved by retransmission of the collided packets instead of via a commonly used backoff mechanism that will lead to longer delay. Such a design is to better fit the proposed scheme into the dynamic and opportunistic environment of CR networks, where the minimization of primary network interference is set as the ultimate goal.

We have conducted extensive simulations to analyze the proposed GESMA scheme, and compare it with other two other channel negotiation approaches by examining the access failure rate and access overhead. The simulation results show that the proposed GESMA scheme achieves comparable performance when compared to the dedicated control channel approach, which verified its effectiveness and efficiency. The simulation also examined the overall performance of the proposed GESMA scheme working under different primary traffic volumes and compared with previously reported counterparts, which further demonstrated its superiority. Furthermore, the analytical model presented is validated.

Chapter 7

Interference Analysis for Cognitive-Empowered Femtocells

In this chapter, the interference of interest in the CEF framework based on difference interfering sources, such as femtocell interference at a macrocell, interference from neighboring femtocell, interference within a femtocell, as well as interference from macrocell are analyzed. The characteristic and probabilistic analysis of the corresponding aggregate interference is derived based on the model of interfering signals using *shot noise* process [116, 117].

7.1 Interference Model

Due to the radio propagation nature of wireless communications, a victim receiver experiences interference from a random number of arbitrary interfering signals. The sources of interfering signals can be a finite number of transmitters of concurrent transmission, and the interfering transmitters are randomly distributed within the radio range of the victim receiver. In the radio frequency propagation model, signals may experience both the path loss and Nakagami-m fading [118, 119].

7.1.1 Path Loss Model

In the path loss model, regarding on the different point-to-point links of particular interest on channel i, the mean pass loss in dB can be simplified as [120]

$$\ell(d) = \underline{a} \begin{bmatrix} \log_{10} d \\ \log_{10} f_c^i \\ 1 \\ n^{(\frac{n+2}{n+1}-0.46)} \\ \epsilon \end{bmatrix}, \tag{7.1}$$

where $\underline{a}$ is the vector that indicates the path loss factor of outdoor radio propagation environment with $\underline{a} = \{40, 30, 0, 49, 0\}$, the path loss of indoor radio with $\underline{a} = \{30, 0, 18.3, 37, 0\}$, as well as the penetration loss of radio wave that penetrate walls from outdoor to indoor with $\underline{a} = \{40, 30, 0, 49, 1\}$, and from indoor to outdoor $\underline{a} = \{30, 0, 18.3, 37, 1\}$; d indicates the distance between an arbitrary transmitter and receiver; f_c^i is the carrier frequency of the channel i, ϵ indicates penetration loss, and n is the number of floors in the path.

7.1.2 Fading Model

In the Nakagami-m fading model, the probability distribution function of the received signal test statistics u_i on channel i can be expressed as

$$f(u_i) = \frac{2m_i^{m_i}}{\Gamma(m_i)E\{u_i^2\}} u_i^{2m_i-1} e^{-m_i u_i^2/E\{u_i^2\}}, \tag{7.2}$$

where $\Gamma(\cdot)$ is the Gamma function, and m_i indicates the fading severity of channel i. Moreover, different values of m_i can model different fading in a heterogenous channel model, such as Rayleigh fading and Rician fading [121, 118].

7.1.3 Shot Noise Model

At the front end of the victim receiver, the composite bandpass waveform received on channel i can be written as

$$r_i(t) = \mathrm{Re}\{[h_c S_{LP}(t) + I(t) + w_{LP}(t)]e^{j2\pi f_c^i}\}, \tag{7.3}$$

where $Re\{\cdot\}$ indicates the real part of a complex value, h_c is the channel impulse response, and $S_{LP}(t)$, $w_{LP}(t)$ refer to an equivalent low-pass representation of the received signal,

and additive white Gaussian noise (AWGN) with zero mean and a known power spectrum density (PSD), respectively. $I(t)$ refer to aggregate interfering signals contributed by the finite number K_I of concurrent transmissions; therefore, based on *shot noise* process, the low-pass received interference waveform can be written as [119]

$$I(t) = \sum_{k=1}^{K_I} S_k g_i(t - T_k), \tag{7.4}$$

where the k^{th} interfering signal arrives at T_k, which is a random variable following Poisson process with rate λ, also known as *intensity* and is related to Media Access Control (MAC) scheme. S_k is an equivalent low-pass representation of received k^{th} interfering signal, $g_i(t)$ is the impulse response of channel i for interfering signals.

7.1.4 Signal-to-Interference Ratio

The total interference power received at the victim receiver x_o on channel i can be estimated as

$$I_i(x_o) = \sum_{k=1}^{K_I} \mathcal{P}_k \beta_i / \ell(|x_o - y_k|) \tag{7.5}$$

where $\mathcal{P}_k$ denotes the transmission power of k^{th} interfering transmitter y_k, β_i is the Nakagamim fading factor. Given that each transmitter is associated with a location, for the sake of simplicity, we use the same notations such as x_o, y_k to respectively indicate the origin and the corresponding location of the k^{th} interfering transmitter on the polar coordinate (θ, z) within the radio range $\Omega(x_o)$ of the victim receiver x_o. As such, from this point on, z_k will be used to indicate the distance $|x_o - y_k|$. Moreover, it is important to note that, according the *shot noise* process, K_I is a random variable that represents the number of concurrently transmission occurrences associated with the applied MAC scheme within $\Omega(x_o)$ on channel i.

Suppose there is a transmitter y_0 sending data to the victim receiver x_o with transmitting power $\mathcal{P}_0$, the signal-to-interference ratio (SIR) at the receiver on channel i can be written as

$$\gamma^* = \frac{\mathcal{P}_0 \beta_i / \ell(z_0)}{I_i(x_o)}. \tag{7.6}$$

7.2 Interference Analysis

In this section, we begin by analyzing the interference of interest based on different interfering sources, followed by the analysis of the characteristics of the aggregate interference at the victim receiver, as well as the derivation the outage probability of the wireless link where the SIR is lower than the target threshold.

7.2.1 Interferences of Interest

From the point of view of femto users, the interference of interests are as follows:

Femtocell interference at a macrocell (I_{FM})

In this case, the victim receiver is the macrocell user which is interfered by the femto users' signals that penetrate walls from the indoor to the outdoor. Since there is no line of sight between femto users and macrocell users when signals penetrate walls, Rayleigh fading is more appropriate for capturing the characteristics of radio environments.

The possible causes of this interference include: 1) the indoor femto users or femto BS are not able to identify severely faded outdoor macrocell users' signals, and thus leading to unwanted accesses to unavailable channels that are being used by macrocell users, and 2) macrocell users returning to previously identified available channels that have been used by femtocell users. As known, the probability of the first cause is determined by probability of identifying the presence of primary user's signal, denoted as P_d, during the spectrum sensing process, while the probability of the second cause is related to the probability of no false alarms, denoted as $1 - P_f$, and the probability of the returning macrocell users. Moreover, the probability of the second cause is given in Eq. (3.4). Since the causes of the interference from the femtocell to the macrocell are independent, the probability of this interference can be evaluated as

$$P_{i,FM} \triangleq 1 - P_d + (1 - P_f)P_{i,re}. \tag{7.7}$$

Interference from neighboring femtocells (I_{FF})

In this case, the victim receivers are the femtocell users that are most likely on the edge of femtocell or in the intersections of neighboring femtocells. Since femtocells are deployed by

users within different sections in a complex building or within different households, there is usually no line of sight between neighboring femtocells. We assume Rayleigh channel fading in this type of radio environment.

The cause of this form of interference is that the neighboring femtocell users access the same channels that are in used by the reference femtocell users. Let $F(t, \mu^j)$ denote the probability distribution of the j^{th} femto traffic arrival with aggregate arrival rate μ^j. In the CEF, the traffic is stochastically distributed onto the channels, and channel i are selected with probability q_i^0 and q_i^j by the reference CEF BS and j^{th} neighboring CEF BS, respectively. Therefore, at the reference femtocell, the probability of interference from neighboring femtocells on channel i can be determined by the earliest traffic arrival from any neighboring femtocell traffic during the transmission duration T, which is expressed as

$$P_{i,FF} \triangleq 1 - F(T, \max(q_i^1 \mu^1, ..., q_i^j \mu^j, ...)). \tag{7.8}$$

Interference within a femtocell (I_F)

Within a femtocell, interference is mainly caused by the CEF BS instructing the same channels to difference femtocell users to sense and launch simultaneous transmission in the vulnerable time when the channels are both identified available at the femtocell users. The vulnerable time is defined as the duration in which an emitted signal can not be detected, i.e., the one-way propagation delay plus detection delay. Therefore, the probability of interference on channel i within a femtocell can be simply determined by the probability of instructing channel i to more than two femtocell users in the vulnerable time, which is denoted ν_i,

$$P_{i,F} \triangleq \nu_i. \tag{7.9}$$

Interference from macrocell (I_{MF})

This case is the opposite of the case associated with femtocell interference at a macrocell, where the victim receiver is the femtocell users being interfered by macrocell signals that penetrate the wall from outdoor to indoor. As such, Rayleigh fading is generally used to characterize the radio environment. Since the interference is also caused by the returning macrocell users, the probability of interference from macrocell users is evaluated by

$$P_{i,MF} \triangleq P_{i,FM}. \tag{7.10}$$

Aggregated Interference

The above analysis gives the picture of the different interference sources and the associated probabilities. At the front of the victim receiver, the aggregated average interference are received within its radio range $\Omega(x_o)$ as

$$\bar{I}_i(x_o) = \mathbb{1}_{FF}(\chi)I_{FF} + \mathbb{1}_F(\chi)I_F + \mathbb{1}_{MF}(\chi)I_{MF}, \tag{7.11}$$

where $\mathbb{1}_*(\chi)$ is the indication function of the different interference sources as

$$\mathbb{1}_*(\chi) = \begin{cases} 1 & if\ \chi \in * \\ 0 & if\ \chi \notin * \end{cases}, \tag{7.12}$$

The expected values of the indication functions for the different interference sources can be expressed by their associated probability of interference,

$$E(\mathbb{1}_*) = P_{i,*}. \tag{7.13}$$

7.2.2 Interference Characteristics

To analyze the characteristics of the aggregate average interference $\bar{I}_i(x_o)$ expressed in Eq. (7.11), we are interested in obtaining the Laplace transform of the shot-noise process of the interference as we can easily derive the distribution and the moments of the aggregate average interference [122].

According to the shot noise process in Eq. (7.4), the arrival time T_k of the k^{th} interfering signal at the victim receiver on the time axis follows a Poisson distribution. Due to the nature of radio propagation delay, there is a direct relationship between the propagation delay, T_k and the distance z_k. Based on this observation, the total number of interfering signal K_I on the time axis is the same on the polar coordinate (θ, z) axis within $\Omega(x_o)$. The corresponding aggregated intensity

$$\lambda(\Omega(x_o)) = \lambda_{FF}(\Omega(x_o)) + \lambda_F(\Omega(x_o)) + \lambda_{MF}(\Omega(x_o)) \tag{7.14}$$

indicates the average number of concurrent interfering transmission in inhomogeneous Poisson point process from different interfering sources, which is dependent on the location on $\Omega(x_o)$, as analyzed in the previous section. Therefore, the shot noise projected on $\Omega(x_o)$ in terms of shot noise amplitude and Dirac delta function $\delta(\cdot)$ can be rewritten as

$$I_i(x_o) = \sum_{*\in\{FF,F,MF\}} \sum_{k_*=1}^{K_*} P_{k_*} u_i / \ell(z_{k_*}) \delta(y - y_{k_*}), \tag{7.15}$$

where $\delta(y - y_{k_*})$ indicates the k^{th} interfering transmitter y_{k_*} from interfering source I_* where $* \in \{FF, F, MF\}$ within $\Omega(x_o)$. Similar to Eq. (7.13), the expected values of the k^{th} interfering transmitter for the different interference sources can be expressed by their associated probability of interference,

$$E(\delta(y - y_{k_*})) = P_{i,*}. \tag{7.16}$$

By not biasing on interfering source, the above equation can be rewritten as

$$I_i(x_o) = \sum_{k=1}^{K_I} \mathcal{P}_k u_i / \ell(z_k) \delta(y - y_k), \tag{7.17}$$

where $\delta(y - y_k)$ indicates the k^{th} interfering transmitter y_k within $\Omega(x_o)$, and $K_I = K_{FF} + K_F + K_{MF}$. The corresponding well-known Laplace transform [123] is given by

$$\begin{array}{rl} \mathcal{L}_I(s) & = \int_{I_i(x_o)} e^{-sI_i(x_o)} dI_i(x_o) \\ & = \exp\left\{ - \int_{\Omega(x_o)} E[1 - \mathrm{e}^{-s\mathcal{P}_k u_i/\ell(z_k)}] \lambda(\Omega(x_o)) d\Omega(x_o) \right\}. \end{array} \tag{7.18}$$

By assuming the fading is independent from the shot noise process [119], and assuming the angle of the interfering transmitter to the victim receiver follows a uniform distribution without loss the generality, the above equation can be simplified as

$$\mathcal{L}_I(s) = \exp\left\{ -2\pi \int_0^\infty \left[1 - \mathcal{L}_{u_i}(s\mathcal{P}_k/\ell(z_k))\right] \lambda(z) z dz \right\}, \tag{7.19}$$

which is consistent with that obtained in [119, 124].

Replacing s by $-\vartheta$ gives the moment generating function of $M_I(\vartheta)$; therefore, the average of interference is then given by

$$E(I) = \frac{dM_I}{d\vartheta}(0) = L_I'(-\vartheta)_{|\vartheta=0}, \tag{7.20}$$

and its variance is given by

$$Var(I) = \mathcal{L}_I''(-\vartheta)_{|\vartheta=0} - [\mathcal{L}_I'(-\vartheta)_{|\vartheta=0}]^2 \tag{7.21}$$

7.2.3 Outage Probability

The outage probability on channel i is defined as the probability that the SIR is smaller than a given threshold γ^o:

$$\begin{aligned} P_i^o &= Prob[\gamma^* < \gamma^o] \\ &= \int\limits_{I_i(x_o)} \int\limits_{\ell(z)} \Pr ob[\mathcal{P}_0 u_i < \gamma^o \ell(z) I(x) | \ell(z), I_i(x_o)] d\ell(z) dI_i(x_o) \\ &= \int\limits_{I_i(x_o} \int\limits_{\ell(z)} \int_0^{\gamma^o \ell(z) I_i(x_o f(u_i) du_i} d\ell(z) dI_i(x_o. \end{aligned} \tag{7.22}$$

In the case of Rayleigh fading, the outage probability can be rewritten as

$$\begin{aligned} P_{i,Ray}^o &= \int\limits_{I_i(x_o} \int_0^z (1 - e^{-\gamma^o \ell(z) I_i(x_o) \ell(z)} dz dI_i(x_o \\ &= \int\limits_{I_i(x_o} [\ell(z) - e^{-\gamma^o \ell(z) I(x)}] dI_i(x_o \\ &= 1 - \mathcal{L}_I[\gamma^o \ell(z) I_i(x_o)]. \end{aligned} \tag{7.23}$$

In the case of Rician fading, the probability of co-channel interference can be expressed as

$$P_{i,Ric}^o = \int\limits_{I_i(x_o)} \int\limits_{\ell(z)} \int_0^{\gamma^o \ell(z) I_i(x_o)} \exp\{-(u_i + \bar{u})\} J_0(u_i \bar{u}) du_i d\ell(z) dI_i(x_o), \tag{7.24}$$

where $\bar{u}$ is the factor of line of sight signal, and $J_0(\cdot)$ is the first order Bessel function.

Chapter 8

Conclusions and Future Work

This research proposed the idea of Cognitive-Empowered Femtocell (CEF): a network composed of elements that dynamically adapt to varying network conditions through learning and reasoning to optimize the performance. CEF represents the network solution of the CR techniques and femtocell networking concept, which has never been developed before and can have a significant impact on ubiquitous broadband communications. In a CEF network, decisions are made by the femto users to meet the requirements of radio resource under coordination, rather than having a complete control of spectrum access and sharing by the central controller. As such, the network intelligence are further moved out towards the end users to achieve cognition as a whole. We identified exciting deployment of the CEF for the early stage of WRAN with CR techniques so that radio resources can be better captured and intelligently selected while cross-tier and inner-tier interference can be mitigated.

8.1 Summary of Contributions

We list the problems and requirements that motivate CEF: network complexity, scarcity of radio resources, cost of deploying macrocell infrastructure, as well as increasing demands of higher data rates and pervasive computing. All of these problems and requirements make current approaches to network design inadequate. This technology is aimed to achieve better spectrum reuse, lower interference, easy integration, wider network coverage, as well as fast and cost effective network deployment. The enabling feature of CEF networking solutions is coordinated spectrum management, which provides the capability for

opportunistic access of radio spectrum resources by exploiting the radio environment for user-centric communications.

Three of the design challenges on the way of interference-free access, spectrum sensing as the first step to accurately identify available spectrum, media access as the second step of limiting interference, interference avoidance as the final step to achieve interference cancelation, are highlighted and can be considered distinct from conventional wireless networks. In the course of the survey of related work, advantages and disadvantages, as well as the tradeoffs are presented.

Having discussed the background and related work of the CR techniques and femtocell networking solution, the system design model and framework are formally defined. The definition of CEF emphasizes its coordinated spectrum management, which provides the capability for opportunistic access of radio spectrum resources by exploiting the radio environment for user-centric communications. This framework consists of two components, spectrum coordination module and end user module, which are respectively equipped at the femto BSs and femto users to facilitate the secondary and dynamic spectrum access.

The spectrum coordination module employs a novel sensing coordination approach that takes the best advantage of conventional stand-alone and cooperative sensing approaches, where better system scalability, efficiency, and complexity can be achieved without losing any performance and ability of interference management. By utilizing a *priori* information such as feature carriers, channel spacing of frequency bands, proactive fast sensing information, as well as user-based class information, the proposed coordination scheme provides intelligence in channel selection of spectrum fine sensing for femto users in the secondary network.

The end user module employs a novel Extended Knowledge-Based Reasoning (EKBR) approach for fine sensing, with a located spectrum range from the femto BS coordination. The optimal number of fine sensings is further refined by jointly considering the learned short-term statistical information and data transmission rate information. The reasoning approach is introduced through an analogy of "seashell collection" to illustrate a graceful balance between data transmission rate and sensing overhead.

Based on the obtained available channels, the actual media access for the femto users is achieved via a Gossip-Enabled Stochastic Media Access (GESMA) scheme built in the end user module. This proposed scheme is particularly designed to solve the media access without involving dedicated control channels. GESMA scheme serves as a MAC scheme in two CEF ad hoc modes: 1) femto users in the same CEF communicate with each other with a coordination channel that is not allowed for control signaling for peer-to-

peer communications; 2) femto users from different femtocell networks try to form an ad hoc network but with no available common coordination channel. As expected, learning from the gossip information makes up for the lack of dedicated control channel, and the MCMC channel selection can capture the uncertainty of the dynamic nature of secondary networks. The incorporation of power control, collision resolution and data fragmentation with GESMA are addressed to limit the interference.

Finally, interference characteristics and outage probability are analyzed for the CEF framework through rigorous mathematic modeling.

8.2 Future Work

Given that this research was the first investigation into combining CR techniques and femtocell network solution, there is plenty of work yet to be done. At the CEF BS, as interference avoidance is limited by the probability of detection p_d associated with the sensing techniques, an effective proactive strategy in interference mitigation is simply to take initial precautions against interference in the sensing coordination module. This prevention of potential interference can be achieved through proper coordination of user nodes.

A proper coordination given by the CEF BS should precariously distribute the channels for CEF users to sense so that the proceeding femtocell traffic can take place in a way such that concurrent transmission on the same channels can be mitigated. We look at Eq. 7.15, the aggregated interference consists of interference from neighboring femtocell I_{FF}, interference within a femtocell I_F, as well as interferences from macrocell I_{MF}. The I_{FF}, I_F known as inner-tier interference are important, non-negligible interfering sources, and their corresponding probabilistic behavior P_{FF} (Eq. 7.8) and P_F (Eq. 7.9) are respectively determined by the q_i^j and ν_i.

To improve interference mitigation, we wish to control q_i^j and ν_i such that the CEF BS can steer and minimize the intensity of intra-tier interference, $\lambda_{FF}\{A\}$, $\lambda_{FF}\{A\}$ in its coverage area A. Therefore, the optimal coordination problem can be formulated as the following minimization problem, where we wish to find the parameters q_i^j and ρ that minimize the aggregate interference $I[q_i^j, \nu_i]$,

$$I[q_i^o, \nu_i] = \sum_{i=1}^{K} \sum_{x \in A} I_i(x), \tag{8.1}$$

over all channels in the coverage area A of the CEF BS.

Moreover, as the femtocell networks underlay the macrocell networks, the interference to the macrocell I_{FM} is highly undesirable while the interference from the macrocell $I_{MF}$is unable to control. However, such cross-tier interference is extremely hard to avoid given the unpredictable returning of macrocell users. Therefore, we limit the probability of femtocell interference at a macrocell $P_{i,FM}$ under an acceptable threshold α for the macrocell users. The maximum transmission time of femtocell users T_{max} with regarding of α cross-tier interference are subject to

$$T_{\max} = \left\{ T \left| \frac{\mathbb{I}_i^{(1)}}{\bar{t}_i} \int_0^T (1 - e^{-t/\mathbb{I}_i^{(1)}}) f_{t_i}(t) dt < \frac{\alpha + p_d - 1}{1 - p_f} \right. \right\}. \tag{8.2}$$

Given the problem formulation, a few open topics and questions are listed.

- Wideband spectrum sensing
  To better realize the level of open spectrum utilization envisioned for CR systems, wideband spectrum sensing [125–127] is highly demanded. Given that energy detection methods are computationally efficient and easy to implement when compared to feature detection methods, they can be considered the natural choice for initial spectrum sensing in wideband CR systems. Very important challenges that we must face when employing an energy detection approach for wideband spectrum sensing are improving accuracy with higher p_d and lower p_f, and efficient PSD estimation in low Signal-to-Noise Ratio (SNR) scenarios.

- Stronger learning and reasoning for advanced inference avoidance
  The CEF framework can be refined by stronger learning and reasoning in future research. A reinforcement learning can be a potential solution of the interference minimization problem. For a mobile phone example, we could think of a move in a particular direction or making a call in a particular place being reinforced when the reception is improved or when a call from that place is successful, thus leading us to increased probability via that direction or at the place. There is also a trade-off between the amount of data and the complexity of the system that should be investigated.

- Implementation issue
  This research focused on designing the CEF framework and then implementing it via simulation. Given the ultimate goal of designing a CEF that is applicable to

real-world environments, a testbed will be developed using embedded devices with off-the-shelf wideband radio transceivers, during which additional design problems will be identified, implementation details will be fleshed out, and the limitations will be revealed.

- Energy-cognizant wireless communication
  Obviously, any cognitive process consume energy, and this results in an increasingly greater divide between power consumption and battery capacity. Therefore, although interference avoidance is one way of energy-cognizant, the protocol design and PHY-MAY layer optimization should also be studied from the view point of energy efficiency.

References

[1] S. Haykin. Cognitive radio: brain-empowered wireless communication. *IEEE Journal on Selected Area in Communications*, 23, Feb. 2005. 1, 2

[2] J. Miltola. Cognitive radio: making software radios more personal. *IEEE Personal Communications*, Aug 1999. 2

[3] FCC. A cognitive radio is a radio that can change its transmitter parameters based on interaction with the environment in which it operates. Technical Report ET Docket No. 03-222, Dec. 2003. 2

[4] F. K. Jondral. Software-defined radio–basics and evolution to cognitive radio. *EURASIP Journal on Wireless Communications and Networking*, (3), 2005. 2

[5] IEEE 802.221.22$^{\text{TM}}$/D0.1. Draft standard for wireless regional area networks part 22: Cognitive wireless ran medium access control (mac) and physical layer (phy) specifications: Policies and procedures for operation in the tv bands, 2006. 3

[6] C. R. Stevenson, C. Cordeiro, E. Sofer, and G. Chouinard. Functional requirement for the 802.22 wran standard, Nov. 2006. 3, 26, 36, 38, 84, 91

[7] R. Y. Kim, J. S. Kwak, and K. Etemad. WiMAX femtocell: Requirements, challenges, and solutions. *IEEE Communication Magazine*, 47, Sept. 2009. 4

[8] V. Chandrasekhar and J. G. Andrews. Femtocell networks: A survey. *IEEE Communications*, 46, Sept. 2008. 4

[9] X.Y. Wang, P.-H. Ho, and K.-C. Chen. Cognitive-Empowered Femtocells: An intelligent paradigm for femtocell networks. *IEEE Communications Magazine*, 2010. submitted. 4

[10] L. Ma, X. Han, and C. Shen. Dynamic open spectrum sharing mac protocol for wireless ad hoc networks. In *Proc. IEEE DySPAN*, Nov. 2005. 6, 18

[11] P. Pawelczak, R. V. Prasad, L. Xia, and I. G. M. M. Niemegeers. Cognitive radio emergency networks - requirements and design. In *Proc. IEEE DySPAN*, Nov. 2005. 18

[12] L.-C. Wang, A. Chen, and D. S. L. Wei. A cognitive mac protocol for qos provisioning in over laying ad hoc networks. In *Proc. IEEE CCNC*, Jan. 2007. 6, 30

[13] D. Cabirc, S. M. Mishar, and R. W. Brodersen. Implementation issue in spectrum sensing for cognitive radios. In *IEEE, Signals, Systems and Computers, Conference Record of the Thirty-Eighth Asilomar Conference*, Nov. 2004. 6, 7

[14] A. Ghasemi and E. S. Sousa. Spectrum sensing in cognitive radio networks: Requirements, challenges and design tradeoffs. *IEEE Communication*, 46, Apr. 2008. 6

[15] T. S. Rappaport. *Wireless Communications: Priciples & Practice*. Prentice-Hall, 1996. 6

[16] W. A. Gardner. *Cyclostationarity in Communications and Signal Processing*. IEEE Press, 1994. 7, 29

[17] I. F. Akyildiz, W. Lee, M. C. Vuran, and S. Mohanty. Next generation/dynamic spectrum access/cognitive radio wireless networks: A survey. *Computer Networks Journal (Elsevier)*, Sept. 2006. 7

[18] X. Y. Wang, A. Wong, and P.-H. Ho. Extended knowledge-based reasoning approach to spectrum sensing for cognitive radio. *IEEE Transactions on Mobile Computing*, 9, Apr. 2010. 12, 25, 50

[19] M. Gandetto and C. Regazzoni. Spectrum sensing: A distributed approach for cognitive terminals. *IEEE Journal on Selected Area in Communications*, 25, Apr. 2007. 15

[20] Z. Quan, S. Cui, and A. H. Sayed. An optimal strategy for cooperative spectrum sensing in cognitive radio networks. In *Proc. IEEE GLOBECOM*, Nov, 2007.

[21] J. Ma and Y. Li. Soft combination and detection for cooperative spectrum sensing in cognitive radio netwroks. In *Proc. IEEE GLOBECOM*, Nov, 2007. 15

[22] K. Lee and A. Yener. Throughput enhancing cooperative spectrum sensing strategies for cognitive radios. In *Proc. IEEE ACSSC*, Nov. 2007. 15

[23] C. Sun, W. Zhang, and K. B. Letaief. Cooperative spectrum sensing for cognitive radios under bandwidth constraints. In *Proc. IEEE WCNC*, Mar. 2007.

[24] L. Chen, J. Wang, and S. Li. An adaptive cooperative spectrum sensing scheme based on the optimal data fusion rule. In *Proc. IEEE ISWCS*, Oct. 2007.

[25] A. Ghasemi and E. S. Sousa. Collaborative spectrum sensing for opportunistic access in fading environments. In *Proc. IEEE DySPAN*, Nov. 2006.

[26] C. Lee and W. Wolf. Energy efficient technique for cooperative spectrum sensing in cognitive radios. In *Proc. IEEE CCNC*, Jan. 2008. 15

[27] C. Lee and W. Wolf. Multiple access-inspired cooperative spectrum sensing for cognitive radio. In *Proc. IEEE MILCOM*, Oct. 2007. 15

[28] G. Ganesan, Y. Li, B. Bing, and S. Li. Spatiotemporal sensing in cognitive radio networks. *IEEE Journal on Selected Area in Communications*, 26, Jan. 2008. 15

[29] G. Ganesan and Y. Li. Cooperative spectrum sensning in cognitive radio, part i: Two user networks. *IEEE Transactions on Wireless Communications*, 6, Jun. 2007. 15

[30] W. Zhang, R.K. Mallik, and K. B. Letaief. Cooperative spectrum sensing optimization in cognitive radio networks. In *Proc. IEEE ICC*, May 2008. 15

[31] S. M. Mishra, A. Sahai, and R. W. Brodersen. Cooperative sensing among cognitive radios. In *Proc. IEEE ICC*, Jun. 2006. 16

[32] X. Y. Wang, A. Wong, and P.-H. Ho. Stochastic channel prioritization for spectrum sensing in cooperative cognitive radio. In *Proc. IEEE CCNC*, Jan. 2009. 16, 41, 44, 51

[33] X. Y. Wang, A. Wong, and P.-H. Ho. Dynamically optimization spatiotemporal prioritization for spectrum sensing in cooperative cognitive radio. *ACM Wireless Networks*, (DOI: 10.1007/s11276-009-0175-0), Apr. 2009. 16

[34] P. Boggs and J. Tolle. Sequential quadratic programming. *Acta Numerica*, 1995. 16

[35] X. Y. Wang, A. Wong, and P.-H. Ho. Prioritized spectrum sensing in cognitive radio based on spatiotemperal statistical fusion. In *Proc. IEEE WCNC*, Apr. 2009. 16, 41, 44, 45, 46, 51

[36] H. Kim and K. G. Shin. Fast discovery of spectrum opportunities in cognitive radio networks. In *Proc. IEEE DySPAN*, Oct. 2008. 16

[37] X. Y. Wang, P.-H. Ho, and A. Wong. Towards efficient spectrum sensing for cognitive radio through knowledge-based reasoning. In *Proc. IEEE DySPAN*, Oct. 2008. 16

[38] D. Datla, R. Rajbanshi, A. Wyglinski, and G. Minden. Fast discovery of spectrum opportunities in cognitive radio networks. In *Proc. IEEE DySPAN*, Apr. 2007. 16, 17

[39] J. Jia, Q. Zhang, and X. Shen. Hc-mac: A hardware-constrained cognitive mac for efficient spectrum management. *IEEE Journal on Selected Areas in Communication*, Jan. 2008. 16, 17, 18, 30, 60, 74

[40] S. Huang, X. Liu, and Z. Ding. On optimal sensing and transmission strategies for dynamic spectrum access. In *Proc. IEEE DySPAN*, Oct. 2008. 16, 17, 74

[41] H. Kim and K. G. Shin. Adaptive mac-layer sensing of spectrum availability in cognitive radio networks. Technical Report, 2006. 16

[42] N. B. Chang and M. Liu. Optimal channel probing and transmission scheduling for opportunistic spectrum access. In *Proc. ACM MobiCom*, Sept. 2007. 17

[43] H. Su and X. Zhang. Cross-layer based opportunistic mac protocols for qos provisionings over cognitive radio wireless networks. *IEEE Journal on Selected Areas in Communications*, 26, Jan. 2008. 18, 74

[44] C. Peng and B. Y. Zhao H. Zheng. Utilization and fairness in spectrum assignment for opportunistic spectrum access. *ACM Mobile Networks and Applications*, 11, Aug. 2006.

[45] A. C. Hsu, D.S. L. Weiy, and C.-C. J. Kuo. A cognitive mac protocol using statistical channel allocation for wireless ad-hoc networks. In *Proc. IEEE WCNC*, Mar. 2007.

[46] C. Cordeiro and K. Challapali. C-MAC: A cognitive mac protocol for multi-channel wireless networks. In *Proc. IEEE DySPAN*, Apr. 2007.

[47] Q. Zhao, L. Tong, A. Swami, and Y. Chen. Decentralized cognitive mac for dynamic spectrum access in ad hoc networks: A pomdp framework. *IEEE Journal on Selected Areas in Communications*, 25, Apr. 2007. 21

[48] B. Yang, G. Feng, Y. Shen, C. Long, and X. Guan. Channel-aware access for cognitive radio networks. *IEEE Transactions on Vehicular Technology*, 58, Sept. 2009. 18

[49] S. L. Wu, C. Y. Lin, Y. C. Tseng, and J. L. Sheu. A multi-channel MAC protocal with power control for multi-hop mobile ad hoc networks. *Computer Journal*, 45, Jan. 2002.

[50] J. Chen and Y.-D. Chen. AMNP: Ad hoc multichannel negotiation protocol for multihop mobile wireless networks. In *Proc. IEEE ICC*, Jun. 2004.

[51] R. Maheshwari, H. Gupta, and S. R. Das. Multichannel MAC protocols for wireless networks. In *Proc. IEEE SECON*, Sept. 2006.

[52] P.-J. Wu and C.-N. Lee. On-demand connection-oriented multi-channel MAC protocol for ad-hoc network. In *Proc. IEEE SECON*, Sept. 2006. 18

[53] J. Zhao, H. Zheng, and G.-H. Yang. Distributed coordination in dynamic spectrum allocation networks. In *Proc. IEEE DySPAN*, Nov. 2005. 19, 20

[54] J. Mo, H.-S. W. So, and J. Walrand. Comparison of multichannel MAC protocols. *Computer Journal*, 7, Jan. 2008. 19

[55] J. So and N. Vaidya. Multi-channel MAC for ad hoc networks: Handling multi-channel hidden terminals using a single transceiver. In *Proc. ACM Mobihoc*, May. 2004. 19

[56] J. Wang, Y. Fang, and D. Wu. A power-saving multi-radio multi-channel MAC protocol for wireless local area networks. In *Proc. IEEE INFOCOM*, Apr. 2006. 19

[57] J. Zhang, G. Zhou, C. Huang, S. H. Son, and J. A. Stankovic. TMMAC: An energy efficient multi-channel mac protocol for ad hoc networks. In *Proc. IEEE ICC*, Jun. 2007. 19

[58] N. D. Jain and S. R. Nasipuri. A multichannel CSMA MAC protocl with receiver-based channel selection for multihop wireless networks. In *Proc. IEEE ICCCN*, Oct. 2007. 19

[59] R. Rozovsky and P. Kumar. SEEDEX: A MAC protocol for ad hoc networks. In *Proc. ACM MobiHoc*, Oct. 2001. 19, 20, 91

[60] P. Bahl, R. Chandra, and J. Dunagan. SSCH: Slotted seeded channel hopping for capacity improvement in IEEE 802.11 ad-hoc wireless networks. In *Proc. ACM Mobicom*, Sept. 2004. 20

[61] H.-S. W. So, J. Walrand, and M. Jeonghoon. McMAC: A parallel rendezvous multi-channel MAC protocol. In *Proc. IEEE WCNC*, Mar. 2007. 19

[62] T. Shu and M. Krunz. Spectrum opportunity-based control channel assignment in cognitive radio networks. In *Proc. IEEE SECON*, Jan. 2009. 20

[63] M. Felegyhazi, M. Cagalj, and J.-P. Hubaux. Efficient mac in cognitive radio systems: A game-theoretic approach. *IEEE Transaction on Wireless Communications*, 8, Apr. 2009. 21

[64] C. Cordeiro, M. Ghosh, D. Cavalcanti, and K. Challapali. Spectrum sensing for dynamic spectrum access of tv bands. In *Proc. IEEE CrownCom*, Aug. 2007. 21, 30, 61

[65] H. Claussen. Performance of macro- and co-sub-band femtocells in a hierarchical cell structure. In *Proc. IEEE PRIMRC*, Sept. 2007. 21

[66] K. Han, Y. Choi, D. Kim, S. Choi M. Na, and K. Han. Optimization of femtocell network configuration under interference constrains. Jun. 2009.

[67] H.-S. Jo, J.-G. Yook, C. Mun, and J. Moon. A self-organized uplink power control for cross-tier interference management in fentocell networks. In *Proc. IEEE MILCOM*, Nov. 2008.

[68] N. Arulselvan, V. Ramachandran, and S. Kalyanasundaram. Distributed power control mechanism for hsdpa femtocells. In *Proc. IEEE VTC Spring*, 2009. 21

[69] V. Chandrasekhar and J. G. Andrews. Uplink capacity and interference avoidance for two-tier femtocell networks. *IEEE Transactions on Wireless Communications*, 8, July 2009. 21

[70] L. G. U. Garcia, K. I. Pedersen, and P. E. Mogensen. Autonomous component carrier selection: Interference management in locol area environments for lte-advanced. *IEEE Communications*, 47, Sept. 2009. 21

[71] C. Snow, L. Lampe, and R. Schober. Impact of WiMAX interference on MB-OFDM UWB system: Analysis and mitigation. *IEEE Transactions on Communications*, 57(9), Sept. 2009. 21

[72] 3GPP. Evolved universal terrestrial radio access (e-utra); physical layer - measurements, Sept. 2009. 21

[73] 3GPP. Institute for information industry (iii) and coiler corporation, interference mitigation for henbs by channel measurements, Aug. 2009. 22

[74] S. Delaere and P. Ballon. Multi-level standardization and business models for cognitive radio: The case of the cognitive pilot channel. In *Proc. IEEE DySPAN*, Oct. 2008. 22

[75] M. Mueck, C. Rom, W. Xu, A. Polydoros, N. Dimitrious, A. S. Diaz, R. Piesiewicz, H. Bogucka, S. Zeisberg, H. Jaekel, T. Renk, F. Jondral, and P. Jung. Smart femtocell controller based distributed cognitive pilot channel. Jun. 2009.

[76] J. Perez-Romero, O. Sallent, R. Agusti, and L. Guipponi. A novel on-demand cognitive pilot channel enabling dynamic spectrum allocation. In *Proc. IEEE DySPAN*, Apr. 2007. 22

[77] M. Andrews, V. Capdevielle, A. Feki, , and P. Gupta. Autonomous spectrum sharing for mixed LTE femto and macro cells deployments. In *Proc. IEEE INFOCOM*, Mar. 2010. 22

[78] S.-Y. Lien and K.-C. Chen. Cognitive radio resource management for QoS guarantees in autonomous femtocell networks. In *Proc. IEEE ICC*, Apr. 2010. 22

[79] L. Lin and B. Li. Cooperative resource management in cognitive WiMAX with femto cells. In *Proc. IEEE INFOCOM*, Mar. 2010. 22

[80] A. E. Leu, B. L. Mark, and M. A. McHenry. A framework for cognitive WiMAX with frequency agility. *Proc. IEEE*, 2009. 22

[81] R. Saracco. Forecating the future of information technology: How to make research investment more cost-effective. *IEEE Communications Magazine*, 41, Dec. 2003. 25

[82] X. Y. Wang and P.-H. Ho. A novel sensing coordination framework for cr-vanets. *IEEE Transactions on Vehicular Technology Special Issue on Cognitive Radio*, pp, 2009. 25

[83] R.W. Brodersen, A. Wolisz, D. Cabric, S.M. Mishra, and D. Willkomm. Corvus: a cognitive radio approach for usage of virtual unlicensed spectrum. White paper, 2004. 26

[84] S. J. Shellhammer, A. K. Sadek, and W. Zhang. Technical chanllenges for cognitive radio in the tv white space spectrum. In *Proc. Information Theory and Applications workshop*, Jan. 2009. 28, 29

[85] F. F. Digham, M. S. Alouini, and M. K. Simon. On the energy detection of unknown signals over fading channels. *IEEE Trans. on Communications*, 55, Jan. 2007. 28, 29, 35

[86] S. Huang, X. Liu, and Z. Ding. Opportunistic spectrum access in cognitive radion networks. In *Proc. IEEE INFOCOM*, Apr. 2008. 29

[87] A. Feldmann and W. Whitt. Fitting mixtures of exponentials to longtail distributions to analyze network performance models. *Performance Evaluation*, 31, Jan. 1998. 30

[88] H. A. B. Salameh, M. M. Krunz, and O. Younis. MAC protocol for opportunistic cognitive radio networks with soft guarantees. *IEEE Transactions on Mobile Computing*, 8, Oct. 2009. 31

[89] T. C. Clancy. Achievable capacity under the interference temperature model. In *Proc. IEEE INFOCOM*, May. 2007. 31

[90] M. J. Osborne. *Game Theory*. Oxford University Press, 2004. 37

[91] S. Geirhofer, L. Tong, and B. Sadler. Cognitive radios for dynamic spectrum access - dynamic spectrum access in the time domain: Modeling and exploiting white space. *IEEE Communications*, 45, May. 2007. 51

[92] S. Mangold, Z. Zhong, K. Challapali, and C. Chou. Spectrum agile radio: radio resource measurements for opportunistic spectrum usage. In *Proc. IEEE GLOBECOM*, Nov. 2004. 51

[93] F. Hou, J. She, P.-H Ho, and X. Shen. A cross-layer design framework for non-real-time polling service in ieee 802.16 networks. *ACM Wireless Networks*, Jun. 2007. 53, 61

[94] B.W. Silverman. *Density Estimation*. Chapman and Hall, London, 1986. 53

[95] John G. Kemeny and J. L. Snell. *Denumerable Markov Chains*. McGraw-Hill, New York, 1976. 56, 88

[96] H.-S. Chen, W. Gao, and D. G. Daut. Signature based spectrum sensing algorithms for IEEE 802.22 WRAN. In *Proc. IEEE ICC*, Jun. 2007. 61

[97] M. Shen, G. Li, and H. Liu. Design tradeoff in ofdma traffic channels. In *Proc. IEEE ICASSP*, May 2004. 61

[98] X. Y. Wang, A. Wong, and P.-H. Ho. Dynamic Markov-chain Monte Carlo channel negotiation for cognitive radio. In *Proc. IEEE INFOCOM*, Mar. 2010. 73, 74

[99] S. Srinivasa and S. A. Jafar. Cognitive radios for dynamic spectrum access - the throughput potential of cognitive radio: A theoretical perspective. *IEEE Communications*, 45, May. 2008. 74

[100] M. Felegyhazi, M. Cagalj, and J.-P. Hubaux. Efficient MAC in cognitive radio systems: A game-theoretic approach. *IEEE Transaction on Wireless Communications*, 8, Apr. 2009.

[101] M. Van der Schaar and F. Fu. Spectrum access games and strategic learning in cognitive radio networks for delay-critical applications. *IEEE Proceedings*, 97, Apr. 2009.

[102] R. Urgaonkar and M. J. Neely. Opportunistic scheduling with reliability guarantees in cognitive radio networks. *IEEE Transaction on Mobile Computing*, 8, Jun. 2009. 74

[103] R. Storn and K. Price. Differential evolution a simple and efficient heuristic for global optimization over continuous spaces. *Journal of Global Optimization*, 11, Apr. 1997. 75

[104] J. Tsitsiklis. Problem in decentralized decision making and computation. Ph. D. dissertation, 1984. 76

[105] D. L. Donoho. De-noising by soft-thresholding. *IEEE Transction on Information Theory*, 41, May 1995. 78

[106] A. Gelman and D. Rubin. Inference from iterative simulation using multiple sequences. *Statistical Science*, 7, 1992. 79

[107] W. Hastings. Monte carlo sampling methods using markov chains and their applications. *Biometrika*, 57, 1970. 79

[108] F. A. Tobagi and L. Kleinrock. Packet switching in radio channels: Part ii-the hidden terminal problem in carrier sense multiple-access and the busy-tone solution. *IEEE Transactions on Communications*, 23, Dec. 1975. 84, 88, 89, 90

[109] J. Deng and Z.J. Hass. Dual busy tone multiple access (DBTMA) — a multiple access control scheme for ad hoc networks. *IEEE Transactions on Communications*, 50, Jun. 2002. 84, 89

[110] B. Sadeghi, V. Kanodia, A. Sabharwal, and E. Knightly. Opportunisitic media access for multirate ad hoc networks. In *Proc. IEEE Mobicom*, Sep. 2002. 84

[111] S. M. Ross. *Introduction to Probability Models*. Elsevier, San Diego, CA, 2006. 86

[112] P. Pawelczak, S. Pollin, H.-S. W. So, A. R. S. Bahai, R. V. Prasad, and R. Hekmat. Performance analysis of multichannel medium access control algorithms for opportunistic spectrum access. *IEEE Transactions on Vehicular Technology*, 58, Jul. 2009. 89

[113] G. Bianchi. Performance analysis of the ieee 802.11 distributed coordination function. *IEEE Journal on Selected Area in Communications*, 18, March. 2000. 89, 91

[114] Omnet. `http://www.omnetpp.org`, 2006. 90

[115] A. Sabharwal, A. Khoshnevis, and E. Knightly. Opportunisitc spectral usage: bounds and a multi-band CSMA/CA protocoal. *IEEE/ACM Transactions on Networking*, 15, Jun. 2007. 91

[116] N. Campbell. The study of discontinuous phenomena. In *Proc. Cambr. Phil. Soc.*, volume 15, 1909. 102

[117] N. Campbell. Discontinuities in light emission. In *Proc. Cambr. Phil. Soc.*, volume 15, 1909. 102

[118] L.-C. Wang and C.-T Lea. Co-channel interference analysis of shadowed Rician channels. *IEEE Communication Letter*, 2(3), Mar. 1998. 102, 103

[119] M. Haenggi, J. G. Andrews, F. Baccelli, O. Dousse, and M. Franceschetti. Stochastic geometry and random graphs for the analysis and design of wireless networks. *IEEE Journal on Selected Area in Communications*, 27(7), 2009. 102, 104, 108

[120] Guidelines for evaluation of radio transmission technologies for IMT-2000. ITU-R M.1225, Feb. 1997. 103

[121] Y. M. Shobowale and K. A. Hamdi. A unified model for interference analysis in unlicensed frequency bands. *IEEE Transaction on Wireless Communication*, 8, Aug. 2009. 103

[122] F. Baccelli, B. Blaszczyszyn, and P. Muhlethaler. An Aloha protocol for multihop mobile wireless networks. *IEEE Transcation on Information Theory*, 25(2), Feb. 2006. 107

[123] S. O. Rice. Mathematical analysis of random noise. *Bell System Technical Journal*, 24, 1945. 108

[124] F. Baccelli, B. Blaszczyszyn, and P. Muhlethaler. Stochastic analysis of spatial and opportunistic aloha. *IEEE Journal on Selected Area in Communications*, 27(7), 2009. 108

[125] S. M. Mishra, R. Tandra, and A. Sahai. IEEE P802.22, Wireless Rans, Wideband sensing and coiler corporation, interference mitigation for henbs by channel measurements, July 2007. 113

[126] Z. Tian and G. Giannakis. Compressed sensing for wideband cognitive radios. In *Proc. IEEE ICASSP*, May 2007.

[127] Y. Polo, Y. Wang, A. Pandharipande, and G. Leus. Spectrum sharing radios. In *Proc. IEEE ICASSP*, Apr. 2009. 113

[128] 3GPP. Lte-fdd henb interference scenarios, May 2009.

[129] Application Note. Building a versatile low latency cognitive radio for multi-mission applications with the ics-572. Technical Report, Sept. 2003.

[130] S. Geirhofer, L. Tong, and B. M. Sadler. Cognitive medium access: Constraining interference based on experimental models. *IEEE Journal on Selected Areas in Communications*, 26, Jan. 2009.

[131] T. Shu and M. Krunz. Coordinated channel access in cognitive radio networks: A multi-level spectrum opportunity perspective. In *Proc. IEEE INFOCOM*, Apr. 2009.